RENORMALIZATION OF GAUGE THEORY ON THE LIGHT CONE WORLD SHEET

By

JIAN QIU

A DISSERTATION PRESENTED TO THE GRADUATE SCHOOL
OF THE UNIVERSITY OF FLORIDA IN PARTIAL FULFILLMENT
OF THE REQUIREMENTS FOR THE DEGREE OF
DOCTOR OF PHILOSOPHY

UNIVERSITY OF FLORIDA

2007

to Lisa Elkenhans

ACKNOWLEDGMENTS

My greatest gratitude toward my advisor Professor Thorn for sparing no effort in helping me obtain deeper understanding of physics and many a timely encouragement to forge on.

TABLE OF CONTENTS

LIST OF TABLES

LIST OF FIGURES

Abstract of Dissertation Presented to the Graduate School
of the University of Florida in Partial Fulfillment of the
Requirements for the Degree of Doctor of Philosophy

RENORMALIZATION OF GAUGE THEORY ON THE LIGHT CONE WORLD SHEET

By

Jian Qiu

August 2007

Chair: Charles Thorn
Major: Physics

We calculated the scattering of gluon, scalar and quarks in gauge theory in the light cone gauge. Some computation techniques suited for the light cone gauge are introduced. We observed some inadequacies of the counter terms suggested in our earlier work, and we suggest a new way of fixing counter terms using Lorentz invariance as a guide. Gluon scattering with massive matter fields in the loop are presented for completeness. The helicity amplitude method is extensively used in this work and is also modified to simplify the light cone gauge calculation.

CHAPTER 1
INTRODUCTION

Gauge theory is generally thought of as the fundamental theory that governs most of the important interactions in particle physics. The standard model of particle physics is based on a gauge theory with a gauge group $SU(3) \otimes SU(2) \otimes U(1)$ minimally coupled to some matter fields. The electro-weak part of this theory has relatively small coupling, and the perturbative calculations produced results that agree with the experiments extremely well. The strong interaction (QCD) has a coupling constant of the size 0.1 at high momentum (short distance) where the perturbative calculation can still give some useful predictions. However, the coupling is of order one around 1 GeV and will tend to infinity at lower momenta. The perturbative calculations cease to make sense at this scale, yet it is at this scale that some interesting phenomena happen. For example, at high energy QCD can be described by quark and gluon fields, while at low energy the quarks become confined and the description in terms of pions and baryons is more relevant. At high energy the quarks enjoy an $SU(2)_L \otimes SU(2)_R$ symmetry, but at low energy the axial vector part of this symmetry is spontaneously broken down. These phenomena are beyond the grasp of perturbation theory, and the quantitative results mainly come from lattice computation. The quest for an analytic solution to the low energy spectrum or a dual description of QCD that suits the low energy and strong coupling has been the focus of many physicists.

Besides its phenomenological importance, gauge theory is also interesting in its own right because of its close connection with topology. A gauge theory consists of a curvature field $F_{\mu\nu}$, satisfying the Bianchi identity $dF = 0$. In QED, the entries of F are simply the electric and magnetic filed E and B, while the Bianchi identity is two of the four Maxwell equations $\nabla \cdot \vec{B} = 0$ and $-\partial\vec{B}/\partial t = \nabla \times \vec{E}$. In general, the Bianchi identity says the two form $F_{\mu\nu}dx^\mu dx^\nu$ is closed, so we cannot simply vary the field strength to obtain the Euler-Lagrange equation. Instead, we write F as dA for some 1-form A, known as the connection 1-form, and vary A rather than F. Although not all closed forms

(forms satisfying $d\omega = 0$) are exact (forms can be written as $\omega = d\tau$), writing F as dA causes no problem in the perturbative calculations, because we are only interested in small fluctuations around $A = 0$. Yet for a non-perturbative computation, a non-trivial configuration of the A field can give important results such as the anomalous breaking of the axial $U(1)$ symmetry. In those cases, we have to manually sum over configurations of different winding numbers. The A field, as its name suggests, is a connection in the gauge bundle, more concretely, the 1-form $A^a_\mu t^a dx^\mu$ acting on the tangent vector $\partial_\mu = \partial/\partial x^\mu$, converts it to a vector $A^a_\mu t^a$ in the direction of the fibre (elements of the Lie group translate a field in the 'vertical' direction). With this connection, we can compare two fields in nearby space-time points using the covariant derivative $D_\mu = \partial_\mu - A_\mu$. The geometrical nature of the gauge theory is not explored in this dissertation, however, the problem of gauge fixing is still important for this work.

Putting aside gauge theory for a moment, we also have a possible alternative description of the strong interaction: string theory. It was initially proposed in order to model the dynamics of the flux tube which is the explanation of confinement in the strong interactions. In analogy with the point particle, where the equation of motion is such that the path traversed by a particle(world line) in space-time is the shortest path, the bosonic string theory studies a one dimensional extended object and the equation of motion is such that the two dimensional surface swept by the string (world sheet) is a minimal surface. An open string has two free ends, they can be given the Chan-Paton degrees of freedom, which are rather like a label that labels the different states of the end of the string. These states can be taken to transform in a representation of a Lie group, say, in the fundamental for one end and anti-fundamental for the other. With this setup, the open string is like a pion which has presumably a quark and an anti-quark at each end and connected by the flux tube. In fact, the scattering amplitude of the open strings reproduces the scattering of gluons in the low energy limit.

The similarity was explored in [1], where 't Hooft looked at the $SU(N)$ gauge theory as $N \to \infty$. In this limit, the adjoint representation of $SU(N)$ can be approximated by $N \otimes \bar{N}$. The A field transforming in the adjoint representation, now carries two indices A^i_j in the large N limit, where ^{i} and $_j$ transform in the N and $\bar{N}$ respectively. Hence a gluon line can be drawn as two lines carrying the ^{i} and $_j$ index each. With this representation, a Feynman diagram will look like Fig.1-1. The ^i_j index corresponds to the Chan-Paton factors. Any closed index loop such as in the middle of Fig.1-1 will be a trace $\mathrm{Tr}\delta^i_j$ producing a factor of N. If a Feynman diagram is drawn with crossed lines, we will lose factors of N, so by keeping only the leading terms in the power of N, we pick out all the planar diagrams. There is a clear analogy between the planar diagrams and the open string scattering diagrams Fig.1-2, where the arrows now indicate the Chan-Paton factors. By summing over all the planar diagrams, we hope to learn something about the non-perturbative nature of the gauge theory.

't Hooft also pioneered the light-cone parametrization of these planar diagrams in [1]. The correspondence between the two graphs in Fig.1-3 is that, a rectangle maps to a propagator, a line (cut) maps to the blank space between two propagators, and the beginning(end) of a line is the splitting(merging) point of two propagators, or simply a 3-point vertex. The success of this parametrization is because in the light-cone, a propagator contains a step function $\theta(x^+p^+)$. This factor says if a propagator is to propagate forward in x^+, it has to carry positive p^+. This parametrization is also used in [6, 7, 8, 9].

The correspondence between gauge field theory and string theory was revolutionized by the AdS/CFT correspondence due to Maldacena [2], a certain superstring theory on an $\mathrm{AdS}_5 \times S^5$ background is equivalent to the $\mathcal{N} = 4$ supersymmetric gauge theory. Detailed proposals of this correspondence were made by Gubser, Klebanov and Polyakov [3] and by Witten [4]. Their idea is the holographic concept, where the Minkowski space $\mathcal{M}^4$ is the boundary of the AdS space, and the correlators in $\mathcal{M}^4$ are computed from the bulk of

AdS. The field theory and its perturbative expansions grasp the weak coupling limit, while the string theory description naturally grasps the strong coupling limit. For example, in [5], the author studied the energy of a string hanging between two static sources in the classical limit (in the context of AdS/CFT duality, classical limit in the string theory corresponds to the strong coupling limit in the field theory), which shows a force that obeys inverse square law, in accordance with the fact that $\mathcal{N} = 4$ SYM is a conformal theory. Despite all the above, a lot of the details of the correspondence still await filling in.

So the establishment of the detailed correspondence between string theory and gauge theory becomes urgent. In [6, 7], the authors proposed a local world sheet description of the (supersymmetric) gauge theory, which maps a Feynman diagram to a world sheet representation. The vertices in this description become the merging and splitting of strings, and the summation of Feynman diagrams becomes a path integral on the (discretized) world sheet. The Feynman rules, or the vertex functions were realized by inserting a local world sheet operator close to the splitting or merging point. There is no need for the representation of a four point vertex, because it is automatically generated when two insertions for three point vertices coincide and produce a contraction term. This is rather fortuitous, for a four point vertex is very unnatural in a string diagram. The summation of all the planar diagrams becomes the summation over whether or not there is a cut in each of the lattice sites. This treatment still has many loose ends to tie up. For example, the problem of renormalization which requires not only a local representation of the bare diagrams on the world sheet but also a local representation of the counter terms. The problem of renormalization for scalar fields on the world sheet was addressed in [8], but was only partially solved for gauge theory in [9] due to some complications.

It is absolutely necessary therefore, to study the renormalization for gauge fields on the world sheet, making sure that the world sheet path integral description at the least will reproduce all the perturbative results before we jump into studying its

non-perturbative side. The checks include, whether all the divergences appearing in the perturbative expansion can be absorbed into target space local counter terms, and whether these counter terms can have a *local* world sheet representation. And most importantly in the case of (supersymmetric) gauge theory, how the regulators will affect gauge covariance and supersymmetry.

Since 't Hooft's planar diagram representation was most easily given in the light cone parametrization, it is natural that we chose to study the gauge theory on the world sheet also in light cone gauge. In this case, in order to study the gauge invariance property, we have to deal with some collateral complications due to the light cone gauge choice and also the issue of infrared divergence which is inherent to a gauge theory. These tasks have been the main focus of my work. In the two papers [13, 14], we studied the gluon scattering in the light cone gauge in great detail and found the need for some counter terms that were quite unexpected. An infrared regulator is also proposed in [14] that is very different from dimensional regulation yet still respects gauge covariance. In [15], the extension to the gauge theory coupled to general matter was made, and some results that are peculiar to $\mathcal{N} = 4$ were observed. Also the cancelation of counter terms between different species was achieved, whose importance will be explained later.

As an extension, the scattering of quarks and scalars in addition to gluons was computed, which showed a need for some new counter terms not given in the previous work. The complete determination of these new counter terms is still a work in progress. And the usage of Lorentz covariance as a guide to fix counter terms will be initiated in the future work section.

The organization of the dissertation is as follows, in Chapter 2, the helicity amplitude method is briefly introduced. This method, when modified to suit the light cone, can greatly increase the flexibility of light-cone gauge, and offers an alternative way to obtain light cone Feynman rules. Some computational details are also given in the same chapter. In Chapter 3, I shall describe the box-reduction technique which occupied a bulk of

the work done in [14], and is essential to our achievement of the cancelation of artificial divergence and the extraction of infrared divergence. In Chapter 4, I shall simply list the results, since the details of the computation are complicated and not very illuminating. Discussion about some known features of supersymmetric gauge theory is given in Chapter 4 too. In Chapter 5, the Bremsstrahlung calculation on the light cone is presented, and the real processes are combined with virtual processes to obtain an IR finite result.
In Chapter 6, I shall give the scattering of gluon with massive matter in the loop for completeness, and the photon scattering amplitude is also presented. I shall conclude this dissertation by pointing out some remaining problems and the outlook for some future work. In the appendices, I shall spell out the spinor notations used in the paper and all the Feynman rules obtained by using the method of Chapter 2.

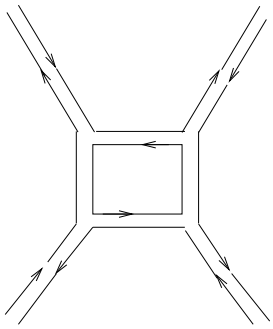

Figure 1-1. Double line notation

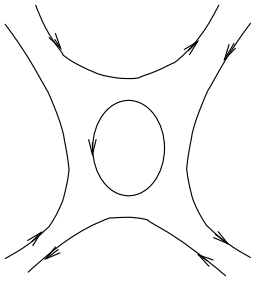

Figure 1-2. Open string scattering diagram

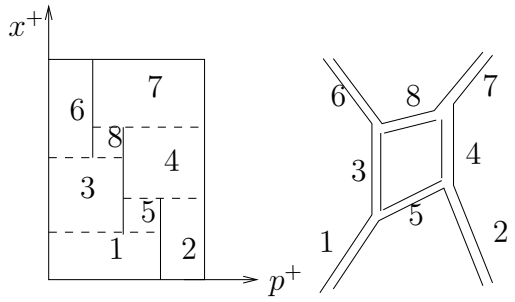

Figure 1-3. Light-cone parametrization

CHAPTER 2
COMPUTATION TECHNIQUES IN THE LIGHT CONE

2.1 Mini Introduction to Spinor Helicity Amplitude Method

This method exploits the covering group of $SO(3,1)$: $SL(2,C)$. Lorentz invariance will be represented as $SL(2,C)$ invariance. By dotting a momentum into the sigma matrices, we obtain a 2 by 2 matrix: $p_\mu \rightarrow p_\mu \sigma^\mu$. If p were light like, we will have $\det(p\cdot\sigma) = p^2 = 0$, so the matrix $p\cdot\sigma$ can be decomposed into a product of two spinors:

$$p\cdot\sigma^{\alpha\dot{\alpha}} = p^\alpha p^{\dot{\alpha}} \tag{2–1}$$

where we have used the same letter for both the momentum and its spinor. p^α ($p^{\dot{\alpha}}$) is the left (right) handed spinor that satisfies the massless Dirac equation. The notation using bracket is commonly used in the literature:

$$p^a \rightarrow |p\rangle; \qquad p_{\dot{a}} \rightarrow |p]; \qquad p_a \rightarrow \langle p|; \qquad p^{\dot{a}} \rightarrow [p| \tag{2–2}$$

Polarization vectors for the gauge particles are also cleverly chosen to minimize the computation [10, 21, 22]. The reader can refer to [11] for a review, and to [12] for some more simplifications and extensions to massive fields.

As an example, a left handed polarization vector ϵ_μ can be given by (up to a normalization factor) $\epsilon_{\dot{a}a} = \eta_{\dot{a}} p_a \Leftrightarrow |\eta\,]\langle p|$, or equivalently $\epsilon^{a\dot{a}} = p^a \eta^{\dot{a}} \Leftrightarrow |p\,\rangle[\eta|$. The handedness can be seen by remembering that γ^μ or σ^μ is the Clebsch-Gordon coefficient for the projection

$$\mathbf{1} \otimes \left(\frac{\mathbf{1}}{\mathbf{2}}\right)_L \rightarrow \left(\frac{\mathbf{1}}{\mathbf{2}}\right)_R \tag{2–3}$$

and that $|\,p\rangle$ is the spinor of a left handed fermion. We have $\epsilon\cdot\bar{\sigma}|\,p\rangle = |\eta\,]\langle p\,|p\,\rangle = 0$. This means that the photon must be left handed so the product of it with a left handed fermion will not have a right handed component.

Another way of seeing the same fact is by inspecting whether the field strength $F_{\mu\nu}$ constructed out of ϵ_μ is anti-selfdual (right handed) or self-dual (left handed).

$$F_{\mu\nu} = -i\,[p_{\dot{a}a}\eta_{\dot{b}}p_b - p_{\dot{b}b}\eta_{\dot{a}}p_a] = -i\left[p_a p_b p_{[\dot{a}}\eta_{\dot{b}]}\right] = -ip_a p_b \epsilon_{\dot{a}\dot{b}}[p\,|\eta\,]$$

The ϵ symbol in the spinor language is given by

$$\epsilon^{\mu\nu\rho\sigma} = \epsilon_{\dot{a}a}{}^{b\dot{b}}{}_{\dot{c}c}{}^{d\dot{d}} = 4i\left[\delta^{\dot{d}}_{\dot{a}}\,\delta^b_a\,\delta^{\dot{b}}_{\dot{c}}\,\delta^d_c - \delta^{\dot{b}}_{\dot{a}}\,\delta^b_c\,\delta^{\dot{d}}_{\dot{c}}\,\delta^d_a\right]$$

so

$$\frac{1}{2}\det g\,\epsilon^{\mu\nu\rho\sigma}F_{\rho\sigma} = i\epsilon^{\mu\nu\rho\sigma}p_\rho A_\sigma = -\left[0 - \epsilon_{\dot{a}\dot{b}}\,p_b p_a[p\,|\,\eta\,]\right] = iF^{\mu\nu} \tag{2–4}$$

hence $*F = iF$.

The reference spinor η can be chosen to our advantage. The most efficient way is to pick it to be a spinor of one of the momenta in the problem. As an illustration, consider the amplitude $\mathcal{M}(1,2,3,4,-,-,+,+)$. Pick

$$\epsilon_1 \sim |1\,\rangle[4|;\ \epsilon_2 \sim |2\,\rangle[4|;\ \epsilon_3 \sim |1\,\rangle[3|;\ \epsilon_4 \sim |1\,\rangle[4| \tag{2–5}$$

They have the property that only the pair ϵ_2 and ϵ_3 have non-vanishing inner product. These polarization vectors are not properly normalized yet, their normalization factors will be put back in at the last step.

Let us look at the t-channel exchange diagram:

$$\left[\epsilon_1\cdot\epsilon_4(p_4-p_1)^\delta + \epsilon_1^\delta(2p_1+p_4)\cdot\epsilon_4 + \epsilon_4^\delta(-2p_4-p_1)\cdot\epsilon_1\right]\frac{ig_{\delta\sigma}}{(p_1+p_4)^2}\left[...\right]^\sigma \tag{2–6}$$

I did not bother to write down the vertex on the right since the left vertex is already zero.

The four-point contact vertex is in fact zero too. Recall that the four-point vertex always involves two pairs of polarization vectors dotted into each other, while we only have one non-zero pair available.

Finally the s-channel exchange diagram:

$$\left[\underline{\epsilon_1\cdot\epsilon_2(p_1-p_2)^\delta}+\epsilon_2^\delta(2p_2+\underline{p_1})\cdot\epsilon_1+\epsilon_1^\delta(-2p_1-\underline{p_2})\cdot\epsilon_2\right]\times\frac{ig_{\delta\sigma}}{(p_1+p_2)^2}$$
$$\left[\underline{\epsilon_3\cdot\epsilon_4(p_3-p_4)^\sigma}+\epsilon_4^\sigma(2p_4+\underline{p_3})\cdot\epsilon_3+\epsilon_3^\sigma(-2p_3-\underline{p_4})\cdot\epsilon_4\right] \tag{2–7}$$

The underlined terms are all zero, and we are left with

$$-4\frac{i}{s}(\epsilon_2\cdot\epsilon_3)\cdot(p_2\cdot\epsilon_1)\cdot(p_3\cdot\epsilon_4)=-\frac{i}{2s}[43]\langle21\rangle[24]\langle21\rangle[34]\langle31\rangle \tag{2–8}$$

As the last step, we need to put in the normalization factors for the polarization vectors: $-[14][24]\langle31\rangle\langle41\rangle/4$, I get

$$-2i\frac{[34]^2\langle12\rangle^2}{st}=-2i\frac{\langle12\rangle^4}{\langle12\rangle\langle23\rangle\langle34\rangle\langle41\rangle} \tag{2–9}$$

The second presentation is holomorphic in the left handed spinors, which will turn out to be interesting later on.

As a slightly more non-trivial example, I shall compute the amplitude $\mathcal{M}(+,+,-,-,-)$ Fig.2-1.

I shall define the polarization vectors to be

$$\epsilon_1=\sqrt{2}\frac{|4]\langle1|}{[14]};\quad \epsilon_2=\sqrt{2}\frac{|4]\langle2|}{[24]}$$
$$\epsilon_3=\sqrt{2}\frac{|3]\langle1|}{\langle13\rangle};\quad \epsilon_4=\sqrt{2}\frac{|4]\langle1|}{\langle14\rangle};\quad \epsilon_5=\sqrt{2}\frac{|5]\langle1|}{\langle15\rangle} \tag{2–10}$$

Here I have used p_1 and p_4 as reference legs. A general observation is that a vertex that involves both legs that are used as reference vanishes, so diagrams 2,3 and 4 are zero. A closer look at the products between a pair of polarization vectors shows that all the diagrams involving four point vertices are zero. We are thus left with only three diagrams to compute.

I will start with some small building blocks according to Fig.2-2:

$$A^\mu = [54]\langle 41\rangle\epsilon_4^\mu - [45]\langle 51\rangle\epsilon_5^\mu \quad B^\mu = [35]\langle 51\rangle\epsilon_5^\mu - [53]\langle 31\rangle\epsilon_3^\mu$$
$$C^\mu = \frac{1}{2}[43]\langle 12\rangle(p_2-p_3)^\mu + [43]\langle 32\rangle\epsilon_3^\mu - [32]\langle 21\rangle\epsilon_2^\mu \quad D^\mu = [42]\langle 21\rangle\epsilon_2^\mu - [41]\langle 12\rangle\epsilon_1^\mu \tag{2–11}$$

With these building blocks, we can calculate further larger blocks Fig.2-3:

$$\begin{aligned} E^\nu &= A_\rho\epsilon_{1\mu}\left[g^{\mu\nu}(1-2-3)^\rho + g^{\nu\rho}(2+3-4-5)^\mu + g^{\rho\mu}(4+5-1)^\nu\right] \\ &= 0 + A^\nu[4|2+3|1\rangle + 0 = -A_\nu[4|5]\langle 5|1\rangle \end{aligned}$$

$$\begin{aligned} F^\nu &= A_\sigma\epsilon_{3\rho}\left[g^{\nu\rho}(1+2-3)^\sigma + g^{\rho\sigma}(3-4-5)^\nu + g^{\sigma\nu}(4+5-1-2)^\rho\right] \\ &= \epsilon_3^\nu\left[\frac{1}{2}[54]\langle 41\rangle[4|2-3|1\rangle - \frac{1}{2}[45]\langle 51\rangle[5|2-3|1\rangle\right] + A^\nu[3|-2|1\rangle \\ &= \epsilon_3^\nu\left[[54]\langle 41\rangle[42]\langle 21\rangle - [45]\langle 51\rangle[52]\langle 21\rangle\right] - A^\nu[3|2|1\rangle \\ &= \epsilon_3^\nu[54]\langle 21\rangle[23]\langle 31\rangle - A^\nu[32]\langle 21\rangle \end{aligned}$$

$$\begin{aligned} G^\nu &= B_\rho\epsilon_{4\sigma}\left[g^{\rho\sigma}(3+5-4)^\nu + g^{\sigma\nu}(4-1-2)^\rho + g^{\nu\rho}(1+2-3-5)^\sigma\right] \\ &= 0 + \epsilon_4^\nu\left[\frac{1}{2}[35]\langle 51\rangle[5|4-2|1\rangle - \frac{1}{2}[53]\langle 31\rangle[3|4-2|1\rangle\right] + \frac{1}{2}B^\nu[4|2-3-5|1\rangle \\ &= \epsilon_4^\nu\left[[35]\langle 51\rangle[54]\langle 41\rangle - [53]\langle 31\rangle[34]\langle 41\rangle\right] + B^\nu[4|2|1\rangle \\ &= \epsilon_4^\nu[35]\langle 41\rangle[42]\langle 21\rangle + B^\nu[42]\langle 21\rangle \end{aligned} \tag{2–12}$$

Finally

$$\begin{aligned}
E^\mu C_\mu &= -A_\mu[4|5]\langle 5|1\rangle\left[\frac{1}{2}[43]\langle 12\rangle(p_2-p_3)^\mu + [43]\langle 32\rangle\epsilon_3^\mu - [32]\langle 21\rangle\epsilon_2^\mu\right] \\
&= -\frac{1}{2}[4|5]\langle 5|1\rangle[43]\langle 12\rangle\left[[54]\langle 41\rangle[4|\frac{2-3}{2}|1\rangle - [45]\langle 51\rangle[5|\frac{2-3}{2}|1\rangle\right] \\
&\quad -0 - \frac{1}{2}[4|5]\langle 5|1\rangle[32]\langle 21\rangle[4|5]\langle 5|1\rangle[54]\langle 21\rangle \\
&= -\frac{1}{2}[4|5]\langle 5|1\rangle[43]\langle 12\rangle\left[[54]\langle 41\rangle[4|\frac{2-3}{2}|1\rangle - [45]\langle 51\rangle[5|\frac{2-3}{2}|1\rangle\right] \\
&= -\frac{1}{2}[4|5]\langle 5|1\rangle\langle 2|1\rangle^2[54]\Big[- [43][42]\langle 41\rangle - [43][52]\langle 51\rangle + [32][45]\langle 51\rangle\Big] \\
&= -\frac{1}{2}[45]^2\langle 21\rangle^3\langle 51\rangle[42][32] \qquad (2\text{–}13)
\end{aligned}$$

$$\begin{aligned}
F^\mu D_\mu &= \left[\epsilon_{3\mu}[54]\langle 21\rangle[23]\langle 31\rangle - A_\mu[32]\langle 21\rangle\right]\left[[42]\langle 21\rangle\epsilon_2^\mu - [41]\langle 12\rangle\epsilon_1^\mu\right] \\
&= \epsilon_2\cdot\epsilon_3[54][42]\langle 21\rangle^2[23]\langle 31\rangle - 0 + \epsilon_5\cdot\epsilon_2[45]\langle 51\rangle[32][42]\langle 21\rangle^2 + 0 \\
&= \frac{1}{2}[34]\langle 21\rangle[54][42]\langle 21\rangle^2[23]\langle 31\rangle + \frac{1}{2}[54]\langle 21\rangle[45]\langle 51\rangle[32][42]\langle 21\rangle^2 \\
&= \frac{1}{2}[54]\langle 21\rangle^4[42]^2[23] \qquad (2\text{–}14)
\end{aligned}$$

$$\begin{aligned}
G^\mu D_\mu &= \left[\epsilon_{4\nu}[35]\langle 41\rangle[42]\langle 21\rangle + B_\nu[42]\langle 21\rangle\right]\left[[42]\langle 21\rangle\epsilon_2^\mu - [41]\langle 12\rangle\epsilon_1^\mu\right] \\
&= 0 - 0 + [42]^2\langle 21\rangle^2\left[\epsilon_5\cdot\epsilon_2[35]\langle 51\rangle - \epsilon_3\cdot\epsilon_2[53]\langle 31\rangle\right] - 0 \\
&= \frac{1}{2}[42]^2\langle 21\rangle^2\left[[54]\langle 21\rangle[35]\langle 51\rangle - [34]\langle 21\rangle[53]\langle 31\rangle\right] \\
&= \frac{1}{2}[42]^3\langle 21\rangle^4[35] \qquad (2\text{–}15)
\end{aligned}$$

Assemble them together:

$$\begin{aligned}
&\frac{G\cdot D}{\langle 21\rangle[12]\langle 35\rangle[53]}+\frac{F\cdot D}{\langle 21\rangle[12]\langle 45\rangle[54]}+\frac{E\cdot C}{\langle 23\rangle[32]\langle 45\rangle[54]}\\
=\;& \langle 21\rangle^3[42]\frac{[42]^2\langle 54\rangle\langle 32\rangle-[42][23]\langle 53\rangle\langle 32\rangle+[45][12]\langle 51\rangle\langle 53\rangle}{2[12]\langle 53\rangle\langle 54\rangle\langle 32\rangle}\\
=\;& \langle 21\rangle^3[42]\frac{[21][41]\langle 51\rangle\langle 13\rangle}{2[12]\langle 53\rangle\langle 54\rangle\langle 32\rangle} \qquad (2\text{–}16)
\end{aligned}$$

After putting back the normalization factor:

$$(-i)^2\frac{\sqrt{2}^5}{[14][24]\langle 13\rangle\langle 14\rangle\langle 15\rangle} \qquad (2\text{–}17)$$

we get

$$-\frac{\sqrt{2}^5\langle 12\rangle^4}{2\langle 12\rangle\langle 23\rangle\langle 35\rangle\langle 54\rangle\langle 41\rangle} \qquad (2\text{–}18)$$

To go to large N_c, we simply multiply it by $(-ig_s\sqrt{N_c/2})^3$.

2.2 The Light Cone Setup

The light cone gauge Feynman rules are usually obtained by the lagrangian method, namely, we first set $A_- = 0$ and integrate out A^-. Then the Feynman rules can be read off from the lagrangian, which is a function only of A^1 and A^2.

Here, I combine the covariant vertex functions with the above spinor helicity method to obtain the Feynman rules in a more flexible way. But this will require us to fix $\eta^a = \eta^{\dot{a}} = [1,0]^T$.

The gluon propagator in light cone gauge is

$$\frac{-i(g^{\mu\nu}-\frac{g^{\mu+}k^\nu}{k^+}-\frac{g^{\nu+}k^\mu}{k^+})}{k^2+i\epsilon} \qquad (2\text{–}19)$$

Note the metric is $diag(1,-1,-1,-1)$ throughout the dissertation. The numerator can be factored into

$$(g^{\mu\nu} - \frac{g^{\mu+}k^{\nu}}{k^{+}} - \frac{g^{\nu+}k^{\mu}}{k^{+}}) = -(\epsilon^{\mu}_{\vee}\epsilon^{\nu}_{\wedge} + \epsilon^{\mu}_{\wedge}\epsilon^{\nu}_{\vee}) - \frac{g^{\mu+}g^{\nu+}}{k^{+2}}k^2 \tag{2–20}$$

Where $\epsilon_{\wedge,\vee}$ are light cone gauge polarization vectors given by

$$\begin{aligned}
\epsilon^{\mu}_{\vee} &= \frac{1}{\sqrt{2}}(\frac{k^1 - ik^2}{k^0 + k^3}, 1, -i, -\frac{k^1 - ik^2}{k^0 + k^3}) = \frac{1}{\sqrt{2}}(\frac{k^{\wedge}}{k^{+}}, 1, -i, -\frac{k^{\wedge}}{k^{+}}) \ ; \ \epsilon_{\wedge} = \epsilon^{*}_{\vee} \\
\epsilon_{\vee} &= -\sqrt{2}|\eta]\langle k| \ ; \ \epsilon_{\wedge} = -\sqrt{2}|k]\langle \eta|
\end{aligned} \tag{2–21}$$

They satisfy $\epsilon \cdot \epsilon^{*} = -1$ and $k \cdot \epsilon = 0$. These polarization vectors are defined both on-shell and off-shell. Note from now on, the definition of $|k]$, $|k\rangle$, $[k|$ and $\langle k|$ will be that of the appendix A, which is slightly different from the conventional ones.

The Feynman rules are obtained by dotting the polarization vectors into the covariant three or four point vertices.

The tri-gluon vertex Fig.2-4, for example, becomes

$$V_{ggg} = gf^{abc}(-\epsilon^{*}_{1\mu})(-\epsilon^{*}_{2\nu})(-\epsilon^{*}_{3\rho})[g^{\mu\nu}(p_1 - p_2)^{\rho} + g^{\nu\rho}(p_2 - p_3)^{\mu} + g^{\rho\mu}(p_3 - p_1)^{\nu}]$$

Setting ϵ_1, $\epsilon_2 = \epsilon_{\wedge}$, $\epsilon_3 = \epsilon_{\vee}$, the above becomes

$$gf^{abc}[(p_2 - p_3)^{+}\frac{p_1^{\wedge}}{p_1^{+}} - (p_2 - p_3)^{\wedge} + (p_3 - p_1)^{+}\frac{p_2^{\wedge}}{p_2^{+}} - (p_3 - p_1)^{\wedge}] = 2gf^{abc}\frac{(p_1 + p_2)^{+}}{p_1^{+}p_2^{+}}K^{\wedge}_{21} \tag{2–22}$$

where $K^{\mu}_{i,j} := (p_i^{+}p_j^{\mu} - p_j^{+}p_i^{\mu})$. They are related to spinor products according to

$$K^{\vee}_{i,j} = p_i^{+}p_j^{+}[p_i|p_j] = p_i^{+}p_j^{+}p_i^{\dot{a}}p_{j\dot{a}}$$

The spinor notation here is also different from the conventional one [20]. The reader can refer to the appendix for an explanation of the spinor notation.

The gluon propagator Eq.2–19 almost factorizes into the product of two polarisation vectors. While the third term on the rhs of Eq.2–20 will make an extra contribution to the four point vertex. For example, consider the t-channel diagram Fig.2-5, the first two terms of Eq.2–20 can be associated with the two tri-gluon vertices, the third term, which describes the mediation of A^-, gives

$$\epsilon^*_{1\mu}\epsilon^*_{4\sigma}V^{\sigma\mu\alpha}\frac{i}{(p_1+p_4)^2}\epsilon^*_{2\nu}\epsilon^*_{3\rho}V^{\nu\rho\beta}\frac{\delta^+_\alpha\delta^+_\beta(p_1+p_4)^2}{(p_1^++p_4^+)^2}=\frac{i\epsilon_1^*\cdot\epsilon_4^*(p_4^+-p_1^+)\epsilon_2^*\cdot\epsilon_3^*(p_2^+-p_3^+)}{(p_1^++p_4^+)^2} \quad (2\text{–}23)$$

What's happening here is that the explicit factor of k^2 in the third term of Eq.2–20 cancels the propagator, effectively making a four point contact vertex.

The fermion-gluon vertex Fig.2-6 is the usual $ig\,\gamma^\mu\,t^a$. We can set $\mu=\wedge$ or $\vee$ by dotting $-\epsilon^*_{\wedge,\vee}$, into μ.[1] Multiplying the spinors to the gamma matrix, we get (assuming now the fermion is left-handed)

$$\begin{aligned}
& ig(t^a)_{bc}\sqrt{2p_1^+p_2^+}(-\epsilon^{*\mu}_\wedge)\left[\begin{array}{cc} 0 & p_2^{\dot\alpha}\end{array}\right]\left|\begin{array}{cc} 0 & (\sigma_\mu)^{\alpha\dot\alpha} \\ (\bar\sigma_\mu)_{\dot\alpha\alpha} & 0\end{array}\right|\left[\begin{array}{c} p_1^\alpha \\ 0\end{array}\right] \\
= \;& -ig(t^a)_{bc}\sqrt{2p_1^+p_2^+}(-\sqrt{2})[p_2\,|\eta\rangle\langle q|p_1\rangle \\
= \;& -2ig(t^a)_{bc}\sqrt{p_1^+p_2^+}\left(\frac{q^\wedge}{q^+}-\frac{p_1^\wedge}{p_1^+}\right)=-2igt^a\frac{\sqrt{p_1^+p_2^+}}{q^+p_1^+}K^\wedge_{p_1,q}\to -2igt^a\frac{p_2^+}{q^+p_1^+}K^\wedge_{p_1,q} \quad (2\text{–}24)
\end{aligned}$$

In Eq.2–24, in order to avoid defining what is $\sqrt{p^+}$, I chose to associate p_2^+ instead of $\sqrt{p_1^+p_2^+}$ to a vertex. This won't cause any problem, since a fermion line either always closes, or end up as an external particle (then the phase of the root can be defined arbitrarily).

[1] Calling polarizations by $\vee$ or $\wedge$ is potentially confusing, especially if you are looking at the diagram up-side-down. So,sometimes it is clearer to associate $\wedge$ with 'in' and $\vee$ with 'out'.

The fermion propagator is given by $ip_\mu\gamma^\mu/(p^2+i\epsilon)$. We can decompose $p\cdot\gamma$ according to

$$\begin{aligned}
p\cdot\sigma &= \sqrt{2}\begin{bmatrix} p^- & -p^\wedge \\ -p^\vee & p^+ \end{bmatrix} = \sqrt{2}p^+\begin{bmatrix} -\frac{p^\wedge}{p^+} \\ 1 \end{bmatrix}\begin{bmatrix} -\frac{p^\vee}{p^+} & 1 \end{bmatrix} + \begin{bmatrix} \frac{p^2}{\sqrt{2}p^+} & 0 \\ 0 & 0 \end{bmatrix} \\
&= \sqrt{2}p^+|p\rangle[p| + \frac{p^2}{\sqrt{2}p^+}|\eta\rangle[\eta| \\
p\cdot\bar\sigma &= \sqrt{2}\begin{bmatrix} p^+ & p^\wedge \\ p^\vee & p^- \end{bmatrix} = \sqrt{2}p^+\begin{bmatrix} 1 \\ \frac{p^\vee}{p^+} \end{bmatrix}\begin{bmatrix} 1 & \frac{p^\wedge}{p^+} \end{bmatrix} + \begin{bmatrix} 0 & 0 \\ 0 & \frac{p^2}{\sqrt{2}p^+} \end{bmatrix} \\
&= \sqrt{2}p^+|p]\langle p| + \frac{p^2}{\sqrt{2}p^+}|\eta]\langle\eta|
\end{aligned} \tag{2–25}$$

Since the fermion propagator almost factorizes too, it is also possible to contract a pair of vertices here. For example, the second term of Eq.2–25 will contribute to Fig.2-7 according to

$$\begin{aligned}
&-g^2(t^d)_{ce}(t^a)_{eb}\sqrt{2p_1^+p_2^+}\,[p_2|(-\epsilon_3^*\cdot\bar\sigma)\frac{i(p_1+p_4)\cdot\sigma}{(p_1+p_4)^2}(-\epsilon_4^*\cdot\bar\sigma)|p_1\rangle \\
&\to -g^2(t^d)_{ce}(t^a)_{eb}\sqrt{2p_1^+p_2^+}\,[p_2\,|(\sqrt{2}|\eta]\langle p_3\,|)\cdot\frac{i}{(p_1+p_4)^2} \\
&\cdot(\frac{(p_1+p_4)^2}{\sqrt{2}(p_1^++p_4^+)}|\eta\rangle[\eta\,|)\cdot(\sqrt{2}|p_4]\langle\eta\,|)\,|p_1\,\rangle \\
&= -2ig^2(t^d)_{ce}(t^a)_{eb}\frac{\sqrt{p_1^+p_2^+}}{p_1^++p_4^+} \;\to\; -2ig^2(t^d)_{ce}(t^a)_{eb}\frac{p_2^+}{p_1^++p_4^+}
\end{aligned} \tag{2–26}$$

The scalar Feynman rules have no suspense in them at all, and can be read off from any field theory book. The Feynman rules that pertain to our calculation will be summarized in the appendix. The main property of the Feynman rules above is the absence of p^-.

2.3 Brief Description of the Calculational Procedure

In the Fig.2-8, the k's and q are the dual momenta. They are related to the real momenta coming into the three legs according to $p_1 = k_1 - k_2$, $p_2 = k_4 - k_1$ and $p_3 = k_2 - k_4$. The unregulated integrands have a symmetry under $k_i \to k_i + a$, which

would ensure that each diagram depends only on the real momenta. But here, as in [13, 14], we use a regulator $\exp(-2\delta q^{\wedge} q^{\vee})$ that breaks this symmetry. Hence, a regulated amplitude can depend on the individual dual momenta. This seemingly unwieldy regulator is designed for the world sheet description, but the result doesn't differ too much when a cut off regulator is used.

The calculation roughly goes as follows,

1. Exponentiate all propagators according to

$$\frac{i}{p^2 + i\epsilon} = \int_0^\infty dT\, e^{iTp^2}$$

For the schematic diagram Fig.2-8. We have

$$\begin{aligned} \Gamma &= \int \frac{d^4q}{(2\pi)^4} \frac{i}{(q-k_2)^2} \frac{i}{(q-k_1)^2} \frac{i}{(q-k_4)^2} \\ &= \int \frac{d^4q}{(2\pi)^4} d^3T_i \exp\left\{ i \sum T_i (q-k_i)^2 \right\} \end{aligned}$$

2. Integrate out q^-, leaving a delta function relating q^+ to the Feynman parameters(this step requires the absence of q^- in all Feynman rules).

$$\Gamma = \int \frac{dq^+ d^2q_\perp}{(2\pi)^3} \frac{1}{2} d^3T_i \delta(\sum T_i k_i^+ - \sum T_i q^+) \exp\left\{ i \sum T_i (q-k_i)^2 \right\}$$

3. Integrate q^1, q^2 using $\exp[-\delta q_\perp^2]$ as a damping factor.

$$\Gamma = \int \frac{dq^+}{16\pi^2} dx_i \delta(\sum x_i - 1) \delta(\sum x_i k_i^+ - q^+) \frac{1}{x_2 x_4 (k_2 - k_4)^2}$$

where $x_i := T_i / \sum T_i$.

Here is the rub: we cannot simply integrate over x_2,x_1 and x_4, because the prefactor of this diagram will have up to second order poles at $q^+ = k_i^+$. In order to show the

cancellation of these poles (gauge artificial divergences), we proceed as follows: first eliminate one Feynman parameter in favour of q^+:

$$k_2^+ < q^+ < k_1^+ : \; x_1 = \frac{x(q^+ - k_2^+)}{k_1^+ - k_2^+}, \;\; x_4 = \frac{(1-x)(q^+ - k_2^+)}{k_4^+ - k_2^+}, \;\; x_2 = 1 - x_1 - x_4, \;\; x \in [0,1]$$

$$k_1^+ < q^+ < k_4^+ : \; x_1 = \frac{(1-x)(q^+ - k_4^+)}{k_1^+ - k_4^+}, \;\; x_2 = \frac{x(q^+ - k_4^+)}{k_2^+ - k_4^+}, \;\; x_4 = 1 - x_1 - x_2, \;\; x \in [0,1]$$

Now $dx_2 dx_1 dx_4 \delta(\sum x_i - 1)\delta(\sum x_i k_i^+ - q^+) = dq^+ dx J$. After integrating out x, we are left with a function of q^+ which is defined differently in different regions: $k_2^+ < q^+ < k_1^+$ and $k_1^+ < q^+ < k_4^+$. All these can be visualized very clearly when we represent a Feynman diagram on the light cone world sheet. The details can be found in [13, 14].

Our observation is that, in each region, all poles cancel.[2] Hence we can perform the final q^+ integral and obtain the results.

To summarize the computation procedure, *perform the q^+ integral last.*

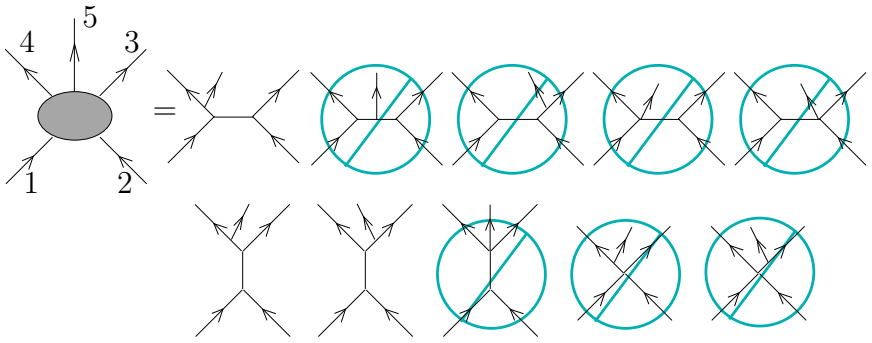

Figure 2-1. Five-point amplitude

[2] in the case helicity conserving amplitude, all poles cancel up to infrared terms, but since infrared divergence is always proportional to a tree, they are easy to recognize and deal with.

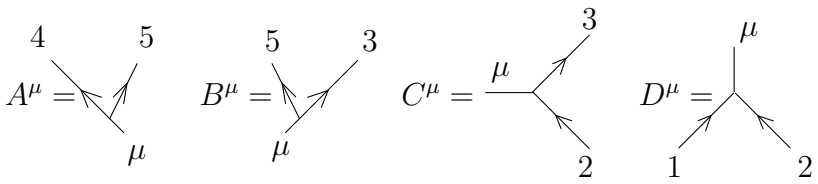

Figure 2-2. Some building blocks that can be computed separately

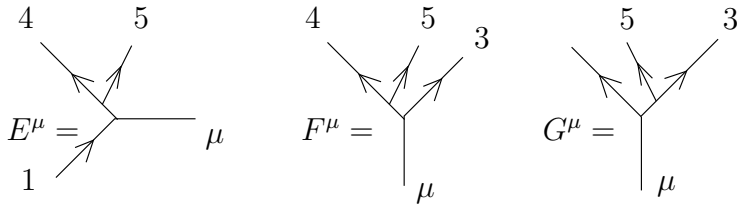

Figure 2-3. Second level building blocks

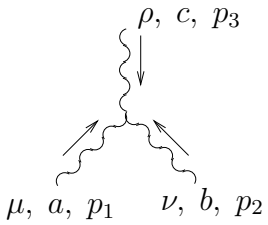

Figure 2-4. Tri-gluon vertex

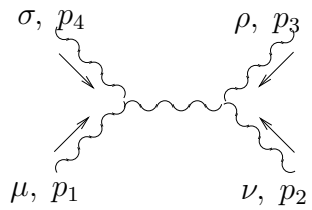

Figure 2-5. Propagator in the t-channel is contracted

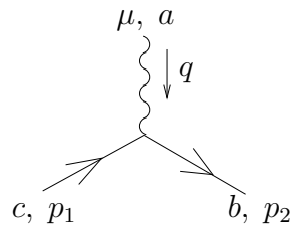

Figure 2-6. Fermion-gluon vertex

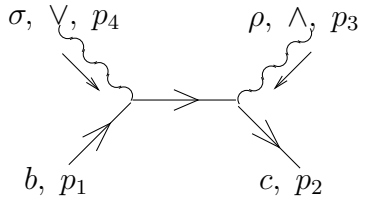

Figure 2-7. Fermion propagator contracted

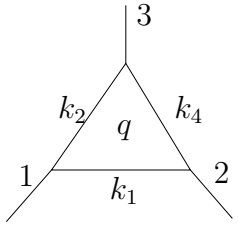

Figure 2-8. Here we assume only $(k_2 - k_4)^2 \neq 0$, and $k_4^+ > k_1^+ > k_2^+$

CHAPTER 3
BOX REDUCTION

This chapter contains a lot of technical details, the reader may skip it for first reading.

Our general procedure for evaluating box diagrams is

1. Evaluate a box diagram that is free of artificial, collinear and infrared divergences using text book method (combining denominator with Feynman's trick, shift the momentum, perform momentum and Feynman parameter integrals, etc).
2. Evaluate a box that contains collinear or infrared divergence but is free of artificial divergence by subtracting those collinear or infrared divergences in the form of triangle diagrams, and then use method 1.
3. A box that has artificial divergences has to be reduced to triangle diagrams.

In the next section, I will describe how to achieve 2 and 3. The dual momenta assignment given by Fig.3-1 will be used through out all the calculations.

3.1 Box with a Helicity Violating Sub-diagram

The Feynman rules for the gluon, scalar and fermion in the light cone gauge are very similar. Any three point vertex will have the following form: $\mathcal{R}(k_i^+)K_{ij}^{\wedge,\vee}$, where $\mathcal{R}(k^+)$ is a rational function of the + component of external momenta and $K_{ij}^{\wedge,\vee} = (p_i^+ p_j^{\wedge,\vee} - p_j^+ p_i^{\wedge,\vee})$ is introduced in the appendix. This allows us to write the numerator of any box diagram as

$$\mathcal{R}(k^+)K_{ij}^{\wedge,\vee}K_{kl}^{\wedge,\vee}K_{mn}^{\wedge,\vee}K_{op}^{\wedge,\vee} \tag{3–1}$$

We can also label a box by the helicity of the four corners, regardless of the details of the boxes. For example the following Fig.3-2 will be abbreviated as $\wedge\wedge\vee\vee$ box.

$\mathcal{R}(k^+)$ in general will contain poles of k^+. These poles are usually interpreted using Cauchy principle value or some other prescriptions. We chose to show directly that these poles are all fake, namely, when we compute a physical quantity, these poles will

be cancelled. To show this would entail us to express the amplitude as a holomorphic functions of k^+ and analyze the poles one by one. But the box integrand in general will have a denominator that is quadratic in the Feynman parameters and k^+. Integrating it by force will introduce logarithm and di-logarithms with various arguments. Although we know of certain relations between (combinations of) di-logarithms and double logarithms, the application of these relations is hard to automate.

Fortunately, for the case at hand, all box diagrams can be reduced to triangle-like integrands, whose manipulations are considerably easier. Here I describe the box reduction technique in detail.

The lower half of the box Fig.3-2 is the 't channel' of $(++-+)$ scattering process, which is zero. So we can replace this 't channel' with minus the 's channel', which will result in a triangle diagram. But since the amplitude is only truly zero on-shell, while the two internal lines are certainly off-shell, I will get some more terms that are proportional to the virtuality of the two internal lines (p_5^2 and p_6^2). Schematically, I have Fig.3-3:

More concretely, Fig.3-3 is written as

$$\begin{aligned} & \frac{1}{(p_1+p_6)^2} K_{16}^{\wedge} K_{52}^{\wedge} \\ = & -\frac{1}{(p_1+p_2)^2} K_{21}^{\wedge} K_{65}^{\wedge} + \frac{p_6^2}{(p_1+p_6)^2(p_1+p_2)^2} K_{52}^{\wedge} K_{21}^{\wedge} + \frac{p_5^2}{(p_1+p_6)^2(p_1+p_2)^2} K_{21}^{\wedge} K_{16}^{\wedge} \end{aligned} \tag{3–2}$$

Clearly, in this case, the box is reduced into three triangle-like diagrams.

Here I list its contribution: First, define some functions that occur ubiquitously:

$$
\begin{aligned}
H_s: &= \frac{(k_4^+ - q^+)(-k_2^+ + q^+)s\delta e^\gamma}{(k_2^+ - k_4^+)^2},\ k_2^+ < q^+ < k_4^+ \\
H_t: &= \frac{(k_3^+ - q^+)(q^+ - k_1^+)t\delta e^\gamma}{(-k_1^+ + k_3^+)^2},\ k_3^+ < q^+ < k_1^+ \\
H_d: &= \frac{(k_3^+ - q^+)(-k_2^+ + q^+)s\delta e^\gamma}{(k_3^+ - k_2^+)(k_4^+ - k_2^+)},\ k_2^+ < q^+ < k_3^+ \\
&= \frac{(q^+ - k_3^+)(k_4^+ - q^+)s\delta e^\gamma}{(k_4^+ - k_2^+)(k_4^+ - k_3^+)},\ k_3^+ < q^+ < k_4^+ \\
\\
H_l: &= \frac{(-k_4^+ + q^+)(k_3^+ - q^+)t\delta e^\gamma}{(k_3^+ - k_4^+)(-k_1^+ + k_3^+)},\ k_3^+ < q^+ < k_1^+ \\
&= \frac{(-k_4^+ + q^+)^2 t\delta e^\gamma}{(k_4^+ - k_1^+)(k_4^+ - k_3^+)},\ k_1^+ < q^+ < k_4^+ \\
H_u: &= \frac{(k_1^+ - q^+)(q^+ - k_2^+)s\delta e^\gamma}{(k_1^+ - k_2^+)(k_4^+ - k_2^+)},\ k_2^+ < q^+ < k_1^+ \\
&= \frac{(q^+ - k_1^+)(-k_4^+ + q^+)s\delta e^\gamma}{(k_4^+ - k_1^+)(k_2^+ - k_4^+)},\ k_1^+ < q^+ < k_4^+ \\
H_r: &= \frac{(-k_2^+ + q^+)^2 t\delta e^\gamma}{(k_1^+ - k_2^+)(k_3^+ - k_2^+)},\ k_2^+ < q^+ < k_3^+ \\
&= \frac{(k_2^+ - q^+)(q^+ - k_1^+)t\delta e^\gamma}{(-k_1^+ + k_2^+)(-k_1^+ + k_3^+)},\ k_3^+ < q^+ < k_1^+
\end{aligned}
\tag{3–3}
$$

Next, I list the results for the two model boxes $\vee\wedge\wedge\vee$ and $\wedge\vee\vee\wedge$.

- $\vee\wedge\wedge\vee$:

$$
\begin{aligned}
&\frac{i}{8\pi^2}\mathrm{Tr}\left[t^a t^b t^c t^d\right] \times \\
&k_2^+ < q^+ < k_3^+ : \\
\\
+\ & 1/4\frac{(q^+ - k_4^+)(q^+ - k_2^+)}{(k_2^+ - k_4^+)s}K_{43}^{\wedge}K_{21}^{\vee}\log(H_s) + 1/8\frac{(q^+ - k_2^+)^2(k_1^+ - k_4^+)(k_3^+ - k_4^+)}{k_2^+ - k_4^+}\log(H_r) \\
-\ & 1/4\frac{(q^+ - k_4^+)(q^+ - k_2^+)}{(k_2^+ - k_4^+)s}K_{43}^{\wedge}K_{21}^{\vee}\log(H_r)
\end{aligned}
$$

$k_3^+ < q^+ < k_1^+$:

$$
\begin{aligned}
+ \quad & 1/4\frac{(q^+ - k_4^+)(q^+ - k_2^+)}{(k_2^+ - k_4^+)s} K_{43}^{\wedge} K_{21}^{\vee} \log(H_s) \\
+ \quad & 1/8\frac{(k_3^+ - k_4^+)(k_2^+ - k_1^+)}{(k_3^+ - k_1^+)(k_2^+ - k_4^+)} \Big((-k_3^+ k_2^+ + k_4^+ k_3^+ - k_4^+ k_2^+ + 2q^+ k_2^+ - {q^+}^2) k_1^+ \\
+ \quad & k_3^+ k_4^+ k_2^+ + {q^+}^2 k_3^+ - 2q^+ k_4^+ k_3^+ - {q^+}^2 k_2^+ + {q^+}^2 k_4^+ \Big) \log(H_t) \\
+ \quad & 1/4\frac{(q^+ - k_4^+)(q^+ - k_2^+)}{(k_2^+ - k_4^+)s} K_{43}^{\wedge} K_{21}^{\vee} \log(H_t) - 1/8\frac{(q^+ - k_4^+)^2 (k_2^+ - k_1^+)(-k_2^+ + k_3^+)}{k_2^+ - k_4^+} \log(H_l) \\
- \quad & 1/4\frac{(q^+ - k_4^+)(q^+ - k_2^+)}{(k_2^+ - k_4^+)s} K_{43}^{\wedge} K_{21}^{\vee} \log(H_l) + 1/8\frac{(q^+ - k_2^+)^2 (k_1^+ - k_4^+)(k_3^+ - k_4^+)}{k_2^+ - k_4^+} \log(H_r) \\
- \quad & 1/4\frac{(q^+ - k_4^+)(q^+ - k_2^+)}{(k_2^+ - k_4^+)s} K_{43}^{\wedge} K_{21}^{\vee} \log(H_r)
\end{aligned}
$$

$k_1^+ < q^+ < k_4^+$:

$$
\begin{aligned}
+ \quad & 1/4\frac{(q^+ - k_4^+)(q^+ - k_2^+)}{(k_2^+ - k_4^+)s} K_{43}^{\wedge} K_{21}^{\vee} \log(H_s) - 1/8\frac{(q^+ - k_4^+)^2 (k_2^+ - k_1^+)(k_3^+ - k_2^+)}{k_2^+ - k_4^+} \log(H_l) \\
- \quad & 1/4\frac{(q^+ - k_4^+)(q^+ - k_2^+)}{(k_2^+ - k_4^+)s} K_{43}^{\wedge} K_{21}^{\vee} \log(H_l)
\end{aligned}
$$

Now assume that its coefficient is $C + A/(q^+ - k_4^+)^2 - 1/(q^+ - k_4^+)^1$, what to do next is to combine this with the coefficients of the $\log H$ terms, then extract the polynomial part through partial fraction and perform the integrals to get its contribution.

$$
\begin{aligned}
- \quad & 1/36 \cdot (k_4^+ - k_3^+)(k_2^+ - k_3^+)(k_1^+ - k_4^+)(k_1^+ - k_2^+)C + 1/8 \cdot \frac{k_1^+ - k_2^+ - k_4^+ + k_3^+}{s} K_{43}^{\wedge} K_{21}^{\vee} \\
- \quad & 1/24 \cdot \frac{({k_1^+}^2 + {k_3^+}^2 - k_1^+ k_2^+ - k_4^+ k_1^+ - k_3^+ k_2^+ - k_4^+ k_3^+ + 2k_4^+ k_2^+)C}{s} K_{43}^{\wedge} K_{21}^{\vee} \\
+ \quad & 1/8 \log(s) \cdot \frac{-k_4^+ + k_2^+ + 2A}{s} K_{43}^{\wedge} K_{21}^{\vee} - 1/24 \log(s) \cdot \frac{(k_2^+ - k_4^+)^2 C}{s} K_{43}^{\wedge} K_{21}^{\vee} \\
+ \quad & 1/24 \log(t) \cdot (k_4^+ - k_3^+)(k_2^+ - k_3^+)(k_1^+ - k_4^+)(k_1^+ - k_2^+)C \\
- \quad & 1/8 \log(t) \cdot \frac{-k_4^+ + k_2^+ + 2A}{s} K_{43}^{\wedge} K_{21}^{\vee} + 1/24 \log(t) \cdot \frac{(k_2^+ - k_4^+)^2 C}{s} K_{43}^{\wedge} K_{21}^{\vee}
\end{aligned}
\tag{3–4}
$$

If its coefficient were $C + A/(q^+ - k_4^+)^2 - 1/(q^+ - k_4^+)^1$, then the result can be obtained from the above by replacing $k_2^+ \leftrightarrow -k_4^+$, $k_1^+ \, (k_3^+) \leftrightarrow -k_1^+ \, (-k_3^+)$.

What is not included in Eq.3–4 is of the form:

$$\left[\frac{...}{(q-k_i)^2} + \frac{...}{q-k_i}\right] \log H \tag{3–5}$$

where ... only depends on the external momenta. The second order poles will have to cancel eventually, the first order pole always combines to become proportional to a tree amplitude with a universal structure.

- $\wedge \vee \vee \wedge$

  $k_2^+ < q^+ < k_3^+$:

$$\begin{aligned}
- \quad & 1/8 \frac{(q^+ - k_4^+)^2(-k_1^+ + k_2^+)(k_3^+ - k_2^+)}{k_2^+ - k_4^+} \log(H_s) \\
+ \quad & 1/8 \frac{(q^+ - k_3^+)^2(k_1^+ - k_4^+)(-k_1^+ + k_2^+)}{k_3^+ - k_1^+} \log(H_d) \\
- \quad & 1/4 \frac{(-k_1^+ + q^+)(q^+ - k_3^+)}{(k_3^+ - k_1^+)(-t)} K_{14}^{\wedge} K_{32}^{\vee} \log(H_d) \\
+ \quad & 1/8 \frac{(-k_1^+ + q^+)^2(k_3^+ - k_4^+)(k_3^+ - k_2^+)}{k_3^+ - k_1^+} \log(H_u) \\
+ \quad & 1/4 \frac{(-k_1^+ + q^+)(q^+ - k_3^+)}{(k_3^+ - k_1^+)(-t)} K_{14}^{\wedge} K_{32}^{\vee} \log(H_u)
\end{aligned}$$

  $k_3^+ < q^+ < k_1^+$:

$$
\begin{aligned}
- \quad & 1/8\frac{(k_3^+-k_4^+)(k_2^+-k_1^+)}{(k_2^+-k_4^+)(k_3^+-k_1^+)}\Big((-k_3^+k_2^+ + 2q^+k_2^+ - k_4^+k_2^+ + k_3^+k_4^+ - {q^+}^2)k_1^+ \\
+ \quad & k_3^+k_4^+k_2^+ + k_3^+{q^+}^2 - 2k_3^+q^+k_4^+ + {q^+}^2k_4^+ - {q^+}^2k_2^+\Big)\log(H_s) \\
- \quad & 1/4\frac{(-k_1^+ + q^+)(q^+ - k_3^+)}{(k_3^+ - k_1^+)(-t)}K_{14}^{\wedge}K_{32}^{\vee}\log(H_s) - 1/4\frac{(-k_1^+ + q^+)(q^+ - k_3^+)}{(k_3^+ - k_1^+)(-t)}K_{14}^{\wedge}K_{32}^{\vee}\log(H_t) \\
- \quad & 1/8\frac{(q^+ - k_3^+)^2(k_1^+ - k_4^+)(k_2^+ - k_1^+)}{k_3^+ - k_1^+}\log(H_d) + 1/4\frac{(-k_1^+ + q^+)(q^+ - k_3^+)}{(k_3^+ - k_1^+)(-t)}K_{14}^{\wedge}K_{32}^{\vee}\log(H_d) \\
+ \quad & 1/8\frac{(-k_1^+ + q^+)^2(k_3^+ - k_4^+)(k_3^+ - k_2^+)}{k_3^+ - k_1^+}\log(H_u) \\
+ \quad & 1/4\frac{(-k_1^+ + q^+)(q^+ - k_3^+)}{(k_3^+ - k_1^+)(-t)}K_{14}^{\wedge}K_{32}^{\vee}\log(H_u)
\end{aligned}
$$

$k_1^+ < q^+ < k_4^+$:

$$
\begin{aligned}
+ \quad & 1/8\frac{(q^+ - k_2^+)^2(k_1^+ - k_4^+)(k_3^+ - k_4^+)}{k_2^+ - k_4^+}\log(H_s) \\
- \quad & 1/8\frac{(-k_3^+ + q^+)^2(k_1^+ - k_4^+)(k_2^+ - k_1^+)}{k_3^+ - k_1^+}\log(H_d) \\
+ \quad & 1/4\frac{(-k_3^+ + q^+)(-k_1^+ + q^+)}{(k_3^+ - k_1^+)(-t)}K_{14}^{\wedge}K_{32}^{\vee}\log(H_d) \\
- \quad & 1/8\frac{(-k_1^+ + q^+)^2(k_3^+ - k_4^+)(k_3^+ - k_2^+)}{k_3^+ - k_1^+}\log(H_u) \\
- \quad & 1/4\frac{(-k_3^+ + q^+)(-k_1^+ + q^+)}{(k_3^+ - k_1^+)(-t)}K_{14}^{\wedge}K_{32}^{\vee}\log(H_u)
\end{aligned}
$$

Now assume that its coefficient is $C + A/(q^+ - k_1^+)^2 - 1/(q^+ - k_1^+)^1$, its contribution would be

$$
\begin{aligned}
- \quad & 1/36 \cdot (k_4^+ - k_3^+)(k_2^+ - k_3^+)(k_1^+ - k_4^+)(k_1^+ - k_2^+)C + 1/8 \cdot \frac{-k_4^+ + k_3^+ + k_1^+ - k_2^+}{(-t)} K_{14}^{\wedge} K_{32}^{\vee} \\
- \quad & 1/24 \cdot \frac{(k_2^+ k_1^+ - 2k_3^+ k_1^+ + k_4^+ k_3^+ + k_1^+ k_4^+ + k_2^+ k_3^+ - k_4^{+2} - k_2^{+2})C}{(-t)} K_{14}^{\wedge} K_{32}^{\vee} \\
+ \quad & 1/24 \log(s) \cdot (k_4^+ - k_3^+)(k_2^+ - k_3^+)(k_1^+ - k_4^+)(k_1^+ - k_2^+)C \\
+ \quad & 1/8 \log(s) \cdot \frac{-k_1^+ + 2A + k_3^+}{(-t)} K_{14}^{\wedge} K_{32}^{\vee} - 1/24 \log(s) \cdot \frac{(k_3^+ - k_1^+)^2 C}{(-t)} K_{14}^{\wedge} K_{32}^{\vee} \\
- \quad & 1/8 \log(t) \cdot \frac{-k_1^+ + 2A + k_3^+}{(-t)} K_{14}^{\wedge} K_{32}^{\vee} + 1/24 \log(t) \cdot \frac{(k_3^+ - k_1^+)^2 C}{(-t)} K_{14}^{\wedge} K_{32}^{\vee}
\end{aligned} \tag{3–6}
$$

Just as in Eq.3–4, the pole terms are dropped here.

3.2 Box without a Helicity Violating Sub-diagram

But of course, not all boxes are going to have a helicity violating subtree, I now turn to a second, much more complicated case Fig.3-4.

Assuming this box diagram can be written as

$$
\left[\frac{A}{(q^+ - k_1^+)^2} + \frac{B}{(q^+ - k_1^+)} \right] K_{16}^{\vee} K_{52}^{\wedge} K_{3,-5}^{\vee} K_{-6,4}^{\wedge} \tag{3–7}
$$

Here I have used the notation of dual momenta to make the formalism more symmetric looking. Write

$$
\begin{aligned}
& \left[\frac{A}{(q^+-k_1^+)^2}+\frac{B}{(q^+-k_1^+)}\right]K_{16}^{\vee}K_{52}^{\wedge} \\
= & \frac{A}{(q^+-k_1^+)^2}(K_{16}^{\vee}K_{52}^{\wedge}+K_{16}^{\wedge}K_{52}^{\vee}-K_{16}^{\wedge}K_{52}^{\vee})+\frac{B}{(q^+-k_1^+)}(K_{16}^{\vee}K_{52}^{\wedge}-K_{16}^{\wedge}K_{52}^{\vee}+K_{16}^{\wedge}K_{52}^{\vee}) \\
= & \frac{A}{(q^+-k_1^+)^2}(K_{16}^{\vee}K_{52}^{\wedge}+c.c)+\frac{B}{(q^+-k_1^+)}(K_{16}^{\vee}K_{52}^{\wedge}-c.c) \\
- & (\frac{A}{(q^+-k_1^+)^2}-\frac{B}{(q^+-k_1^+)})K_{16}^{\wedge}K_{52}^{\vee} \\
= & \frac{A}{(q^+-k_1^+)^2}\frac{1}{2}(k_1^+-q^+)(-k_1^++q^+)s \\
+ & \frac{A}{(q^+-k_1^+)^2}\frac{1}{2}\left[(k_4^+-k_1^+)(k_2^+-q^+)+(k_1^+-k_2^+)(q^+-k_4^+)\right](q-k_1)^2 \\
+ & \frac{A}{(q^+-k_1^+)^2}\frac{1}{2}(-k_1^++k_2^+)(-k_1^++q^+)(q-k_4)^2 \\
+ & \frac{A}{(q^+-k_1^+)^2}\frac{1}{2}(-k_4^++k_1^+)(k_1^+-q^+)(q-k_2)^2 \\
+ & \frac{B}{(q^+-k_1^+)}(K_{21}^{\vee}K_{65}^{\wedge}-c.c)\frac{(q^+-k_1^+)}{(k_4^+-k_2^+)} \\
- & (\frac{A}{(q^+-k_1^+)^2}-\frac{B}{(q^+-k_1^+)})K_{16}^{\wedge}K_{52}^{\vee}
\end{aligned}
\tag{3–8}
$$

Notice that the first four terms in Eq.3–8 contain covariant products of momenta: s, $(q-k_1)^2$, $(q-k_4)^2$ $(q-k_2)^2$. The coefficient of s is simply $-sA/2$ (the annoying $1/(q^+-k_1^+)^2$ has disappeared, the fifth term also has this property). Terms like $(q-k_i)^2$ will simply cancel one of the four propagators, effectively making a triangle-like terms.

Now Let us look at the sixth term of Eq.3–8. Putting back the factor of $K_{3,-5}^{\vee}K_{-6,4}^{\wedge}$ gives $[A/(q^+-k_1^+)^2-B/(q^+-k_1^+)]K_{16}^{\wedge}K_{52}^{\vee}K_{3,-5}^{\vee}K_{-6,4}^{\wedge}$. Now that two $\wedge$'s (or $\vee$) are next to each other, this term is in fact nothing but the previous model diagram.

In summary, the evaluation of the second, fifth and sixth terms of Eq.3–8 goes through without further twist. However, the first(hence forth called half scalar box), third and fourth term have collinear divergence individually (on top of the infrared divergence), some more manipulations are needed.

Subtraction of Collinear Divergence: A collinear divergence in a virtual process happens when the momenta flowing through two internal propagators connected to a common massless external leg become parallel. For a box diagram, there can be a collinear divergence at each massless corner. When only transverse components propagates in the loop, the vertex function will vanish due to helicity conservation. So, a bona fide box in light cone gauge will have no collinear problem. However, in the manipulations of Section 3.2, we have tampered with the vertex structures of the lower sub-tree, so there will be collinear divergences in some of the resulting pieces. But they will cancel when all the pieces are collected.

The collinear divergence in a box diagram can be located into two triangle-like diagrams. This process is rather like doing a partial fraction. Consider

$$K^{\vee}_{3,-5}\cdot\ K^{\wedge}_{-6,4}\frac{i}{(q-k_1)^2}\frac{i}{(q-k_4)^2}\frac{i}{(q-k_3)^2}\frac{i}{(q-k_2)^2} \tag{3–9}$$

Take limit $q \to k_4$ (so the right propagator is soft). Eq.3–9 becomes

$$K^{\vee}_{3,-5}\cdot\ K^{\wedge}_{4,3}\frac{i}{(q-k_1)^2}\frac{i}{(q-k_4)^2}\frac{i}{(q-k_3)^2}\frac{i}{s} \tag{3–10}$$

Take limit $q \to k_1$ (so the bottom propagator is soft). Eq.3–9 becomes

$$K^{\vee}_{3,-5}\cdot\ K^{\wedge}_{1,4}\frac{i}{(q-k_1)^2}\frac{i}{(q-k_4)^2}\frac{i}{t}\frac{i}{(q-k_2)^2} \tag{3–11}$$

Naturally, if these two 'poles' are subtracted from Eq.3–9, we should have a term free of collinear divergence, which will be demonstrated next.

According to Chapter 2, the Schwinger representation of Eq.3–9 is (with H given by $x_1x_3t + x_2x_4s + \mu^2$, where μ is a small mass used here to regulate temporarily the possible collinear divergences)

$$
\begin{aligned}
&\int \frac{T^3 dT \delta(\Sigma x_i - 1) d^4 x_i}{2T(2\pi)^3} \exp\left(-iTq_\perp^2 + iTH\right) \\
&\left[(k_4^+ - k_3^+)q^\vee + x_2 K_{43}^\vee + x_1 K_{32}^\vee\right]\left[(k_3^+ - k_2^+)q^\wedge + x_4 K_{43}^\wedge + x_1 K_{14}^\wedge\right] \\
= &\int \frac{T^3 dT \delta(\Sigma x_i - 1) d^4 x_i}{2T(2\pi)^3} \exp\left(-iTq_\perp^2 + iTH\right) \\
&\left[\frac{1}{2}(k_4^+ - k_3^+)(k_3^+ - k_2^+)q_\perp^2 + x_2 x_4 K_{43}^\vee K_{43}^\wedge + x_1 x_4 K_{32}^\vee K_{43}^\wedge + x_2 x_1 K_{43}^\vee K_{14}^\wedge + x_1^2 K_{32}^\vee K_{14}^\wedge\right] \\
= &\int \frac{T^3 dT \delta(\Sigma x_i - 1) d^4 x_i}{16\pi^2 T} \exp iTH \\
&\left[\frac{1}{2}\frac{(k_4^+ - k_3^+)(k_3^+ - k_2^+)}{(iT)^2} + \frac{x_2 x_4}{iT} K_{43}^\vee K_{43}^\wedge + \frac{x_1 x_4}{iT} K_{32}^\vee K_{43}^\wedge + \frac{x_2 x_1}{iT} K_{43}^\vee K_{14}^\wedge + \frac{x_1^2}{iT} K_{32}^\vee K_{14}^\wedge\right]
\end{aligned}
$$

Integrate over T:

$$
\begin{aligned}
&\int \frac{1}{8\pi^2}\delta(\Sigma x_i - 1) dx_i \\
&[-\frac{1}{4H}(k_4^+ - k_3^+)(k_3^+ - k_2^+) + \frac{x_2 x_4}{2H^2} K_{43}^\vee K_{43}^\wedge + \frac{x_1 x_4}{2H^2} K_{32}^\vee K_{43}^\wedge + \frac{x_2 x_1}{2H^2} K_{43}^\vee K_{14}^\wedge + \frac{x_1^2}{2H^2} K_{32}^\vee K_{14}^\wedge]
\end{aligned}
$$

The first two terms won't have collinear divergence, the μ can be set to zero, but the rest will have to be evaluated with a small μ to regulate the collinear divergences.

There are basically two types of Feynman parameter integrals in this case. The others are either finite or could be obtained from these two.

$$
\begin{aligned}
&\int_{\Sigma x_i \le 1} \frac{x_1^2}{(x_1 x_3 t + x_2 x_4 s + \mu^2)^2} \\
= &\frac{1}{2st}\log^2\frac{\mu^2}{s} - \frac{s}{2t(s+t)^2}\log^2\frac{s}{t} + \frac{2}{st}\log\frac{\mu^2}{s} + \frac{1}{t(s+t)}\log(\frac{s}{t}) + \frac{4}{st} - \frac{\pi^2 s}{2t(s+t)^2} \\
&\int_{\Sigma x_i \le 1} \frac{x_1 x_2}{(x_1 x_3 t + x_2 x_4 s + \mu^2)^2} \\
= &-\frac{1}{2(s+t)^2}\log^2\frac{s}{t} - \frac{2}{st}\log\frac{\mu^2}{s} - \frac{1}{t(s+t)}\log(\frac{s}{t}) - \frac{2}{st} - \frac{\pi^2}{2(s+t)^2}
\end{aligned} \tag{3–12}
$$

Collecting all the divergent terms from Eq.3–9:

$$
\begin{aligned}
(3\text{–}9)_{div} &= \frac{iA}{8\pi^2}\left[\frac{1}{8(-t)}\log^2\mu^2+\frac{1}{2(-t)}\log\mu^2-\frac{1}{4(-t)}\log s\log\mu^2\right]K^{\vee}_{32}K^{\wedge}_{14} \\
&- \frac{iA}{8\pi^2}\frac{1}{4(-t)}\log\mu^2\cdot(K^{\vee}_{43}K^{\wedge}_{14}+K^{\wedge}_{43}K^{\vee}_{32}) \qquad (3\text{–}13)
\end{aligned}
$$

Eq.3–10 and Eq.3–11 simply give

$$
\begin{aligned}
& K^{\vee}_{3,-5}\cdot\ K^{\wedge}_{4,3}\frac{i}{(q-k_1)^2}\frac{i}{(q-k_4)^2}\frac{i}{(q-k_3)^2}\frac{i}{s} \\
= & \int\frac{T^2dTdx_1dx_3dx_4\delta(\sum x_i-1)}{2T(2\pi)^3} \\
& \left[-\frac{k_4^+-k_3^+}{(-t)}q^{\vee}-\frac{x_1}{(-t)}K^{\vee}_{32}-\frac{0}{(-t)}K^{\vee}_{43}\right]K^{\wedge}_{43}\ \exp\left(-iTq_{\perp}{}^2+iTH\right) \\
= & \frac{1}{8\pi^2}[\log\mu^2+2-\log(-t)]\frac{1}{2s(-t)}K^{\wedge}_{43}K^{\vee}_{32}
\end{aligned}
$$

$$
\begin{aligned}
& K^{\vee}_{3,-5}\cdot\ K^{\wedge}_{1,4}\frac{i}{(q-k_1)^2}\frac{i}{(q-k_4)^2}\frac{i}{t}\frac{i}{(q-k_2)^2} \\
= & \int\frac{T^2dTdx_1dx_2dx_4\delta(\sum x_i-1)}{2T(2\pi)^3} \\
& \left[-\frac{k_4^+-k_3^+}{(-t)}q^{\vee}-\frac{x_1}{(-t)}K^{\vee}_{32}-\frac{x_2}{(-t)}K^{\vee}_{43}\right]K^{\wedge}_{14}\ \exp\left(-iq_{\perp}{}^2+iH\right) \\
= & \frac{1}{8\pi^2}[(\log s-2)\log\mu^2-\frac{1}{2}\log^2\mu^2-(\frac{1}{2}\log^2 s+4-2\log s)]\frac{1}{2s(-t)}K^{\vee}_{32}K^{\wedge}_{14} \\
+ & \frac{1}{8\pi^2}[\log\mu^2+2-\log s]\frac{1}{2s(-t)}K^{\vee}_{43}K^{\wedge}_{14}
\end{aligned}
$$

This, multiplied by $-sA/2$, is the same as the half scalar box contribution Eq.3–13.

The complete contribution of Eq.3–9 with Eq.3–10 and 3–11 subtracted is (pole terms omitted)

$$
\begin{aligned}
&\frac{1}{8\pi^2}A\log\frac{s}{t}\Bigg[-\frac{1}{8}\frac{s(-k_3^+ + k_4^+)(-k_2^+ + k_3^+)}{(-t)-s} \\
&-\frac{1}{4}\frac{s}{((-t)-s)(-t)}K_{14}^{\wedge}K_{32}^{\vee} + \frac{1}{4}\frac{s}{((-t)-s)(-t)}K_{14}^{\wedge}K_{43}^{\vee} + \frac{1}{4((-t)-s)}K_{43}^{\wedge}K_{32}^{\vee}\Bigg] \\
+\quad &\frac{1}{8\pi^2}A[\log^2\frac{s}{t}+\pi^2]\Bigg[-\frac{1}{16}\frac{s(-k_3^+ + k_4^+)(-k_2^+ + k_3^+)(-t)}{((-t)-s)^2} \\
&-\frac{1}{8}\frac{s^2}{((-t)-s)^2(-t)}K_{14}^{\wedge}K_{32}^{\vee} + \frac{1}{8}\frac{s}{((-t)-s)^2}K_{14}^{\wedge}K_{43}^{\vee} + \frac{1}{8}\frac{s}{((-t)-s)^2}K_{43}^{\wedge}K_{32}^{\vee}\Bigg] \qquad (3\text{–}14)
\end{aligned}
$$

So, when evaluating Eq.3–9, which is collinearly divergent by itself, I shall subtract Eq.3–10 and 3–11 from it, to make 3–9 finite.

Next I will show that Eq.3–10 and Eq.3–11 also cancel the collinear divergence in the third and fourth term of Eq.3–8. Putting the triangle-like terms in Eq.3–8 together with Eq.3–10, 3–11:

$$
\begin{aligned}
&\left[(-k_1^+ + k_2^+)(-k_1^+ + q^+)(q-k_4)^2 + (-k_4^+ + k_1^+)(k_1^+ - q^+)(q-k_2)^2\right] \\
&\frac{1}{(q^+ - k_1^+)^2}\frac{i}{(q-k_1)^2}\frac{i}{(q-k_2)^2}\frac{i}{(q-k_3)^2}\frac{i}{(q-k_4)^2}K_{3,-5}^{\vee}K_{-6,4}^{\wedge} \\
+\quad &K_{3,-5}^{\vee}\cdot K_{4,3}^{\wedge}\frac{i}{(q-k_1)^2}\frac{i}{(q-k_4)^2}\frac{i}{(q-k_3)^2}\frac{i}{s}s \\
+\quad &K_{3,-5}^{\vee}\cdot K_{1,4}^{\wedge}\frac{i}{(q-k_1)^2}\frac{i}{(q-k_4)^2}\frac{i}{t}\frac{i}{(q-k_2)^2}s \qquad (3\text{–}15)
\end{aligned}
$$

Suppose $q-k_1=\lambda(p_1-p_2)$, $q-k_2=(1+\lambda)(p_1-p_2)$. The above expression becomes

$$
\begin{aligned}
&\frac{1}{(q-k_1)^2}\frac{1}{(q-k_2)^2}K_{3,-5}^{\vee}\times \\
&\left[\frac{(-k_1^+ + k_2^+)}{\lambda(k_1^+ - k_2^+)}\frac{1}{(1+\lambda)t}(1+\lambda)K_{14}^{\wedge} + 0 + 0 + \frac{1}{\lambda s}s\frac{1}{t}K_{14}^{\wedge}\right] = 0
\end{aligned}
$$

Suppose $q-k_1=\lambda(p_4-p_1)$, $q-k_4=(\lambda-1)(p_4-p_1)$. The above expression becomes

$$\frac{1}{(q-k_1)^2}\frac{1}{(q-k_4)^2}K^{\vee}_{3,-5}\times$$
$$\left[0+\frac{(-k_4^+ + k_1^+)}{-\lambda(k_4^+ - k_1^+)}\frac{1}{(\lambda-1)t}(K^{\wedge}_{14}+\lambda K^{\wedge}_{24})+K^{\wedge}_{4,3}\frac{1}{(1-\lambda)t}\frac{1}{s}s+K^{\wedge}_{1,4}\frac{1}{t}\frac{1}{\lambda s}s\right]=0$$

Thus all the collinear divergences cancel.

The complete contribution of 3–10 and 3–11 and third fourth term of Eq.3–8 are quite complicated. I observed that the rational part of their contribution is zero, so if there is a way to get the logarithmic parts through some other methods (such as unitarity), we can be spared all these ordeals.

To summarize, I have subtracted 3–10 and 3–11 from Eq.3–9 and then added them back to the triangle-like terms in Eq.3–8 to make both parties collinearly finite. I want to add that the introduction of μ will not mess up gauge covariance as people would normally think.

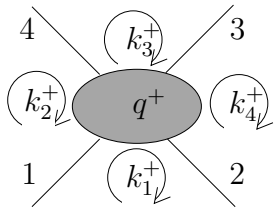

Figure 3-1. Dual momentum assignment with $k_2^+ < k_3^+ < k_1^+ < k_4^+$

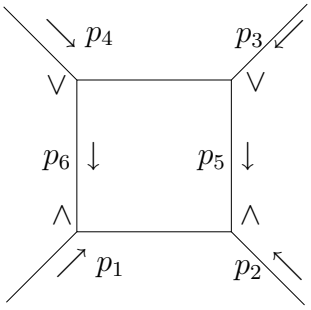

Figure 3-2. Model box with a helicity violating subtree

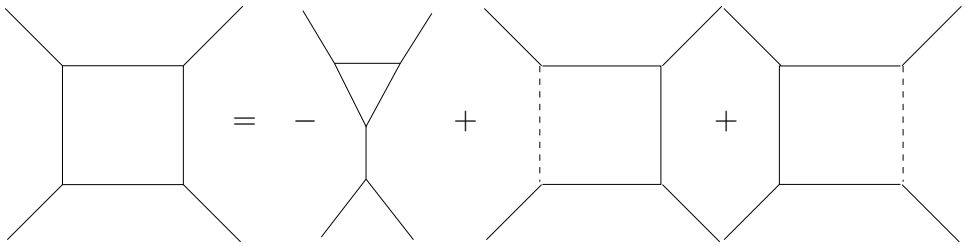

Figure 3-3. Graphical representation of box reduction

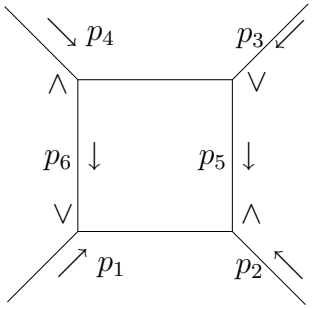

Figure 3-4. Model box with alternating helicity

CHAPTER 4
MASSLESS AMPLITUDES

I will be following [21] and decompose an n-particle amplitude into

$$\mathcal{M}_n = \sum_{perm'} \mathrm{Tr}(t^{a_1} t^{a_2} ... t^{a_n}) M(p_1, \epsilon_1; p_2, \epsilon_2; ...; p_n, \epsilon_n) \tag{4–1}$$

where $perm'$ is over non cyclic permutations for complex representations, non cyclic and non reflexive permutations for real representations. In the following results, the representation is assumed to be the adjoint representation.

4.1 Two Point Functions

A factor of $-ig^2/(16\pi^2) f^{cad} f^{dbc} = ig^2/(16\pi^2)\mathrm{Tr}\left[t^a t^b\right]$ will be omitted in the following list.

4.1.1 Gluon Self-Energy

Refer to Fig.4-1

$$\begin{aligned}
\Pi(g+, g+; s) &= -\frac{1}{3}\left[k_1^{\wedge 2} + k_1^{\wedge} k_3^{\wedge} + k_3^{\wedge 2}\right] \\
\Pi(g+, g+; q) &= \frac{4}{3}\left[k_1^{\wedge 2} + k_1^{\wedge} k_3^{\wedge} + k_3^{\wedge 2}\right] \\
\Pi(g+, g+; g) &= -\frac{2}{3}\left[k_1^{\wedge 2} + k_1^{\wedge} k_3^{\wedge} + k_3^{\wedge 2}\right]
\end{aligned} \tag{4–2}$$

where the first two arguments in Π tell the species of particle and the helicity, and the third denotes the particle in the loop. For the above assignment of helicity, the contribution should be zero due to Lorentz covariance. They are only nonzero because the regulator used here doesn't respect Lorentz covariance. This is purely an artifact, and it has to be cancelled by a counter term. Also, it can be observed that $\Pi(g+, g+, s) \times N_s + \Pi(g+, g+; q)_F \times N_f + \Pi(g+, g+; g) \times N_g = 0$ in the $\mathcal{N} = 4$ SYM case.

$$\Pi(g+,g^+;s) = \frac{1}{6}p^+p^\wedge$$
$$\Pi(g+,g^+;q) = -\frac{2}{3}p^+p^\wedge$$
$$\Pi(g+,g^+;g) = \frac{7}{3}p^+p^\wedge + \text{IR terms} \tag{4–3}$$

The notation g^+ simply means that I am using $|\eta]\langle\eta|$ or $g^{\mu+}$ as polarization vector. The first two terms should also be zero due to Lorentz covariance, so they have to be set to zero with counter terms.

Here are the helicity conserving 2 point functions:

$$\begin{aligned}
\Pi(g+,g-;s) &= \int_0^1 dx x(1-x)p^2 \log x(1-x)p^2\delta e^\gamma \\
&= p^2\left[\frac{5}{18} - \frac{1}{6}\log p^2\delta e^\gamma\right] \\
\Pi(g+,g-;q) &= 2\int_0^1 dx\left[x^2+(1-x)^2\right]p^2 \log x(1-x)p^2\delta e^\gamma \\
&= p^2\left[\frac{26}{9} - \frac{4}{3}\log p^2\delta e^\gamma\right] \\
\Pi(g+,g-,g) &= 2\int_0^1 dx\left[\frac{x}{1-x}+\frac{1-x}{x}+x(1-x)\right]p^2 \log x(1-x)p^2\delta e^\gamma \\
&= p^2\left[-\frac{67}{9} + \frac{11}{3}\log p^2\delta e^\gamma + \int_0^1 dx\left[\frac{2}{1-x}+\frac{2}{x}\right]\log x(1-x)p^2\delta e^\gamma\right]
\end{aligned} \tag{4–4}$$

Here x is in fact $(q^+ - k_1^+)/(k_3^+ - k_1^+)$.

Several comments are in order:

In the last line of Eq.4–4, the x integral is certainly divergent, this is due to the artificial divergence. This divergent integral is what we call the infrared term (with x interpreted as $(q^+ - k_1^+)/(k_3^+ - k_1^+)$. Temporarily forgetting about these infrared terms, it is easily observed that the sum of these diagrams is zero with the $\mathcal{N} = 4$ field content. I shall comment on this later.

In the above list, all quadratic divergence $1/\delta$ are omitted. Due to the way the light cone world sheet computation is setup, all the tadpoles are being dropped. These tadpoles will only contribute to the quadratic $1/\delta$ divergence. As a result, the $1/\delta$ terms can actually have non-trivial p^+ dependence. When the p^+ dependence is of the type $1/p^+$, it can be interpreted as a world sheet cosmological constant as in [13]. While in other cases, the p^+ dependence could be of the form $(1/p^+)\log p^+$, whose interpretation has not been fully understood yet.

There is one small point about numerics that I want to point out here. The 2 point function naturally comes with a color structure of $f^{cad}f^{dbc} = -\mathrm{Tr}\left[t^a t^b\right]$, when we try to fit the 2 point functions into the big picture as in Fig.4-2, the trace factor becomes (assuming that t^a is in a real representation):

$$\begin{aligned} & f^{abe}\mathrm{Tr}[t^e t^f]f^{fcd} = \mathrm{Tr}[(-i)[t^a,t^b](-i)[t^c,t^d]] \\ = \; & -\mathrm{Tr}[t^a t^b t^c t^d] + \mathrm{Tr}[t^a t^b t^d t^c] + \mathrm{Tr}[t^b t^a t^c t^d] - \mathrm{Tr}[t^b t^a t^d t^c] \\ & \to -2\mathrm{Tr}[t^a t^b t^c t^d] \end{aligned} \tag{4–5}$$

Also, there is always another factor of i^2 coming from the two propagators connecting to the 2 point function.

As a comparison, I shall give the two point function that describes the 'propagation' of A^-. The argument g^+ means that I am taking the polarization vector to be $g^{\mu+}$.

$$\begin{aligned} \Pi(g^+,g^+;s) &= p^{+2}\left[\frac{4}{9} - \frac{1}{6}\log p^2\delta e^\gamma\right] \\ \Pi(g^+,g^+;q) &= p^{+2}\left[\frac{20}{9} - \frac{4}{3}\log p^2\delta e^\gamma\right] \\ \Pi(g^+,g^+,g) &= p^{+2}\left[\frac{8}{9} - \frac{1}{3}\log p^2\delta e^\gamma\right] \end{aligned}$$

We observe that the logarithmic piece that will give a cut matches between $\Pi(g+,g-)$ and $\Pi(g^+,g^+)$ when the loop particle is fermion or scalar. This is a hint that we shall use counter terms to enforce the total agreement between $\Pi(g+,g-)$ and $\Pi(g^+,g^+)$, due to the

consideration of Lorentz covariance. This observation shall be a guide to fix counter terms later on.

Clearly, there is a mismatch when the gluon is in the loop. This mismatch is due to the presence of infrared divergences in $\Pi(g+, g-, g)$, while $\Pi(g^+, g^+, g)$ is free of infrared divergence.

4.1.2 Fermion and Scalar Self-Energy

$$\begin{aligned}\Pi(\bar{q}+, q+) &= \int_0^1 dx \frac{-2+3x-3x^2}{(1-x)x} p^2 \log x(1-x)p^2\delta e^\gamma \\ &= p^2\left[-6+3\log p^2\delta e^\gamma + \int_0^1 dx \left[\frac{-2}{1-x}+\frac{-2}{x}\right]\log x(1-x)p^2\delta e^\gamma\right]\end{aligned}$$

The divergent x integral is likewise interpreted as infrared term.

I shall also give the result when I use $|\eta\rangle$ or $|\,\eta]$ as spinors instead of $|p\rangle$ or $|\,p]$.

$$\Pi(\bar{q}^+, q^+) = \sqrt{2}p^+\left[2-\log p^2\delta e^\gamma\right]$$

where p flows with the direction of the fermion line. We again observe a mismatch of $\log p^2$ term, due to the infrared divergence.

The scalar self-energy diagram is given by

$$\begin{aligned}\Pi(s, s) &= \int_0^1 dx \frac{-2+4x-4x^2}{(1-x)x} p^2 \log x(1-x)p^2\delta e^\gamma \\ &= p^2\left[-8+4\log p^2\delta e^\gamma + \int_0^1 dx \left[\frac{-2}{1-x}+\frac{-2}{x}\right]\log x(1-x)p^2\delta e^\gamma\right]\end{aligned}$$

4.2 Three Point Functions

The general structure of 3 point function Fig.4-3 is

$$\left(\text{const} + \log p_o^2\right)\text{ tree} + \alpha\text{ term} + \text{const}(k_{2\perp} + k_{1\perp} + k_{4\perp})$$

The α term will arise if the off-shell leg has unlike helicity.

A factor of $g^3/8\pi^2 f^{dae} f^{ebf} f^{fcd} = ig^3/8\pi^2 \mathrm{Tr}[t^a t^b t^c]$ is omitted.

4.2.1 Gluon Vertex Correction

$$\begin{aligned}
\Gamma(g+,g+,g-;s) &= \frac{-2p_3^+}{p_1^+ p_2^+} K_{2,1}^{\wedge} \left[\frac{1}{6} \log p_o^2 \delta e^{\gamma} - \frac{1}{9} - \alpha \frac{1}{6} \frac{p_1^+ p_2^+}{p_3^{+2}} \right] \\
\Gamma(g+,g+,g-;q) &= \frac{-2p_3^+}{p_1^+ p_2^+} K_{2,1}^{\wedge} \left[\frac{4}{3} \log p_o^2 \delta e^{\gamma} - \frac{32}{9} + \alpha \frac{2}{3} \frac{p_1^+ p_2^+}{p_3^{+2}} \right] \\
\Gamma(g+,g+,g-;g) &= \frac{-2p_3^+}{p_1^+ p_2^+} K_{2,1}^{\wedge} \left[-\frac{11}{3} \log p_o^2 \delta e^{\gamma} + \frac{70}{9} - \alpha \frac{1}{3} \frac{p_1^+ p_2^+}{p_3^{+2}} \right] + \text{IR terms} \quad (4\text{–}6)
\end{aligned}$$

where $\alpha = 1$ if leg 3 is off shell and 0 otherwise, and p_o is the momentum of the only off-shell leg. The infrared terms present in the gluon triangle diagram will eventually be combined with infrared terms from other diagrams to become proportional to a tree. They are given in [14] and are not repeated here.

All of the above also contain an anomalous term:

$$\begin{aligned}
\Gamma(g+,g+,g-;s)_{ano} &= \frac{1}{3}(k_2^{\wedge} + k_1^{\wedge} + k_4^{\wedge}) \\
\Gamma(g+,g+,g-;q)_{ano} &= -\frac{4}{3}(k_2^{\wedge} + k_1^{\wedge} + k_4^{\wedge}) \\
\Gamma(g+,g+,g-;g)_{ano} &= \frac{2}{3}(k_2^{\wedge} + k_1^{\wedge} + k_4^{\wedge})
\end{aligned}$$

here the k's are dual momenta, they arise because δ is an exponential damping factor of the transverse dual momenta. Had we used a cut off regulator ($(q_\perp - k_{1\perp})^2 < \Lambda$ for example) instead of δ, the anomalous terms would change according to

$$(k_{2\perp} + k_{1\perp} + k_{4\perp}) \to (k_{2\perp} - k_{1\perp}) + (k_{4\perp} - k_{1\perp})$$

These polynomial terms must be canceled by counter terms.

The MHV triangles (with all three legs having the same helicity) give

$$\begin{aligned}
\Gamma(g+,g+,g+;s) &= \frac{(K^{\wedge}_{21})^3}{p_1^+p_2^+p_3^+}\left[\frac{2}{3p_o^2}\right] \\
\Gamma(g+,g+,g+;q) &= \frac{(K^{\wedge}_{21})^3}{p_1^+p_2^+p_3^+}\left[\frac{-8}{3p_o^2}\right] \\
\Gamma(g+,g+,g+;g) &= \frac{(K^{\wedge}_{21})^3}{p_1^+p_2^+p_3^+}\left[\frac{4}{3p_o^2}\right]
\end{aligned} \tag{4–7}$$

Here, we again observe that with $\mathcal{N}=4$ SYM field content, the gluon vertex correction vanishes.

As a comparison, I shall give the result when the off shell leg takes on + component.

$$\begin{aligned}
\Gamma(g+,g-,g^+;s) &= -(p_1^+-p_2^+)\left[\frac{1}{6}\log p_o^2\delta e^{\gamma}-\frac{5}{18}\right] \\
\Gamma(g+,g-,g^+;q) &= -(p_1^+-p_2^+)\left[\frac{4}{3}\log p_o^2\delta e^{\gamma}-\frac{26}{9}\right] \\
\Gamma(g+,g-,g^+;g) &= -(p_1^+-p_2^+)\left[-\frac{5}{3}\log p_o^2\delta e^{\gamma}+\frac{31}{9}\right]+\text{IR terms} \\
\Gamma(g+,g+,g^+) &= 0
\end{aligned} \tag{4–8}$$

Although $\Gamma(g+,g-,g^+)$ are not directly used in the computation of the scattering amplitudes, they are a guide to fix the counter terms

4.2.2 Fermion Vertex Correction

The fermion vertex correction Fig.4-4 is given by

$$\Gamma(q+,\bar{q}+,g+) = \frac{2}{q^+}K^{\wedge}_{p_2,q}\left[-3\log p_o^2\delta e^{\gamma}+6\right]+\text{IR terms} \tag{4–9}$$

The notation here is that: q means an incoming fermion line while $\bar{q}$ means an outgoing fermion line; $q+$ means that the fermion is right handed; $g+$ means that the gluon is right handed which corresponds to $\wedge$. The reader can refer to Fig.4-4. The factor $ig^3/(8\pi^2)\mathrm{Tr}[t^at^bt^c]$ is omitted as usual. The other combination is

$$\Gamma(q+,\bar{q}+,g-) \;=\; \frac{2p_2^+}{q^+p_1}K^{\vee}_{p_1,q}\left[-3\log p_o^2\delta e^{\gamma}+6\right]+\text{IR terms} \qquad (4\text{–}10)$$

While $\Gamma(q-,\bar{q}-,g+)$, $\Gamma(q+,\bar{q}+,g-)$; and $\Gamma(q-,\bar{q}-,g-)$, $\Gamma(q+,\bar{q}+,g+)$ are related by charge conjugation[1] . These results up to the IR terms are the same with any one of the legs being off shell.

We can also have the case when a gluon is off shell but taking on + component.

$$\Gamma(q+,\bar{q}+,g^+) \;=\; 2p_2^+\left[-\log p_o^2\delta e^{\gamma}+2\right]+\text{IR terms}$$

4.2.3 Scalar Vertex Correction

Scalar vertex Fig.4-5 is given by

$$\Gamma(s,s,g+) \;=\; \frac{2}{q^+}K^{\wedge}_{2,1}\left[-4\log p_o^2\delta e^{\gamma}+\frac{17}{2}\right]+(k_2^{\wedge}+k_1^{\wedge}+k_4^{\wedge})+\text{IR terms} \qquad (4\text{–}11)$$

with $\Gamma(s,s,g-)$ equal to $\Gamma(s,s,g+)$ with the obvious change of $\wedge$ to $\vee$. This result is also the same up to IR terms with any one of the legs being off-shell.

4.2.4 Four-Point Functions

The box diagrams are too cumbersome to present here, but I do want to point out that, up to the infrared terms, the total contribution of the box diagrams in a specific amplitude is surprisingly simple. I shall list the rational part of the contribution of some boxes in conjunction with the scattering processes in which they occur.

4.3 Scattering Amplitudes

I shall start with gluon scattering, with a factor of $ig^4/(8\pi^2)\mathrm{Tr}[t^at^bt^ct^d]$ omitted.

[1] up to the external line factors which are defined asymmetrically, see the explanation below Eq.2–24

4.3.1 Helicity Violating Amplitudes

The tree level amplitude for four gluons with the same helicity is zero. At one loop, the amplitude is

$$\begin{aligned} A(g+,g+,g+,g+;s) &= \frac{4}{3}\frac{K^{\wedge}_{43}K^{\wedge}_{32}K^{\wedge}_{21}K^{\wedge}_{14}}{p_1^+p_2^+p_3^+p_4^+st} \\ A(g+,g+,g+,g+;q) &= -\frac{16}{3}\frac{K^{\wedge}_{43}K^{\wedge}_{32}K^{\wedge}_{21}K^{\wedge}_{14}}{p_1^+p_2^+p_3^+p_4^+st} \\ A(g+,g+,g+,g+;g) &= \frac{8}{3}\frac{K^{\wedge}_{43}K^{\wedge}_{32}K^{\wedge}_{21}K^{\wedge}_{14}}{p_1^+p_2^+p_3^+p_4^+st} \end{aligned} \tag{4–12}$$

The tree level amplitude with only one unlike helicity is zero too. At one loop level, the amplitude is

$$\begin{aligned} A(g+,g+,g+,g-;s) &= \frac{1}{6}(s+t)\frac{K^{\wedge 2}_{13}p_2^+p_4^+}{K^{\wedge}_{43}K^{\vee}_{32}K^{\vee}_{21}K^{\wedge}_{14}} \\ A(g+,g+,g+,g-;q) &= \frac{-2}{3}(s+t)\frac{K^{\wedge 2}_{13}p_2^+p_4^+}{K^{\wedge}_{43}K^{\vee}_{32}K^{\vee}_{21}K^{\wedge}_{14}} \\ A(g+,g+,g+,g-;g) &= \frac{1}{3}(s+t)\frac{K^{\wedge 2}_{13}p_2^+p_4^+}{K^{\wedge}_{43}K^{\vee}_{32}K^{\vee}_{21}K^{\wedge}_{14}} \end{aligned} \tag{4–13}$$

It is easily observable that the helicity violating amplitude is zero if there is any amount of supersymmetry [17]. For example:

$$\begin{aligned} \mathcal{N}=1: \; & -\frac{16}{3}\times\frac{1}{2}+\frac{8}{3}\times 1=0 \quad -\frac{2}{3}\times\frac{1}{2}+\frac{1}{3}\times 1=0 \\ \mathcal{N}=2: \; & -\frac{16}{3}\times 1+\frac{8}{3}\times 1+\frac{4}{3}\times 2=0 \quad -\frac{2}{3}\times 1+\frac{1}{3}\times +\frac{1}{6}\times 2=0 \\ \mathcal{N}=3(4): \; & -\frac{16}{3}\times 2+\frac{8}{3}\times 1+\frac{4}{3}\times 6=0 \quad -\frac{2}{3}\times 2+\frac{1}{3}\times 1+\frac{1}{6}\times 6=0 \end{aligned} \tag{4–14}$$

Since for gluon scattering up to one loop, adding supersymmetry is simply taking into account the multiplicity of each species, hence $\mathcal{N}=3$ is the same as $\mathcal{N}=4$.

In the list of amplitudes, the fermions are assumed to be dirac, this explains the strange looking 1/2 multiplicity for the fermions in the first line of Eq.4–14.

4.3.2 Helicity Conserving Amplitudes

The helicity conserving amplitude is non-zero at tree level. They are given by [20]

$$A(g+,g+,g-,g-) = ig^2 f^{abe} f^{ecd} \frac{-2K_{12}^{\wedge 4} p_3^+ p_4^+}{K_{43}^{\wedge} K_{32}^{\wedge} K_{21}^{\wedge} K_{14}^{\wedge} p_1^+ p_2^+}$$
$$A(g+,g-,g+,g-) = ig^2 f^{abe} f^{ecd} \frac{-2K_{13}^{\wedge 4} p_2^+ p_4^+}{K_{43}^{\wedge} K_{32}^{\wedge} K_{21}^{\wedge} K_{14}^{\wedge} p_1^+ p_3^+} \tag{4–15}$$

The factor $f^{abe} f^{ecd}$ can be converted to $-1/C(G)\mathrm{Tr}\left[[t^a,t^b][t^c,t^d]\right] \rightarrow -2/C(G)\mathrm{Tr}\left[t^a t^b t^c t^d\right]$. Here I have chosen t^a to be the structure constants, while most literature picks t^a to be in the fundamental representation. So, instead of the one loop amplitude gaining a factor of N_c, here the tree amplitude is *down* by a factor of N_c.

At one loop level, the amputated Green's function is (with external leg corrections omitted)

$$
\begin{aligned}
A(g+,g+,g-,g-;s) &= \frac{-2K_{12}^{\wedge 4}p_3^+p_4^+}{K_{43}^\wedge K_{32}^\wedge K_{21}^\wedge K_{14}^\wedge p_1^+p_2^+}\left[\frac{1}{18}+\frac{1}{6}\log\delta e^\gamma t\right]-\frac{1}{6}\times+\frac{1}{3}\\
A(g+,g+,g-,g-;q) &= -2\left\{\frac{-2K_{12}^{\wedge 4}p_3^+p_4^+}{K_{43}^\wedge K_{32}^\wedge K_{21}^\wedge K_{14}^\wedge p_1^+p_2^+}\left[\frac{19}{9}-\frac{2}{3}\log\delta e^\gamma t\right]-\frac{1}{3}\times+\frac{2}{3}\right\}\\
A(g+,g+,g-,g-;g) &= \frac{-2K_{12}^{\wedge 4}p_3^+p_4^+}{K_{43}^\wedge K_{32}^\wedge K_{21}^\wedge K_{14}^\wedge p_1^+p_2^+}\left[-\left(\log^2\frac{s}{t}+\pi^2\right)-\frac{11}{3}\log\delta e^\gamma t+\frac{73}{9}\right]\\
&\quad -\frac{1}{3}\times+\frac{2}{3}
\end{aligned}
\tag{4–16}
$$

$$
\begin{aligned}
A(g+,g-,g+,g-;s) &= \frac{-2K_{13}^{\wedge 4}p_2^+p_4^+}{K_{43}^\wedge K_{32}^\wedge K_{21}^\wedge K_{14}^\wedge p_1^+p_3^+}\left[-\frac{s^2t^2}{2(s+t)^4}\left(\log^2\frac{s}{t}+\pi^2\right)\right.\\
&\quad \left.+\frac{s(2t^2-5st-s^2)}{6(s+t)^3}\log\frac{s}{t}+\frac{1}{6}\log\delta e^\gamma s+\frac{ts}{2(s+t)^2}+\frac{1}{18}\right]\\
&\quad -\frac{1}{6}\times+\frac{1}{3}\\
A(g+,g-,g+,g-;q) &= -2\left\{\frac{-2K_{13}^{\wedge 4}p_2^+p_4^+}{K_{43}^\wedge K_{32}^\wedge K_{21}^\wedge K_{14}^\wedge p_1^+p_3^+}\left[\frac{st(t^2+s^2)}{2(s+t)^4}\left(\log^2\frac{s}{t}+\pi^2\right)\right.\right.\\
&\quad \left.+\frac{s(5t^2+st+2s^2)}{3(s+t)^3}\log\frac{s}{t}-\frac{2}{3}\log\delta e^\gamma s+\frac{ts}{(s+t)^2}+\frac{19}{9}\right]\\
&\quad \left.-\frac{1}{3}\times+\frac{2}{3}\right\}\\
A(g+,g-,g+,g-;g) &= \frac{-2K_{13}^{\wedge 4}p_2^+p_4^+}{K_{43}^\wedge K_{32}^\wedge K_{21}^\wedge K_{14}^\wedge p_1^+p_3^+}\left[-\frac{(s^2+st+t^2)^2}{(t+s)^4}\left(\log^2\frac{s}{t}+\pi^2\right)\right.\\
&\quad \left.+\frac{s}{3}\frac{(14t^2+19st+11s^2)}{(s+t)^3}\log\frac{s}{t}-\frac{11}{3}\log\delta e^\gamma s+\frac{ts}{(s+t)^2}+\frac{73}{9}\right]\\
&\quad -\frac{1}{3}\times+\frac{2}{3}
\end{aligned}
\tag{4–17}
$$

The symbol $\times$ above is the relevant four point vertex: $-2(p_1^+p_3^++p_2^+p_4^+)/[(p_1^++p_4^+)(p_2^++p_3^+)]$ or $2(p_2^+p_3^++p_1^+p_4^+)[(p_1^++p_2^+)(p_3^++p_4^+)]+2(p_1^+p_2^++p_3^+p_4^+)/[(p_1^++p_4^+)(p_2^++p_3^+)]$.

Here I also give the rational contribution of the corresponding box diagrams:

$$
\begin{aligned}
B(g+,g+,g-,g-;s) &= \frac{4}{9} - \text{all } \alpha \text{ terms} \\
B(g+,g+,g-,g-;q) &= -\frac{16}{9} - \text{all } \alpha \text{ terms} \\
B(g+,g+,g-,g-;g) &= \frac{8}{9} - \text{all } \alpha \text{ terms} \\
B(g+,g-,g+,g-;s) &= \frac{1}{9} + \frac{st}{2(s+t)^2}\frac{-2K_{13}^{\wedge 4}p_2^+p_4^+}{K_{43}^{\wedge}K_{32}^{\wedge}K_{21}^{\wedge}K_{14}^{\wedge}p_1^+p_3^+} \\
B(g+,g-,g+,g-;q) &= -\frac{4}{9} - \frac{2st}{(s+t)^2}\frac{-2K_{13}^{\wedge 4}p_2^+p_4^+}{K_{43}^{\wedge}K_{32}^{\wedge}K_{21}^{\wedge}K_{14}^{\wedge}p_1^+p_3^+} \\
B(g+,g-,g+,g-;g) &= \frac{2}{9} + \frac{st}{(s+t)^2}\frac{-2K_{13}^{\wedge 4}p_2^+p_4^+}{K_{43}^{\wedge}K_{32}^{\wedge}K_{21}^{\wedge}K_{14}^{\wedge}p_1^+p_3^+}
\end{aligned}
\tag{4–18}
$$

So, the rational part of a box diagram vanishes in $\mathcal{N}=4$ SYM together with the earlier observation that two and three point functions vanish in $\mathcal{N}=4$ SYM. This agrees with the 'no-triangle' assertion and some other technical observations that are commonly used nowadays to simplify the computation of $\mathcal{N}=4$ SYM amplitudes. Using a box reduction procedure [18], an integrand with d powers of momenta in the numerator and n propagators can be reduced to tensor box integrals of degree up to $d+4-n$. For gauge interactions, all three point vertices have one power of momenta, so there is n powers of momenta in the numerator of an n-gon diagram. Then the result of reduction is a combination of degree four box integrals, and some of the degree four box integrals can be further reduced to triangle and bubble integrals. In $\mathcal{N}=4$ SYM, due to the ultraviolet cancelation between different species, the degree of an n-gon integrand will be n-4, so the result of reduction is thus scalar box integrals. This essentially is the 'no triangle' assertion, which we did observe in Section 4.2 of vertex corrections. While it can also be shown that the scalar box integrals will not in any way produce rational terms, this I have explicitly shown in the above list.

The gluon scattering in $\mathcal{N}=4$ SYM is very simple (up to infrared terms):

$$
\begin{aligned}
A(g+,g+,g-,g-;SYM) &= \frac{-2K_{12}^{\wedge 4}p_3^+p_4^+}{K_{43}^{\wedge}K_{32}^{\wedge}K_{21}^{\wedge}K_{14}^{\wedge}p_1^+p_2^+}\left[-\left(\log^2\frac{s}{t}+\pi^2\right)\right] \\
A(g+,g-,g+,g-;SYM) &= \frac{-2K_{13}^{\wedge 4}p_2^+p_4^+}{K_{43}^{\wedge}K_{32}^{\wedge}K_{21}^{\wedge}K_{14}^{\wedge}p_1^+p_3^+}\left[-\left(\log^2\frac{s}{t}+\pi^2\right)\right] \qquad (4\text{–}19)
\end{aligned}
$$

without any need for counter terms.

4.3.3 Restoring Gauge Covariance

So far, we have only studied the pure gluon scattering, and we have encountered some non-gauge-covariance (non-Lorentz-Covariance) such as the hanging four point vertex. We have to complete everything to a tree in order to maintain Lorentz covariance. At four point level, the spinor structure of the leading order amplitude is the unique one that agrees with all the helicity assignment. So for the result to be Lorentz covariant, it has to be proportional to the leading order. This remains true to all orders if supersymmetry is present according to [17], which says MHV amplitudes are proportional to tree amplitudes.

We cannot just simply use a counter-term to cancel the hanging four point vertex, because they are not polynomials in external momenta. However, we can adjust the relative strength of the exchange diagram to the contact diagram by adding a term proportional to p^2 to the self-energy term Eq.4–4. This modification only changes the field strength renormalization by a constant, hence is perfectly allowed. With this term, the coefficient of s and t channel exchange diagram is shifted. So if we pick the numerical factor in front of p^2 to be $-1/6,\ -1/3,\ -1/3$ for scalar, fermion and gluon respectively, then they will match the coefficient of the lone four point vertex, completing it to a full tree. This brings about a change in the numerical factor: $1/18 \to -5/18$, $19/9 \to 13/9$, $73/9 \to 67/9$ [14].

I have also done the computation with dimension regulation. The procedure was to use dimension regulation to regulate the transverse momentum integral, and as soon as this is done, ϵ will be set to zero. Hence the infrared regulator is still k^+. The computation shows that the hanging four point vertex and the pure number will vanish,

this is expected since I have used a gauge invariant regulator. The numerical factor in this scheme will come out in agreement with [23], who used dimension regulation through and through, (not that the numerical factor is any thing important, as it can be altered by a redefinition of coupling constant).

This type of counter-term will be put to a more severe test later on when we consider the scattering of not just gluons but quarks and scalars. These counter terms had better be universal in the sense that they are only the property of the self-energy bubble, and should not depend upon what process it is embedded into.

4.3.4 All 2-2 Processes

$$\begin{aligned} A(s,s,g+,g-) &= \frac{8K_{13}^{\wedge 2}K_{14}^{\vee 2}}{sp_3^+p_4^+p_1^{+2}}\Big[9-\frac{2(s+2t)}{(s+t)}\log\delta e^\gamma s-\frac{2s}{(s+t)}\log\delta e^\gamma t \\ &\quad -\frac{s^2+st+t^2}{(s+t)^2}\left(\log^2\frac{s}{t}+\pi^2\right)\Big]-\frac{1}{2}\times\left[1+\frac{(p_2^+-p_1^+)(p_4^+-p_3^+)}{(p_1^++p_2^+)^2}\right]+1 \end{aligned}$$

$$A(g+,s,g-,s)=\frac{-8K_{21}^{\wedge 2}K_{32}^{\vee 2}}{stp_1^+p_3^+p_2^{+2}}\left[9-2\log\delta e^\gamma s-2\log\delta e^\gamma t-\left(\log^2\frac{s}{t}+\pi^2\right)\right]-1\times(-2)$$

$$\begin{aligned} A(s,s,s,s) &= \Big[\frac{59s^2+77st+59t^2}{3st}-\frac{3(2s+3t)}{s}\log\delta e^\gamma s \\ &- \frac{3(2t+3s)}{t}\log\delta e^\gamma t-\frac{2(s^2+t^2)}{st}\left(\log^2\frac{s}{t}+\pi^2\right)\Big] \\ &- \frac{1}{2}\times\left[\frac{(p_1^+-p_2^+)(p_3^+-p_4^+)}{(p_1^++p_2^+)^2}+\frac{(p_4^+-p_1^+)(p_2^+-p_3^+)}{(p_2^++p_3^+)^2}\right] \end{aligned}$$

while $A(s,s,s,s)_0 = 2(s^2+st+t^2)/(st)$.The above are the processes only involving bosons, the scheme for picking counter term described in Section 4.3.3 remains valid, namely, we can find a universal set of numerical factors that will complete all the above amplitudes into trees. This set can be chosen as -1/3 for $\Pi(g+,g-;g)$, -1/3 for $\Pi(g+,g-;q)$, -1/6 for $\Pi(g+,g-;s)$ and -1/2 for $\Pi(s,s)$.

However, when fermions are involved, I failed to find a universal set of counter terms that will fix the problem. I shall list the result of the computation first.

$$A(q-,q-,\bar{q}-,\bar{q}-)=\frac{-4K_{21}^{\wedge}K_{43}^{\vee}}{tp_1^+p_2^+}\left[\frac{67}{9}-\frac{11}{3}\log\delta e^{\gamma}t-\left(\log^2\frac{s}{t}+\pi^2\right)\right]-\frac{1}{3}\times\frac{-4p_3^+p_4^+}{(p_1^++p_4^+)^2} \tag{4–20}$$

$$\begin{aligned}A(q-,\bar{q}-,q-,\bar{q}-)=&\frac{4K_{13}^{\wedge}K_{24}^{\vee}(s+t)}{stp_1^+p_3^+}\\&\left[\frac{67}{9}-\frac{11}{3}\frac{t}{s+t}\log\delta e^{\gamma}s-\frac{11}{3}\frac{s}{s+t}\log\delta e^{\gamma}t-\frac{2s^2+st+2t^2}{2(s+t)^2}\left(\log^2\frac{s}{t}+\pi^2\right)\right]\\&-\frac{1}{3}\times\left[\frac{4p_2^+p_4^+}{(p_1^++p_4^+)^2}-\frac{4p_2^+p_3^+}{(p_1^++p_2^+)^2}\right]\end{aligned} \tag{4–21}$$

The notation here is that a 'q' represents an incoming fermion line, a '$\bar{q}$' represents an outgoing one, '+' corresponds to right handedness while '−' corresponds to left handedness. So the process corresponding to Eq.4–20 and Eq.4–21 is Fig.4-6:

$$A(q-,\bar{q}-,q+,\bar{q}+)=\frac{-4K_{14}^{\wedge}K_{32}^{\vee}}{sp_1^+p_3^+}\left[\frac{67}{9}-\frac{11}{3}\log\delta e^{\gamma}s-\left(\log^2\frac{s}{t}+\pi^2\right)\right]-\frac{1}{3}\times\frac{-4p_2^+p_4^+}{(p_1^++p_2^+)^2}$$

In fact, by charge conjugation, $A(q-,\bar{q}-,q+\bar{q}+)$ can be related to $A(q-,\bar{q}-,\bar{q}-,q-)$, which then can be obtained from rotating $A(q-,q-,\bar{q}-,\bar{q}-)$ clockwise by one notch (up to the external line factors). As was explained in Section 2.2, instead of associating $\sqrt{p^+}$ to each fermion line, I only associate a factor of p^+ to an outgoing line, but nothing to an incoming line. This is simply because a square root always causes troubles in automated computation. For example, $-4K_{14}^{\wedge}K_{32}^{\vee}/(sp_1^+p_3^+)$ should really be $-4K_{14}^{\wedge}K_{32}^{\vee}/(s\sqrt{p_1^+p_2^+p_3^+p_4^+})$, which is quite clear as the latter is Lorentz covariant (can be written as spinor products), but the former is not. The phase of the square root here can be given arbitrarily.

$$A(s,s,q-,\bar{q}-) =$$
$$\frac{4K_{13}^{\wedge}K_{14}^{\vee}}{sp_1^+p_3^+}\left[\frac{92}{9}-\frac{29}{6}\log\delta e^{\gamma}s-\frac{2t+s}{2(s+t)}\left(\log^2\frac{s}{t}+\pi^2\right)\right]-\frac{2}{3}\times\frac{2p_4^+(p_2^+-p_1^+)}{(p_1^++p_2^+)^2}$$

So far, the effect of using a non-covariant regulator is the mismatch between the exchange vertex and 4 point vertex in the final result. However, in the case of gluon fermion scattering, the mismatch is much worse.

$$\begin{aligned}A(g+,g-,q-,\bar{q}-) &= \frac{-8K_{13}^{\wedge 2}K_{32}^{\vee}K_{24}^{\vee}}{stp_1^+p_2^+p_3^{+2}}\left[6-3\log\delta e^{\gamma}s-\left(\log^2\frac{s}{t}+\pi^2\right)\right]\\ &\quad -\frac{1}{3}\times\text{s channel tree}\end{aligned}$$

$$\begin{aligned}A(g+,g-,q+,\bar{q}+) &= \frac{8K_{14}^{\wedge}K_{13}^{\wedge}K_{32}^{\vee 2}}{stp_1^+p_2^+p_3^+p_4^+}\left[6-3\log\delta e^{\gamma}s-\left(\log^2\frac{s}{t}+\pi^2\right)\right]\\ &\quad -\frac{1}{3}\times\text{s channel tree}\end{aligned}$$

Here we see that the mismatch is between s and t channel. By s-channel tree, I mean the s-channel exchange diagram and also its descendent four point vertex.

$$A(g+,q-,g-,\bar{q}-) = \frac{-8K_{21}^{\wedge 2}K_{43}^{\vee}K_{32}^{\vee}}{stp_1^+p_3^+p_2^{+2}}\left[6-3\log\delta e^{\gamma}t-\left(\log^2\frac{s}{t}+\pi^2\right)\right]$$

Here, it is mere coincidence that everything matches (the planar condition eliminates the u-channel tree).

The problem of fixing counter terms will be revisited in the future work discussion.

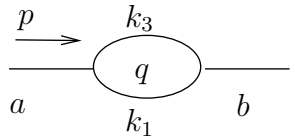

Figure 4-1. Two-point function and the dual momentum assignment

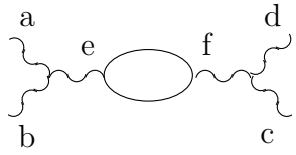

Figure 4-2. A self-energy diagram embedded in a scattering process

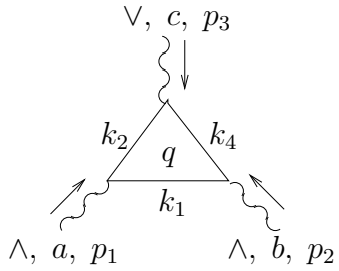

Figure 4-3. Triangle diagram

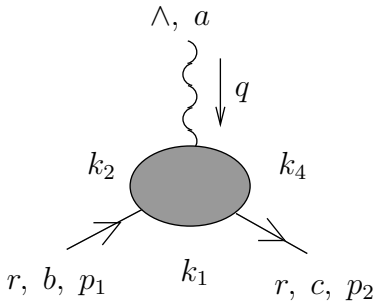

Figure 4-4. Fermion vertex correction corresponding to Eq.4–9

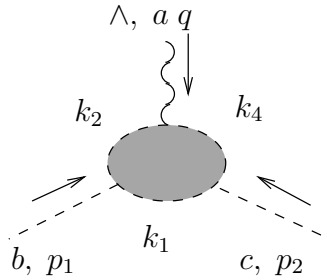

Figure 4-5. Scalar vertex correction corresponding to Eq.4–11

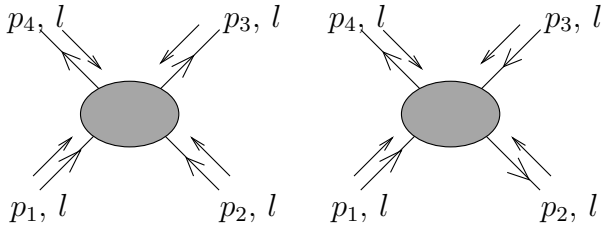

Figure 4-6. Four-fermion scattering corresponding to Eq.4–20 and Eq.4–21

CHAPTER 5
BREMSSTRAHLUNG IN LIGHT CONE

In this chapter, I shall deal with the infrared terms.

5.1 A List of Infrared Terms

All the amplitudes given in Section 4.3.4 are amputated Green's function, the external leg corrections are not included. As we can see that the self-energy diagram always contains a term $\log \delta e^{\gamma} p^2 x(1-x)$, which gives a multi-particle branch cut on the positive real axis, stopping us from doing wave function renormalization. This can be cured by summing over collinear emissions or absorptions from the external legs. The analysis of [14] showed that doing so is equivalent to replacing $\log \delta e^{\gamma} p^2 x(1-x)$ with $\log \delta e^{\gamma} \Delta^2 x(1-x)$, Δ being the jet resolution. For $\Pi(g,g,g,g;s)$ or $\Pi(g,g,g,g,q)$, this substitution alone is enough to regulate the infrared divergence (the triangle or box diagrams involving fermions or scalars are devoid of further infrared divergences). While all the other processes (whenever there is a gluon propagator juxtaposed between two massless external legs), the computation is fraught with IR terms. But these IR terms when combined finally, are universal, which shows that they are physical infrared divergences, instead of light cone gauge artifices. Here I list all of them first.

All momenta appearing below are dual momenta, with the real momenta given by $p_1^+ = k_1^+ - k_2^+$, $p_2^+ = k_4^+ - k_1^+$, $p_3^+ = k_3^+ - k_4^+$, $p_4^+ = k_2^+ - k_3^+$ and $k_2^+ < k_3^+ < k_1^+ < k_4^+$, see Fig.5-1.

$$\frac{ig^4}{8\pi^2}\mathrm{Tr}[t^a t^b t^c t^d] \times$$

$k_2^+ < q^+ < k_3^+$

$$\log\frac{(k_4^+-q^+)(-k_2^++q^+)s\delta e^\gamma}{(k_2^+-k_4^+)^2}\left[\frac{1}{q^+-k_3^+}+\frac{1}{q^+-k_1^+}\right]$$
$$+\quad \log\frac{(k_1^+-q^+)(q^+-k_2^+)s\delta e^\gamma}{(k_1^+-k_2^+)(k_4^+-k_2^+)}\left[-\frac{2}{q^+-k_1^+}\right]$$
$$+\quad \log\frac{(k_3^+-q^+)(-k_2^++q^+)s\delta e^\gamma}{(k_3^+-k_2^+)(k_4^+-k_2^+)}\left[-\frac{2}{q^+-k_3^+}\right]$$
$$+\quad \log\frac{(-k_2^++q^+)^2 t\delta e^\gamma}{(k_1^+-k_2^+)(k_3^+-k_2^+)}\left[\frac{2}{q^+-k_2^+}\right]$$

$k_3^+ < q^+ < k_1^+$

$$\log\frac{(k_4^+-q^+)(-k_2^++q^+)s\delta e^\gamma}{(k_2^+-k_4^+)^2}\left[-\frac{1}{q^+-k_3^+}+\frac{1}{q^+-k_1^+}\right]$$
$$+\quad \log\frac{(k_3^+-q^+)(q^+-k_1^+)t\delta e^\gamma}{(-k_1^++k_3^+)^2}\left[-\frac{1}{q^+-k_2^+}+\frac{1}{q^+-k_4^+}\right]$$
$$+\quad \log\frac{(k_2^+-q^+)(q^+-k_1^+)s\delta e^\gamma}{(-k_1^++k_2^+)(k_2^+-k_4^+)}\left[-\frac{2}{q^+-k_1^+}\right]$$
$$+\quad \log\frac{(q^+-k_3^+)(k_4^+-q^+)s\delta e^\gamma}{(k_4^+-k_2^+)(k_4^+-k_3^+)}\left[\frac{2}{q^+-k_3^+}\right]$$
$$+\quad \log\frac{(-k_4^++q^+)(k_3^+-q^+)t\delta e^\gamma}{(k_3^+-k_4^+)(-k_1^++k_3^+)}\left[-\frac{2}{q^+-k_4^+}\right]$$
$$+\quad \log\frac{(k_2^+-q^+)(q^+-k_1^+)t\delta e^\gamma}{(-k_1^++k_2^+)(-k_1^++k_3^+)}\left[\frac{2}{q^+-k_2^+}\right]$$

$k_1^+ < q^+ < k_4^+$

$$\log\frac{(k_4^+-q^+)(-k_2^++q^+)s\delta e^\gamma}{(k_2^+-k_4^+)^2}\left[-\frac{1}{q^+-k_3^+}-\frac{1}{q^+-k_1^+}\right]$$
$$+\quad \log\frac{(q^+-k_1^+)(-k_4^++q^+)s\delta e^\gamma}{(k_4^+-k_1^+)(k_2^+-k_4^+)}\left[\frac{2}{q^+-k_1^+}\right]$$
$$+\quad \log\frac{(q^+-k_3^+)(k_4^+-q^+)s\delta e^\gamma}{(k_4^+-k_2^+)(k_4^+-k_3^+)}\left[\frac{2}{q^+-k_3^+}\right]$$
$$+\quad \log\frac{(-k_4^++q^+)^2 t\delta e^\gamma}{(k_4^+-k_1^+)(k_4^+-k_3^+)}\left[-\frac{2}{q^+-k_4^+}\right]$$

The above is always multiplied by the corresponding tree amplitude (by a tree, I mean whatever I wrote in front of the square bracket in the list of amplitudes). As long as the process has infrared divergence, the infrared divergence will be of the above form.

The infrared terms above will be combined with soft Bremsstrahlung and collinear emission (absorptions) along with the self-energy insertions on the external legs to give a finite result. The basic idea is the same as the standard treatment of infrared divergence. That is, we insist on measuring jets (within a certain resolution Δ) rather than gluons or quarks.

5.2 Bremsstrahlung Process

I will be focusing on final state bremsstrahlung radiation (region between leg 3 and 4) Fig.5-2, and study the four gluon core scattering process as an example.

$p_i,\ i = 1 \ldots 4$ and k are assumed to be incoming, and k will be called the extra one for now. The momenta of the 2-2 core process will be denoted as j_i, $i = 1 \ldots 4$ (j for jet). Possible sources of divergence associated with region 34 are

1. k is collinear with p_3 or p_4
2. k is soft.

We can look at roughly how each type of divergences get canceled. From Fig.5-3, it is quite natural to guess that the collinear divergence arising from k being parallel with p_3 is going to be cancelled by the corresponding self-energy bubble on leg 3. The cancellation will work as long as k is not too soft. We can make sure of this by setting k^+ away from zero as a cut off. What happens when $k \to 0$ is that we lose coherence. More concretely, when k is not too soft, we only need to worry about the case when it is attached to p_3. When $k \sim 0$, it can be attached to either p_3 or p_4. So we will be considering the following cancelation of Fig.5-4.

There is no natural boundary as to when k is soft enough. In fact, we can first impose an artificial boundary A, such that when $k^+ > A$ we use the scheme in Fig.5-3, when $k^+ < A$ we use the scheme in Fig.5-4. When the dust settles the A dependence disappears.

The method described above was used in [14], it involves a careful analyzing of phase space to avoid double counting. However the beautiful Parke-Taylor expression for helicity amplitudes greatly simplifies the computation: the first diagram in Fig.5-2 is given by (in the large N_c limit)

$$\begin{aligned} & \left| (g\sqrt{N_c})^3 \frac{\langle p_1|p_2\rangle^4}{\langle p_1|p_2\rangle\langle p_2|p_3\rangle\langle p_3|k\rangle\langle k|p_4\rangle\langle p_4|p_1\rangle} \right|^2 \\ = & \frac{g^6 N_c^3}{2} \frac{(p_1\cdot p_2)^4}{(p_1\cdot p_2)(p_2\cdot p_3)(p_3\cdot k)(k\cdot p_4)(p_4\cdot p_1)} \end{aligned} \tag{5–1}$$

It's quite clear from Eq.5–1 that when k is collinear with $p_{3,4}$ or soft, there will be divergences.

As stated before, we have to set k^+ away from zero in order to cut off infrared divergence, but this does not regulate collinear divergence, so a temporary cut-off ϵ will be used tentatively to cut off collinear divergence.

In order to parameterize the phase space, define (refer to Fig.5-5)

$$x = \frac{2Q\cdot(-p_3)}{Q^2},\ y = \frac{2Q\cdot(-p_4)}{Q^2},\ Q = p_1 + p_2 \tag{5–2}$$

The integration region of x and y is depicted in Fig.5-5, we will only be integrating x and y in the 'L' shaped region. R is related to detector resolution according to $R := \Delta^2/s$. The physical meaning of these cuts is quite clear: when $x \sim 1$, $k\cdot p_4 = 1/2(k+p_4)^2 = 1/2(Q+p_3)^2 = 1/2Q^2(1-x) = 0$; when $x, y \sim 1$, $k\cdot Q \sim 0$ (since Q is time-like, $k \sim 0$). Here and after, s and t will denote the Mandelstam invariants for the 2-2 core process.

A trick used in [24] turned out useful. Write

$$\begin{aligned} \frac{1}{(p_3\cdot k)(k\cdot p_4)} &= \frac{1}{(p_3\cdot k)(k\cdot(p_3+p_4))} + \frac{1}{(p_4\cdot k)(k\cdot(p_3+p_4))} \\ &= \frac{2}{s(1-y)}\frac{2}{s(2-x-y)} + \frac{2}{s(1-x)}\frac{2}{s(2-x-y)} \end{aligned} \tag{5–3}$$

The first term will only diverge when p_3 and k are collinear and(or) k is soft. The second term will only diverge when p_4 and k are collinear and(or) k is soft. For the second term, the integration of x and y in area A: $1-R<x<1-\epsilon;\ 1-x<y<1$ is divergent, but finite in the area B : $1-R<y<1;\ 1-y<x<1-R$. These two areas will be treated slightly differently.

- Region A:

Since $x\sim 1$, p_4 and k are either collinear or k is soft. All x at innocuous places can be set to be 1. Further define L to be a reference (light-like, $L^0>0$) 4-vector, such that $L\cdot p=p^+$. Now the 3 body phase space integral is given by

$$\frac{sx}{64(2\pi)^5}d\Omega_3 dx d\Omega_{4k}$$

$d\Omega_3$ is the angular integral of p_3. $d\Omega_{4k}$ includes the angular integral of p_4 and k, dx represents the integral of the norm of $\vec{p}_3$. Note that if the phase space integral is isotropic, it can be written as the standard form $sdx\,dy/128\pi^3$ for a 3-body final state. We can factorize the phase space integral into $[1/(8(2\pi)^2)d\Omega_3]\,[sx/(8(2\pi)^3)dxd\Omega_{4k}]$. Here p_3 is picked out as 'the special one', since in region A, p_3 is always hard, and is almost equal to j_3 of the 2-2 core process. I will integrate out $[sx/(8(2\pi)^3)d\Omega_{4k}]$, while the $[1/(8(2\pi)^2)d\Omega_3]$ part is what should be compared to the 2-2 process.

The second term of Eq.5–3 is parameterized as

$$\begin{aligned}
&\frac{g^6N_c^3}{2}\frac{(p_1\cdot p_2)^4}{(p_1\cdot p_2)(p_2\cdot p_3)(p_4\cdot k)(k\cdot(p_4+p_3))(p_4\cdot p_1)} \qquad (5\text{–}4)\\
=\ &\frac{g^6N_c^3s^4}{4s(p_2+p_3)^2(p_4+p_1)^2}\cdot\frac{1}{(p_4\cdot k)(k\cdot(p_4+p_3))}\\
=\ &\frac{g^6N_c^3s^4}{s(p_2+p_3)^2(p_4+p_1)^2}\cdot\frac{1}{s(1-x)s(2-x-y)}
\end{aligned}$$

As $x \sim 1$, $(p_2+p_3)^2 \sim t$, $(p_1+p_4)^2 \sim yt$. The first approximation is always good in region A, the second is good as long as p_4 is not too soft. Plug in the phase space integral, thus arriving at

$$\begin{aligned} & \int \frac{sx}{64\pi^3}\frac{g^6 N_c^3 s^2}{st(yt)}\cdot\frac{1}{(1-x)(2-x-y)}dxd\Omega_{4k} \\ = & \int \frac{x}{64\pi^3}g^2 N_c A_{core}^2\cdot\frac{1}{(1-x)(2-x)}(\frac{1}{y}+\frac{1}{2-x-y})dxd\Omega_{4k} \end{aligned} \tag{5–5}$$

where $A_{core} = g^4 N_c^2 (s/t)^2$, let us drop the factor $g^2 N_c A_{core}^2$ hereafter.

$d\Omega_{4k}$ can be expressed as

$$\begin{aligned} d\Omega_{4k} &:= \frac{2dudv}{\sqrt{(u_1-u)(u-u_0)}} \\ u &:= 1-\frac{2(1-y)}{x} \\ v &:= 1-\frac{2|k^+|}{|Q^+ + p_3^+|} \sim 1-\frac{2|k^+|}{|j_4^+|},\ (|k^+|<\lambda|j_4^+|) \\ w &:= 1-\frac{2|p_3^+|(1-x)}{|Q^+ + p_3^+|x} := 1-\frac{2b(1-x)}{x},\ b=\frac{|j_3^+|}{|j_4^+|} \end{aligned} \tag{5–6}$$

We can first pick a particular value of p_3, then go to the CM frame of $p_1+p_2+p_3$ to evaluate the invariant expression $\delta(k+p_4+p_1+p_2+p_3)\delta(k^2)\delta(p_4^2)d^4k\ d^4p_4$. Notice in this frame, u is in fact $\cos(\hat{p_3 k})$, v is $\cos(\hat{Lk})$ and w is $\cos\hat{p_3 L}$. Then after some exercises in Euclidean geometry in Fig.5-6, we can obtain the expression for $d\Omega_{4k}$.

$u_{0,1} := vw \pm \sqrt{(1-v^2)(1-w^2)}$ are the lower/upper limit of u (y) integral. The limit placed upon k^+ is for breaking the Bose symmetry between p_4 and k and to make sure that the approximation $(p_1+p_4)^2 \sim yt$ works (the λ dependence will drop out).

Performing the u integral using

$$\int_{-1}^{1} \frac{1}{a+bx}\frac{1}{\sqrt{1-x^2}} = \frac{\pi}{\sqrt{a^2-b^2}}\ (a>b>0)$$
$$= -\frac{\pi}{\sqrt{a^2-b^2}}\ (-a>b>0)$$

$$\int_{1-2\lambda}^{1} dv \int_{1-R}^{1-\epsilon} dx \frac{sx}{64\pi^3} A_{core}^2 \cdot \frac{1}{(1-x)(2-x)}\frac{2}{x}$$
$$(\frac{2\pi}{\sqrt{(\frac{2}{x}-1+u_1)(\frac{2}{x}-1+u_0)}} + \frac{2\pi}{\sqrt{(\frac{2}{x}-1-u_1)(\frac{2}{x}-1-u_0)}}) \qquad (5\text{–}7)$$

The first square root can be obtained from the second one by replacing v by $-v$. So I will only compute the second square-root. The following indefinite integral will perhaps be useful:

$$\int dx \frac{1}{\sqrt{x^2+1}}\frac{1}{a+bx} = \frac{1}{\sqrt{a^2+b^2}} \log \frac{-b+ax+\sqrt{(a^2+b^2)(x^2+1)}}{a+bx}$$

The second term of Eq.5–7 becomes

$$\frac{1}{16\pi^2}\int_{1-2\lambda}^{1} \frac{dv}{1-v}\Bigg[\log\frac{1-v}{\epsilon(1+v)}$$
$$+ \log\frac{-\left[(1-v)+(1+v-2b)R\right]+\sqrt{\left[(1-v)+(1+v-2b)R\right]^2+8bR^2(1+v)}}{4bR}\Bigg] \qquad (5\text{–}8)$$

here we have treated the two cut-off's R and ϵ differently: ϵ is set to zero with fixed v (fixed k^+) while R is taken to be small but non-zero. This treatment agrees with the strategy given in the paragraph above Eq.5–1. Notice the second term in the square bracket is finite (when k^+ is kept away from zero), while the first will be combined with self mass contributions to cancel the ϵ dependence.

We can make a change of variable (the y below is not the previous y):

$$-[(1-v)+(1+v-2b)R]+\sqrt{[(1-v)+(1+v-2b)R]^2+8bR^2(1+v)}=4bRy$$
$$\rightarrow \quad 1-v=2R\frac{1-by^2-y(1-b)}{y(1-R)+R};\ \frac{dv}{dy}=-2R\frac{b(1-R)y^2+2bRy+1-bR}{[R+y(1-R)]^2} \tag{5–9}$$

then the integral becomes

$$\begin{aligned}&\frac{1}{16\pi^2}\int_{y_0}^{y_1}\frac{b(1-R)y^2+2bRy+1-bR}{[R+y(1-R)][1-by^2-y(1-b)]}\log y+\frac{1}{16\pi^2}\int_{1-2\lambda}^{1}\frac{dv}{1-v}\log\frac{1-v}{\epsilon(1+v)}\\ =\ &\frac{1}{16\pi^2}\int_{y_0}^{y_1}\left[\frac{1-R}{[R+y(1-R)]}+\frac{1}{1-y}-\frac{1}{y+1/b}\right]\log y+\frac{1}{16\pi^2}\int_{1-2\lambda}^{1}\frac{dv}{1-v}\log\frac{1-v}{\epsilon(1+v)}\end{aligned} \tag{5–10}$$

where $y_0\simeq R(1-\lambda)/\lambda;\ y_1=1$. The above integral becomes

$$\begin{aligned}&\frac{1}{16\pi^2}\left[\int_{y_0}^{y_1}\frac{1-R}{[R+y(1-R)]}\log y-\frac{\pi^2}{6}-\mathrm{dilog}(1+b)\right]+\frac{1}{16\pi^2}\int_{1-2\lambda}^{1}\frac{dv}{1-v}\log\frac{1-v}{\epsilon(1+v)}\\ =\ &\frac{1}{16\pi^2}\Bigg[-\frac{1}{2}\log^2 R-\mathrm{dilog}\frac{1}{\lambda}+\log R\frac{1-\lambda}{\lambda}\log\lambda-\frac{\pi^2}{3}-\mathrm{dilog}(1+b)\\ +\ &\int_{1-2\lambda}^{1}\frac{dv}{1-v}\log\frac{1-v}{\epsilon(1+v)}\Bigg]\end{aligned} \tag{5–11}$$

We can do one more thing to make it more symmetric: as b always comes in pairs with $1/b$, we may replace $\mathrm{dilog}(1+|j_3^+/j_4^+|)$ with $-1/4\log^2|j_3^+/j_4^+|-\pi^2/12$ by using the formula $\mathrm{dilog}[1/(1-x)]+\mathrm{dilog}[1/x]=-\pi^2/6-1/2\log^2(1/x-1)$.

The first term of Eq.5–7 is obtained from the above by substituting v to $-v$ and the limit of y integral becomes $y\in[0,R\lambda/(1-\lambda)]$. We get

$$
\begin{aligned}
& \frac{1}{16\pi^2}\left[\mathrm{dilog}\frac{1}{1-\lambda}+\log R\frac{\lambda}{1-\lambda}\log\frac{1}{1-\lambda}+\int_{1-2\lambda}^{1}\frac{dv}{1+v}\log\frac{1+v}{\epsilon(1-v)}\right] \\
= & \frac{1}{16\pi^2}\Bigg\{-\mathrm{dilog}\frac{1}{\lambda}-\frac{\pi^2}{6}-\log R\log(1-\lambda)-\frac{1}{2}\log^2\lambda+\frac{1}{2}\log^2(1-\lambda) \\
& +\frac{1}{2}\left[-2\mathrm{dilog}\lambda-\log^2(1-\lambda)+\frac{\pi^2}{3}+2\log\epsilon\log(1-\lambda)\right]\Bigg\} \\
= & \log\frac{\epsilon}{R}\log(1-\lambda) \qquad (5\text{–}12)
\end{aligned}
$$

In fact, by noticing that $du/\sqrt{(u_1-u)(u-u_0)}$ behaves like (π times) δ function as $x\sim 1$, I can set $y=1-x(1-u)/2$ to be $1-x(1-v)/2\sim(1+v)/2$ in the first term of Eq.5–5, which will lead to the same result in a much quicker way.

- Region B

Now p_4 is the hard momentum, $(p_4+p_1)^2$ is equal to t, while $(p_3+p_2)^2$ is approximated as xt. The three body phase space integral should likewise be factored as $d\Omega_4 dy d\Omega_{3k}$. Since there is no need here to hold k^+ fixed, and the restriction $|k^+|<\lambda'|Q^+ + p_4^+|$ can be lifted, $sy/(8(2\pi)^3)dyd\Omega_{3k}$ is simply $sdxdy/(16\pi^2)$. Here I have used a different partition: λ', because the partition associated to leg 3 need not be the same as leg 4.

$$
\begin{aligned}
& \int\frac{g^6N_c^3 sydyd\Omega_{3k}}{(8(2\pi)^3)}\frac{s^4}{s(p_2+p_3)^2(p_4+p_1)^2}\frac{1}{s(1-x)s(2-x-y)} \\
= & \int\frac{g^6N_c^3 sdxdy}{16\pi^2}\frac{s^4}{s(xt)t}\cdot\frac{1}{s(1-x)s(2-x-y)}=\frac{1}{16\pi^2}\frac{\pi^2}{12}g^2N_cA_{core}^2 \qquad (5\text{–}13)
\end{aligned}
$$

I have dealt with the first term of Eq.5–3, the second is similar:

$$
\begin{aligned}
& \frac{1}{16\pi^2}\Bigg[-\frac{1}{2}\log^2 R-\mathrm{dilog}\frac{1}{\lambda'}+\log R\frac{1-\lambda'}{\lambda'}\log\lambda'-\frac{\pi^2}{3}-\mathrm{dilog}(1+|j_4^+/j_3^+|) \\
+ & \int_0^{\lambda'|j_3^+|}\frac{dk^+}{k^+}\log\frac{k^+}{\epsilon(|j_3^+|-k^+)}+\frac{\pi^2}{12} \\
+ & \mathrm{dilog}\frac{1}{1-\lambda'}+\log R\frac{\lambda'}{1-\lambda'}\log\frac{1}{1-\lambda'}+\int_0^{\lambda'|j_3^+|}\frac{dk^+}{|j_3^+|-k^+}\log\frac{|j_3^+|-k^+}{\epsilon k^+}\Bigg] \qquad (5\text{–}14)
\end{aligned}
$$

So far, I have covered the first diagram of Fig.5-2 when k does not dominate over neither p_3 nor p_4 ($k^+ < \lambda|j_4^+|$, $k^+ < \lambda'|j_3^+|$). To complete the region $k^+ > \lambda|j_4^+|$, we need to do a computation in region 14.

$$\begin{aligned} & \frac{g^6 N_c^3 s^4}{4s(p_2+p_3)^2(p_4+p_1)^2} \cdot \frac{1}{(p_4\cdot k)(k\cdot(p_4+p_3))} \\ = \; & \frac{g^6 N_c^3 s^3}{8(p_2+p_3)^2(k\cdot(p_4+p_3))}\left[-\frac{1}{p_4\cdot k}\frac{1}{p_4\cdot(k-p_1)}+\frac{1}{p_4\cdot p_1}\frac{1}{p_4\cdot(k-p_1)}\right] \end{aligned} \tag{5–15}$$

with $(k+p_4)^2 < Rs$ and $|k^+| > \lambda|j_4^+|$. One point that I should have emphasized earlier is that in the presence of $1/(p_4\cdot k)$, we can only make approximations controlled by $\mathcal{O}(p_4\cdot k)$, and similarly in the presence of $1/(p_4\cdot p_1)$, we can only make approximations controlled by $\mathcal{O}(p_4\cdot p_1)$, otherwise there will be errors of the type $R\log\epsilon$. This rule makes the evaluation of the first term much easier: we can set k to be parallel to p_4 in all the irrelevant terms.

$$-\frac{g^6 N_c^3 s^3}{8(p_2+p_3)^2(k\cdot(p_4+p_3))}\frac{1}{p_4\cdot k}\frac{1}{p_4\cdot(k-p_1)} = -\frac{g^6 N_c^3 s^3}{8t(k\cdot(p_4+p_3))}\frac{1}{p_4\cdot k}\frac{1}{p_4\cdot(k-p_1)}$$

Now set up a parametrization for region 14:

$$\tilde{x} = \frac{2p_1\cdot(p_1-p_4-k)}{(p_1-p_4-k)^2} \qquad \tilde{y} = \frac{-2k\cdot(p_1-p_4-k)}{(p_1-p_4-k)^2}$$

Abbreviate (p_1-p_4-k) as T. Then $k\cdot p_4$ can be worked out as $1/2(1-\tilde{x})T^2$. With this parametrization:

$$-\frac{g^6 N_c^3 s^3}{8t(k\cdot(p_4+p_3))}\frac{1}{p_4\cdot k}\frac{1}{p_4\cdot(k-p_1)} = -\frac{g^6 N_c^3 s^3}{t\tilde{y}s}\frac{1}{(1-\tilde{x})T^2}\frac{1}{(2-\tilde{x}-\tilde{y})T^2}$$

In the limit $\tilde{x}=1$, $T^2=|t|$. In fact, the above expression can be calculated without effort, simply by identifying λ as $1-\lambda$ and b as $p_1^+/|p_4^+|$ (p_1 and p_4 here are the core values), we can borrow the result from Eq.5–11.

$$
\begin{aligned}
- & \int \frac{g^6 N_c^3 T^2 d\tilde{x} d\Omega_{4k}}{64\pi^3} \frac{s^3}{t\tilde{y}s} \frac{1}{(1-\tilde{x})T^2} \frac{1}{(2-\tilde{x}-\tilde{y})T^2} \\
= & \frac{g^2 N_c A_{core}^2}{16\pi^2} \Bigg[-\frac{1}{2}\log^2 \tilde{R} - \mathrm{dilog}\frac{1}{1-\lambda} + \log\tilde{R}\frac{\lambda}{1-\lambda}\log(1-\lambda) - \frac{\pi^2}{3} - \mathrm{dilog}(1+\frac{j_1^+}{|j_4^+|}) \\
+ & \int_{\lambda|j_4^+|}^{|j_4^+|} \frac{dk^+}{|j_4^+|-k^+} \log\frac{|j_4^+|-k^+}{\tilde{\epsilon}k^+} \Bigg] \\
+ & \frac{1}{16\pi^2} \left[\mathrm{dilog}\frac{1}{\lambda} + \log\tilde{R}\frac{1-\lambda}{\lambda}\log\frac{1}{\lambda} + \int_{\lambda|j_4^+|}^{|j_4^+|} \frac{dk^+}{k^+} \log\frac{k^+}{\tilde{\epsilon}(|j_4^+|-k^+)} \right] \qquad (5\text{–}16)
\end{aligned}
$$

Comparing this to Eq.5–11, 5–12, we see that the λ dependence cancels.

Now we look at the second term of Eq.5–15, it in fact can be interpreted as a false jet, since it will make a contribution when p_4 is parallel with p_1, thus the final state will be a three well separated jets unless p_4 is soft. Our task is to compute this term in the region $2k\cdot p_4 < Rs$ with $|j_4^+| > |k^+| > \lambda|j_4^+|$. This region can be dissembled into a part $\{1-\tilde{x} < \tilde{R}\}\bigcap\{\tilde{y} < 1-\tilde{R}\}$, which produces a $1/(16\pi^2)\pi^2/12$ (the restriction on k^+ makes no difference).

There is the other part: $\{1-\tilde{x} < \tilde{R}\}\bigcap\{1-\tilde{y} < \tilde{R}\}\bigcap\{|k^+| > \lambda|j_4^+|\}$. Here I only lay out the strategy if one were to compute it honestly. First compute in region $\{1-\tilde{y} < \tilde{R}\}$ with no restriction on k^+, then subtract the entire region of $\{\tilde{x} < 1-\tilde{R}\}\bigcap\{1-\tilde{y} < \tilde{R}\}$ again with no restriction on k^+. The validity of this strategy lies in the fact that there exists an upper limit of order $\mathcal{O}(\tilde{R})$ for $|p_4^+|$, beyond which there is no intersection with the region $\{1-\tilde{x} < \tilde{R}\}\bigcap\{1-\tilde{y} < \tilde{R}\}$, while the limit $|k^+| > \lambda|j_4^+|$ translated to $|p_4^+| < (1-\lambda)|j_4^+|$ is well beyond the said upper limit.

Yet in practice, the condition that we can only make approximation of order $p_4\cdot p_1 = 0$ makes the evaluation (and interpretation) quite hard. So we make a compromise, and allow for errors of $R\log\epsilon$, trusting that it will go away with a complete calculation. I shall set not only $p_4\cdot p_1 = 0$ but also $p_4\cdot k = 0$. Then, this term will cancel against some disconnected diagrams which will be explained later.

So the completed result for Eq.5–4 is

$$\frac{1}{16\pi^2}\Big[-\frac{1}{2}\log^2\tilde{R}-\frac{\pi^2}{4}-\mathrm{dilog}(1+\frac{j_1^+}{|j_4^+|})+\int_0^{|j_4^+|}\frac{dk^+}{|j_4^+|-k^+}\log\frac{|j_4^+|-k^+}{\tilde{\epsilon}k^+}\Big]$$
$$+\quad\frac{1}{16\pi^2}\Big[-\frac{1}{2}\log^2 R-\frac{\pi^2}{4}-\mathrm{dilog}(1+\frac{|j_3^+|}{|j_4^+|})+\int_0^{|j_4^+|}\frac{dk^+}{k^+}\log\frac{k^+}{\epsilon(|j_4^+|-k^+)}\Big] \tag{5–17}$$

It makes a similar contribution associated to leg 3, with some suitable substitutions.

Let us take a look at the self-energy bubble on leg 4 Fig.5-7, calculated with a cut off $K^i_{4,k}K^i_{4,k}/p_4^+k^+>\mu^2$ to regulate the on shell divergence. ϵ should be in this case identified with μ^2/s and $\tilde{\epsilon}$ with $\mu^2/|t|$.

The wave function renormalization of these diagrams are (with the 1/2 from '$\sqrt{Z}$' and another 2 since it enters as a cross term):

$$\begin{aligned}
\text{left:}\quad & \int_0^1\frac{1}{16\pi^2}\Big[\frac{1}{x}+\frac{1}{1-x}\Big]\log x(1-x)\mu^2\\
\text{middle:}\quad & \int_0^1\frac{1}{16\pi^2}\frac{(1-x)^3}{x}\log x(1-x)\mu^2\\
\text{right:}\quad & \int_0^1\frac{1}{16\pi^2}\frac{x^3}{1-x}\log x(1-x)\mu^2
\end{aligned} \tag{5–18}$$

where x is $|k^+|/|j_4^+|$. Not all of Eq.5–18 will contribute to region 34. For now, I only take the first line. Combine Eq.5–18 to the expression above:

$$\frac{1}{16\pi^2}\Big[-\frac{1}{2}\log^2 R-\frac{1}{2}\log^2\tilde{R}-\frac{\pi^2}{2}-\mathrm{dilog}(1+\frac{|j_3^+|}{|j_4^+|})-\mathrm{dilog}(1+\frac{j_1^+}{|j_4^+|})$$
$$+\quad\int_0^{|j_4^+|}\frac{dk^+}{k^+}\log\frac{k^{+2}s}{j_4^{+2}}+\int_0^{|j_4^+|}\frac{dk^+}{|j_4^+|-k^+}\log\frac{(|j_4^+|-k^+)^2|t|}{j_4^{+2}}\Big]$$

Thus, the effect of a self-mass insertion is to replace ϵ by $1/sx(1-x)$ or $1/|t|x(1-x)$.

Fig.5-8 represents all the diagrams that contribute to the Bremsstrahlung process. The second diagram of Fig.5-2 or Fig.5-8, when combined with the second line of Eq.5–18, will contribute to leg 4:

$$\frac{1}{16\pi^2}\Big[-\frac{1}{2}\log^2 R-\frac{\pi^2}{4}-\mathrm{dilog}(1+\frac{|j_3^+|}{|j_4^+|})$$
$$+\int_0^{|j_4^+|}\frac{dk^+}{k^+}\log\frac{k^{+2}s}{j_4^{+2}}+\int_0^1(-3+3x-x^2)\log x(1-x)Rs\Big] \qquad (5\text{–}19)$$

Note its contribution here should be attributed to region 34. This diagram won't contribute to region 14, because it remains finite when $p_4 \to 0$.

The third is similar to the second:

$$\frac{1}{16\pi^2}\Big[-\frac{1}{2}\log^2\tilde{R}-\frac{\pi^2}{4}-\mathrm{dilog}(1+\frac{j_1^+}{|j_4^+|})$$
$$+\int_0^{|j_4^+|}\frac{dk^+}{k^+}\log\frac{k^{+2}|t|}{j_4^{+2}}+\int_0^1(-3+3x-x^2)\log x(1-x)R|t|\Big] \qquad (5\text{–}20)$$

Note that it is credited to region 14.

In summary, the contribution from Bremsstrahlung plus self-mass insertion to region 34 is

$$\frac{1}{16\pi^2}\Big[-2\log^2\frac{\Delta^2}{s}-\pi^2-2\left(-\frac{\pi^2}{6}-\frac{1}{2}\log^2\frac{|j_3^+|}{|j_4^+|}\right)$$
$$+2\int_0^{|j_4^+|}\frac{dk^+}{k^+}\log\frac{k^{+2}s}{j_4^{+2}}+2\int_0^{|j_3^+|}\frac{dk^+}{k^+}\log\frac{k^{+2}s}{j_3^{+2}}+\frac{67}{9}-\frac{11}{3}\log\Delta^2\Big]$$

And a symmetric contribution to region 14:

$$\frac{1}{16\pi^2}\Big[-2\log^2\frac{\Delta^2}{|t|}-\pi^2-2\left(-\frac{\pi^2}{6}-\frac{1}{2}\log^2\frac{p_1^+}{|p_4^+|}\right)$$
$$+2\int_0^{|j_4^+|}\frac{dk^+}{k^+}\log\frac{k^{+2}|t|}{j_4^{+2}}+2\int_0^{j_1^+}\frac{dk^+}{k^+}\log\frac{k^{+2}|t|}{j_1^{+2}}+\frac{67}{9}-\frac{11}{3}\log\Delta^2\Big]$$

As a summary, although the kinematics in 14 and 34 region are very different, the results are almost symmetric up to the false jets that I haven't included. Next, we study how to combine these results to the virtual process, and defer the discussion of the false jets.

5.3 Combining with the Infrared Terms from the Virtual Process

The list of infrared terms in Section 5.1 can be rewritten in a more symmetric form that is independent of the relative size of the dual momenta:

Region 34:

$$\frac{-1}{8\pi^2}\left[\int_0^{|p_4^+|}\frac{dk^+}{k^+}\log\frac{k^{+2}s}{|p_4^+||p_3^+|}+\int_0^{|p_3^+|}\frac{dk^+}{k^+}\log\frac{k^{+2}s}{|p_3^+||p_4^+|}\right.$$
$$\left.+\int_{-|p_4^+|}^{|p_3^+|}\frac{dk^+}{k^+}\log\frac{(|p_3^+|-k^+)|p_4^+|}{(|p_4^+|+k^+)|p_3^+|}\right] \tag{5–21}$$

Region 12:

$$\frac{-1}{8\pi^2}\left[\int_0^{|p_1^+|}\frac{dk^+}{k^+}\log\frac{k^{+2}s}{|p_1^+||p_2^+|}+\int_0^{|p_2^+|}\frac{dk^+}{k^+}\log\frac{k^{+2}s}{|p_1^+||p_2^+|}\right.$$
$$\left.+\int_{-|p_1^+|}^{|p_2^+|}\frac{dk^+}{k^+}\log\frac{(|p_2^+|-k^+)|p_1^+|}{(|p_1^+|+k^+)|p_2^+|}\right]$$

Region 41:

$$\frac{-1}{8\pi^2}\left[\int_0^{|p_1^+|}\frac{dk^+}{k^+}\log\frac{k^{+2}(-t)}{|p_1^+||p_4^+|}+\int_0^{|p_4^+|}\frac{dk^+}{k^+}\log\frac{k^{+2}(-t)}{|p_1^+||p_4^+|}\right.$$
$$\left.+\int_{|p_4^+|}^{|p_1^+|}\frac{dk^+}{k^+}\log\frac{(|p_1^+|-k^+)|p_4^+|}{(k^+-|p_4^+|)|p_1^+|}\right]$$

Region 23:

$$\frac{-1}{8\pi^2}\left[\int_0^{|p_2^+|}\frac{dk^+}{k^+}\log\frac{k^{+2}(-t)}{|p_2^+||p_3^+|}+\int_0^{|p_3^+|}\frac{dk^+}{k^+}\log\frac{k^{+2}(-t)}{|p_2^+||p_3^+|}\right.$$
$$\left.+\int_{|p_3^+|}^{|p_2^+|}\frac{dk^+}{k^+}\log\frac{(|p_2^+|-k^+)|p_3^+|}{(k^+-|p_3^+|)|p_2^+|}\right]$$

The first two terms of Eq.5–21 cancels the divergence of Eq.5–19, while the last term integrates to be $-1/(16\pi^2)\left[-\pi^2-\log^2\left(p_3^+/p_4^+\right)\right]$. Finally, all the non-covariance pieces cancel and everything falls together nicely:

$$\frac{1}{8\pi^2}[-\log^2\frac{\Delta^2}{s}+\frac{\pi^2}{3}+\frac{67}{18}-\frac{11}{6}\log\Delta^2] \tag{5–22}$$

is the total contribution of virtual and Bremsstrahlung processes to region 34. While for region 14 we have similarly:

$$\frac{1}{8\pi^2}[-\log^2\frac{\Delta^2}{|t|}-\frac{2\pi^2}{3}+\frac{67}{18}-\frac{11}{6}\log\Delta^2] \tag{5–23}$$

Thus, we can write down the total scattering probability:

$$\begin{aligned}
&P(g+,g+,g-,g-;g)_1 = \\
&P(g+,g+,g-,g-;g)_0\Bigg[1+\frac{g_s^2N_c}{8\pi^2}\times \\
&\Bigg[-2\log^2\frac{\Delta^2}{s}-2\log^2\frac{\Delta^2}{|t|}-\frac{\pi^2}{3}+\frac{67}{9}-\frac{11}{3}\log\frac{\delta\Delta^4e^\gamma}{|t|}+\log^2\frac{s}{|t|}\Bigg]\Bigg]
\end{aligned}$$

$$\begin{aligned}
&P(g+,g-,g+,g-;g)_1 = \\
&P(g+,g-,g+,g-;g)_0\Bigg[1+\frac{g_s^2N_c}{8\pi^2}\times \\
&\Bigg[-2\log^2\frac{\Delta^2}{s}-2\log^2\frac{\Delta^2}{|t|}-\frac{\pi^2}{3}+\frac{67}{9}-\frac{11}{3}\log\frac{\delta\Delta^4e^\gamma}{s} \\
&\frac{(s^2+st+t^2)^2}{(t+s)^4}\log^2\frac{s}{|t|}-\frac{s}{3}\frac{(14t^2+19st+11s^2)}{(t+s)^3}\cdot\log\frac{s}{|t|}-\frac{ts}{(t+s)^2}\Bigg]\Bigg]
\end{aligned}$$

And the probability with $\mathcal{N}=4$ SYM is

$$
\begin{aligned}
& P(g+,g+,g-,g-;SYM)_1 \\
= \;& P(g+,g+,g-,g-)_0\Big[1+\frac{g^2N_c}{8\pi^2}\Big[-2\log^2\frac{\Delta^2}{s}-2\log^2\frac{\Delta^2}{|t|}-\frac{\pi^2}{3}+[\frac{67}{9}-\frac{5}{18}N_s-\frac{26}{9}N_f] \\
+ \;& \log\frac{\delta e^\gamma\Delta^4}{|t|}[-\frac{11}{3}+\frac{1}{6}N_s+\frac{4}{3}N_f]+\log^2\frac{s}{|t|}\Big]\Big]
\end{aligned}
$$

$$
\begin{aligned}
& P(g+,g-,g+,g-;SYM)_1 \\
= \;& P(g+,g+,g-,g-)_0\Big[1+\frac{g^2N_c}{8\pi^2}\Big[-2\log^2\frac{\Delta^2}{s}-2\log^2\frac{\Delta^2}{|t|}-\frac{\pi^2}{3}+[\frac{67}{9}-\frac{5}{18}N_s-\frac{26}{9}N_f] \\
+ \;& \log\frac{\delta e^\gamma\Delta^4}{s}[-\frac{11}{3}+\frac{1}{6}N_s+\frac{4}{3}N_f] \\
+ \;& \frac{1}{2(s+t)^4}\log^2\frac{s}{|t|}[s^2t^2N_s+2st(s^2+t^2)N_f+2(s^2+st+t^2)^2] \\
+ \;& \frac{1}{6(s+t)^3}\log\frac{s}{|t|}[-s(2t^2-5st-s^2)N_s+4s(5t^2+st+2s^2)N_f-2s(14t^2+19st+11s^2)] \\
+ \;& \frac{st}{2(s+t)^2}[-N_s+4N_f-2]\Big]\Big] \qquad (5\text{–}24)
\end{aligned}
$$

5.4 The Inclusion of Disconnected Diagrams

In this section I will discuss certain disconnected diagrams Fig.5-9, whose importance was explained in [16].

Only the cross term between the first and others in Fig.5-9 has the correct power in coupling constant, and the factor $2E_k(2\pi)^3\delta^3(\vec{k}-\vec{k}') = (2\pi)^4\delta^4(k-k')$ corresponding to the forward particle line will force the two extra legs to have the same momentum.

The fourth and fifth diagram of Fig.5-9 look rather like self-energy diagrams, and indeed they will receive the same factor of $1/2$ discount just as self-energy diagrams on the external legs do. The fourth (resp. fifth) diagram will have to be evaluated first with p_4 (resp. p_1) off shell. When the dust settles, any term that do not contain p_1^2 or p_4^2 will be dropped just the same as we are wont to drop the tadpole diagrams.

We have insisted on having two partons scattering into two jets, so the two extra gluons have to be soft. The Feynman rules give (with the approximation $k \sim 0$)

$$\left(-ig\sqrt{\frac{N_c}{2}}\right)^2 A^2_{core}\left\{-\frac{8p_1\cdot p_4}{(k+p_1)^2(k-p_4)^2}\right\}\sim -g^6N_c^3\frac{s^2}{t^2}\frac{t}{2(k\cdot p_1)(k\cdot p_4)} \tag{5–25}$$

to be evaluated in the region $(k-p_3)^2<\Delta^2$ and $(k-p_4)^2<\Delta^2$.

Next I show that it will cancel the false jet terms. Setting $p_4\cdot p_1=0$ and $p_4\cdot k=0$ in the second term of Eq.5–15:

$$\frac{g^6N_c^3s^3}{8(p_2+p_3)^2(k\cdot(p_4+p_3))}\frac{1}{p_4\cdot p_1}\frac{1}{p_4\cdot(k-p_1)}\sim\frac{g^6N_c^3s^3}{4ts}\frac{1}{p_4\cdot p_1}\frac{1}{p_4\cdot(k-p_1)}$$

The third diagram of Fig.5-8 will double the above. To make comparison with the disconnected diagrams, we need to identify k with p_4 and p_4 with $-k$:

$$2\times\frac{g^6N_c^3s^3}{4ts}\frac{1}{p_4\cdot p_1}\frac{1}{p_4\cdot(k-p_1)}\to\frac{g^6N_c^3s^3}{2ts}\frac{1}{(-k\cdot p_1)(-k\cdot(p_4-p_1))} \tag{5–26}$$

The fifth and seventh diagram will give a similar contribution:

$$2\times\frac{g^6N_c^3s^3}{8(p_2+p_3)^2(k\cdot(p_1+p_2))}\frac{1}{p_1\cdot p_4}\frac{1}{p_1\cdot(k-p_4)}\sim\frac{g^6N_c^3s^3}{2ts}\frac{1}{p_1\cdot p_4}\frac{1}{p_1\cdot(k-p_4)}$$

Now identify k with p_1 and p_1 with k:

$$\frac{g^6N_c^3s^3}{2ts}\frac{1}{p_1\cdot p_4}\frac{1}{p_1\cdot(k-p_4)}\to\frac{g^6N_c^3s^3}{2ts}\frac{1}{(k\cdot p_4)(k\cdot(p_1-p_4))} \tag{5–27}$$

The sum of Eq.5–26 and Eq.5–27 cancels Eq.5–25. The cancelation above is ad hoc and certainly not the prettiest. For one thing, we have made approximations of order $\mathcal{O}(R\log\epsilon)$, for another, the interpretation of the disconnected diagrams as false jets is not intuitive. However we can see the similarity between Fig.5-9 and the false jet terms: 5–26 (resp. 5–27) would be a lot more natural had p_4(resp. p_1) be an incoming(resp. outgoing) particle. While if we could change the sign of k^0 in Fig.5-9, they would all become true

loop diagrams. So both the false jets and Fig.5-9 have the 'incoming-outgoing-reversed' problem. I believe a better way of dealing with them is possible.

In [14], the false jets come more naturally. They come from the diagrams with leg 4 *absorbing* a gluon collinear with itself, or leg 1 *emitting* a gluon collinear with itself. These processes suffer collinear divergences, and they are cured by the fourth and fifth diagram in Fig.5-9, while the cross term between them is canceled by the second and third in Fig.5-9.

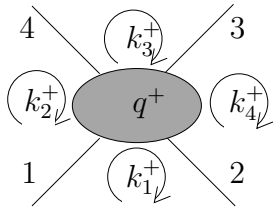

Figure 5-1. Dual momentum assignment

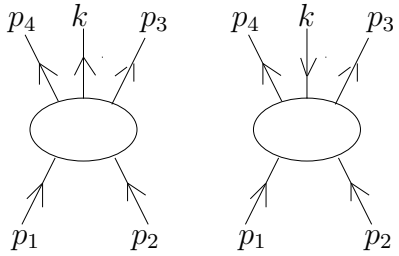

Figure 5-2. Two diagrams with an extra 'unseen' gluon the arrows indicate helicities,all momenta are incoming

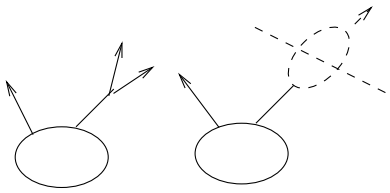

Figure 5-3. Cancelation of collinear divergence

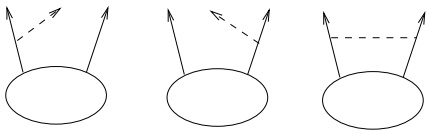

Figure 5-4. Cancelation of the soft bremsstrahlung radiation against a virtual process

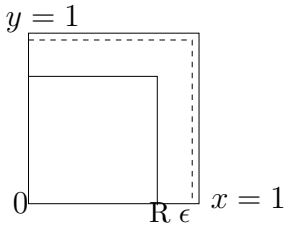

Figure 5-5. Phase space integration region of x and y

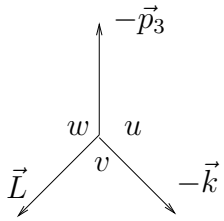

Figure 5-6. Configuration of $\vec{k}$, $\vec{p}_3$ and $\vec{L}$ in the CM frame of $p_1 + p_2 + p_3$

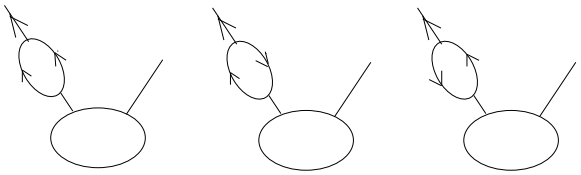

Figure 5-7. Self-energy bubble on leg 4, they will cancel the ϵ dependence in the Bremsstrahlung

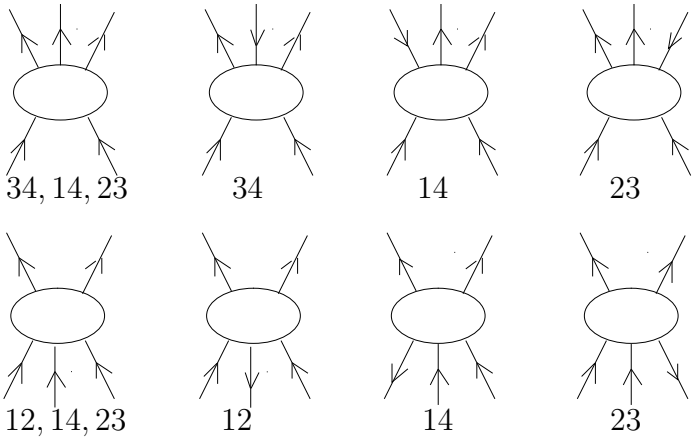

Figure 5-8. All non-vanishing Bremsstrahlung processes, the numbers underneath them are the regions they contribute to

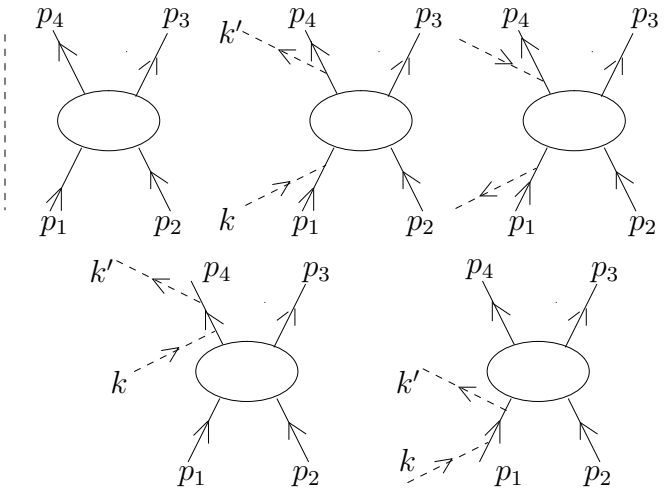

Figure 5-9. Disconnected Bremsstrahlung with two extra 'unseen' gluons

CHAPTER 6
GLUON SCATTERING WITH MASSIVE MATTER FIELDS

I only computed gluon scattering amplitude with massive matter in the loop, for these are the only processes without any internal gluon propagators. If it were not so, we have to devise a way to regulate the infrared divergences. Dimension regulation certainly works, and the entire problem is reduced to calculating the 'box coefficients'. But this is simply bringing coals to Newcastle, as there are people who have already developed the technique and can do it a hundred times faster than me. The new thing about our calculation is the physical infrared cut off that does have a meaning, yet I haven't worked out how to incorporate this cut off into massive amplitudes.

6.1 Computation Technique

The main difficulty for the massive field calculation is the Feynman parameter integrals. Indeed, I can only reduce all Feynman parameter integrals into a set of three definitive integrals. They are

$$\begin{aligned} I(s) &:= \int_0^1 dx \frac{s}{sx(1-x)+M} = \frac{4s}{\sqrt{s^2+4Ms}} \sinh^{-1}\sqrt{\frac{s}{4M}} \\ J(s) &:= \int_0^1 dx \frac{1}{x} \log\frac{sx(1-x)+M}{M} = 2\left(\sinh^{-1}\sqrt{\frac{s}{4M}}\right)^2 \\ K(s,t) &:= \int_0^1 dx \frac{st}{stx(1-x)+M(s+t)} \log\frac{(sx(1-x)+M)(tx(1-x)+M)}{M^2} \end{aligned} \quad (6\text{–}1)$$

Where M is in fact $-m^2+i\epsilon$. As $M \to 0$:

$$\begin{aligned} I(s) &\sim 2\log\frac{s}{M} \\ J(s) &\sim \frac{1}{2}\log^2\frac{s}{M} \\ K(s,t) &\sim -\pi^2 + 2\log\frac{s}{M}\log\frac{t}{M} \\ K(s,t)-2J(s)-2J(t) &\sim -\pi^2 - \log^2\frac{s}{t} \end{aligned} \quad (6\text{–}2)$$

For example, a simple integral:

$$\int_0^1 \delta(x_1+x_2+x_3+x_4-1)dx_1dx_2dx_3dx_4 \frac{x_1x_2(1-x_1-x_2)}{(x_1x_3t+x_2x_4s+M)^2}$$

can be reduced to

$$-\frac{M}{s^2(s+t)}J(s)-\frac{M}{t^2(s+t)}J(t)-\frac{M}{2st(s+t)}K(s,t)+\frac{1}{2st}$$

The definition of Eq.6–1 is in accord with [27, 31]. The last integral of Eq.6–1 can be expressed as dilogarithm and logarithms. In [30], the author gave two equivalent expressions of the box integrals, one in terms of dilogarithms the other in terms of hypergeometric functions. But for the purpose of this paper, I find it most convenient to use Eq.6–1 to spell out the results.

The Feynman rules for scalar fields remain good, but the decomposition Eq.2–25 does not, since it introduces $1/q^+$ factors into the Feynman rules. This will complicate the already complicated Feynman parameter integral. Also q^+ and q^- will be treated the same in contrast to the massless case, where q^- is integrated out and q^+ is given by $\sum x_i k_i^+ / \sum x_i$.

In order to organize the gamma matrix algebra in the fermion part of the calculation, we make use of the factorizability of gluon polarisation vectors Eq.2–21 to reduce products of gamma matrices to products of $K_{ij}^\mu = p_i^+ p_j^\mu - p_j^+ p_i^\mu$, which had been proved to be quite handy. For example, if we are to calculate the diagram Fig.4-1. We would write down:

$$\Pi(g+,g-,q) = (ig)^2 \mathrm{Tr}(t^a t^b) \frac{\mathrm{Tr}\left([(q-k_1)\cdot\gamma+m]\gamma_\mu[(q-k_3)\cdot\gamma+m]\gamma_\nu\right)(-\epsilon_\vee^\mu)(-\epsilon_\wedge^\nu)}{(-i)\left[(q-k_1)^2-m^2\right](-i)\left[(q-k_3)^2-m^2\right]} \quad (6\text{–}3)$$

The numerator can be written as

$$\mathrm{Tr}\left[\left|\begin{array}{cc} m & (q-k_1)\cdot\sigma \\ (q-k_1)\cdot\bar{\sigma} & m \end{array}\right|\left|\begin{array}{cc} 0 & -\sqrt{2}|\eta\rangle[k_3-k_1| \\ -\sqrt{2}|k_1-k_3]\langle\eta| & 0 \end{array}\right|\times\right.$$
$$\left.\left|\begin{array}{cc} m & (q-k_3)\cdot\sigma \\ (q-k_3)\cdot\bar{\sigma} & m \end{array}\right|\left|\begin{array}{cc} 0 & -\sqrt{2}|k_1-k_3\rangle[\eta| \\ -\sqrt{2}|\eta]\langle k_3-k_1| & 0 \end{array}\right|\right]$$
$$= 2[\eta|q-k_1|\eta\rangle[k_3-k_1|q-k_3|k_1-k_3\rangle + 2\langle k_1-k_3|q-k_1|k_3-k_1]\,\langle\eta|q-k_3|\eta]$$
$$+\langle k_1-k_3|m|\eta\rangle\,[k_3-k_1|m|\eta] + [\eta|m|k_3-k_1]\langle\eta|m|k_1-k_3\rangle \qquad (6\text{–}4)$$

For the notation of spinor, see the appendix. The standard procedure of momentum integration tell us to shift $q \to q + xk_1 + (1-x)k_3$, and to replace $q^\mu q^\nu$ by $q^2 g^{\mu\nu}/4$, etc:

$$\begin{aligned} & [\eta|q-k_1|\eta\rangle[k_3-k_1|q-k_3|k_1-k_3\rangle \\ = \;& [\eta|(1-x)(k_3-k_1)|\eta\rangle[k_3-k_1|x(k_1-k_3)|k_1-k_3\rangle + [\eta|\bar{\sigma}^\mu_{\dot{a}a}|\eta\rangle[k_3-k_1|\bar{\sigma}^\nu_{\dot{b}b}|k_1-k_3\rangle\frac{g_{\mu\nu}q^2}{4} \\ = \;& (1-x)\sqrt{2}(k_3-k_1)^+\sqrt{2}\frac{x(k_1-k_3)^2}{2(k_1-k_3)^+} + [\eta|k_3-k_1]\langle k_1-k_3|\eta\rangle\,\frac{q^2}{2} \\ = \;& -x(1-x)(k_1-k_3)^2 + \frac{q^2}{2} \end{aligned} \qquad (6\text{–}5)$$

here we have used an identity:

$$\bar{\sigma}^\mu_{\dot{a}a}\bar{\sigma}^\nu_{\dot{b}b}g_{\mu\nu} = 2\epsilon_{\dot{a}\dot{b}}\epsilon_{ab}; \quad \sigma^{a\dot{a}}_\mu\sigma^{b\dot{b}}_\nu g^{\mu\nu} = 2\epsilon^{ab}\epsilon^{\dot{a}\dot{b}} \qquad (6\text{–}6)$$

For a more complicated example, a string of spinor products becomes (with q shifted to $q + x_2k_2 + x_1k_1 + x_4k_4 + x_3k_3$)

$$\begin{aligned} & [p_1|q-k_2|p_4\rangle[\eta|q-k_3|p_3\rangle \\ = \;& [p_1|q + x_1(k_1-k_2) + x_4(k_4-k_2) + x_3(k_3-k_2)|p_4\rangle \\ & [\eta|q + x_2(k_2-k_3) + x_1(k_1-k_3) + x_4(k_4-k_3)|p_3\rangle \\ = \;& [p_1|\eta]\langle p_3|p_4\rangle\frac{q^2}{2} + [p_1|x_4p_2|p_4\rangle[\eta|x_2p_4 - x_1p_2|p_3\rangle \\ = \;& (-1)\frac{1}{p_3^+p_4^+}K^\wedge_{43}\frac{q^2}{2} + \frac{\sqrt{2}x_4}{p_1^+p_2^+p_4^+}K^\vee_{12}K^\wedge_{42}(\frac{\sqrt{2}x_2}{p_3^+}K^\wedge_{34} - \frac{\sqrt{2}x_1}{p_3^+}K^\wedge_{32}) \end{aligned} \qquad (6\text{–}7)$$

Basically, all of the spinor products can be reduced to one of the K_{ij}'s, and the reader can find in the appendix some practical details as to how to organize the products of K_{ij}'s. After the momentum integral is done, we can perform the Feynman parameter integrals using Eq.6–1.

However, there is one more complication due to the δ regulator: the integration over $q^{\wedge(\vee)}$ is different from $q^{+(-)}$. Since the momentum integration is no longer homogeneous, the replacement of $q^\mu q^\nu$ by $q^2 g^{\mu\nu}/4$ is problematic. But fortunately, when doing the contraction of $q^\mu q^\nu \to g^{\mu\nu} q^2/4$, $q^{\wedge(\vee)}$ and $q^{+(-)}$ will never coexist. For example, in the first line of Eq.6–5, only q^+ will appear in the first bracket while only $q^\wedge$, $q^\vee$, q^- appears in the second bracket. So, when we make the replacement $q^\mu q^\nu \to g^{\mu\nu} q^2/4$, we should remember that q^2 actually means $q_\parallel^2$. Another example, if we have a spinor product such as in the first line of Eq.6–7, $q^\wedge$, $q^\vee$, q^- will appear in both brackets, then q^2 means $q_\perp^2$ this time.

6.2 Self-Energy Diagrams

A factor of $-ig^2/(16\pi^2) f^{cad} f^{dbc} = ig^2/(16\pi^2)\mathrm{Tr}\left[t^a t^b\right]$ will be omitted.

For Fig.4-1, the results are

$$\begin{aligned}
\Pi(g+,g-;s)_m &= -\left[\frac{1}{6}p^2 \log \delta e^\gamma m^2 + \frac{1}{12}\frac{(p^2-4m^2)^2}{p^2} I(p^2) - \frac{5}{18}p^2 + \frac{4}{3}m^2\right] \\
\Pi(g+,g-;q)_m &= -\frac{4}{3}p^2 \log \delta e^\gamma m^2 - \frac{2}{3}\frac{(p^2-4m^2)(p^2+2m^2)}{p^2} I(p^2) + \frac{26}{9}p^2 + \frac{16}{3}m^2
\end{aligned} \tag{6–8}$$

The gluon mass counter term in the expressions above has been removed already.

6.3 Triangle Diagrams

A factor of $g^3/(8\pi^2) f^{dae} f^{ebf} f^{fcd} = ig^3/(8\pi^2)\mathrm{Tr}[t^a t^b t^c]$ is omitted.

For Fig.4-3:

$$
\begin{aligned}
\Gamma(g+,g+,g-;s)_m &= \frac{-2p_3^+}{p_1^+p_2^+}K_{21}^\wedge\Big[\frac{1}{6}\log m^2\delta e^\gamma + (p_o^2-4m^2)(\frac{(p_o^2-4m^2)}{12p_o^4}+\alpha\frac{p_1^+p_2^+}{p_3^{+2}}\frac{m^2}{p_o^4})I(p_o^2)\\
&\quad -\alpha\frac{p_1^+p_2^+}{p_3^{+2}}\frac{m^2}{p_o^2}J(p_o^2)-\frac{1}{9}+\frac{4m^2}{3p_o^2}-\alpha\frac{1}{6}\frac{p_1^+p_2^+}{p_3^{+2}}(1+\frac{24m^2}{p_o^2})\Big]\\
\Gamma(g+,g+,g-;q)_m &= -2\frac{-2p_3^+}{p_1^+p_2^+}K_{21}^\wedge\Big[-\frac{2}{3}\log m^2\delta e^\gamma\\
&\quad +(p_o^2-4m^2)(-\frac{(p_o^2+2m^2)}{3p_o^4}+2\alpha\frac{p_1^+p_2^+}{p_3^{+2}}\frac{m^2}{p_o^4})I(p_o^2)\\
&\quad -2\alpha\frac{p_1^+p_2^+}{p_3^{+2}}\frac{m^2}{p_o^2}J(p_o^2)+\frac{16}{9}+\frac{8m^2}{3p_o^2}-\alpha\frac{1}{3}\frac{p_1^+p_2^+}{p_3^{+2}}(1+\frac{24m^2}{p_o^2})\Big]
\end{aligned}
\tag{6–9}
$$

where $\alpha = 1$ if leg 3 is off shell and 0 otherwise, and p_o is the off shell momentum. Their anomalous terms are identical with the massless result, which agrees with the fact that anomalous terms are UV effects.

For an MHV triangle:

$$
\begin{aligned}
\Gamma(g+,g+,g+;s)_m &= \frac{(K_{21}^\wedge)^3}{p_1^+p_2^+p_3^+}\Big[-\frac{4m^2(p_o^2-4m^2)}{p_o^6}I(p_o^2)+\frac{4m^2}{p_o^4}J(p_o^2)+\frac{2(p_o^2+24m^2)}{3p_o^4}\Big]\\
\Gamma(g+,g+,g+;q)_m &= -2\frac{(K_{21}^\wedge)^3}{p_1^+p_2^+p_3^+}\Big[-\frac{8m^2(p_o^2-4m^2)}{p_o^6}I(p_o^2)+\frac{8m^2}{p_o^4}J(p_o^2)+\frac{4(p_o^2+24m^2)}{3p_o^4}\Big]
\end{aligned}
\tag{6–10}
$$

6.4 Scattering Amplitudes

A factor of $ig^4/(8\pi^2)\mathrm{Tr}[t^at^bt^ct^d]$ is omitted.

$$
\begin{aligned}
A(g+,g+,g+,g+;s)_m &= 8\frac{K_{43}^\wedge K_{32}^\wedge K_{21}^\wedge K_{14}^\wedge}{p_1^+p_2^+p_3^+p_4^+st}\Big[\frac{1}{6}-\frac{m^4}{st}K(s,t)\Big]\\
A(g+,g+,g+,g+;q)_m &= -16\frac{K_{43}^\wedge K_{32}^\wedge K_{21}^\wedge K_{14}^\wedge}{p_1^+p_2^+p_3^+p_4^+st}\Big[\frac{1}{3}-\frac{2m^4}{st}K(s,t)\Big]
\end{aligned}
\tag{6–11}
$$

$$
\begin{aligned}
& A(g+,g+,g+,g-;s)_m \\
= \;& \frac{K_{13}^{\wedge 2} p_2^+ p_4^+}{K_{43}^{\wedge} K_{32}^{\vee} K_{21}^{\vee} K_{14}^{\wedge}} \Big[-\frac{(2t+s)tm^2}{2(s+t)s}(1-\frac{4m^2}{s})I(s) - \frac{(2s+t)sm^2}{2(s+t)t}(1-\frac{4m^2}{t})I(t) \\
& + \frac{(2s+t)t^2m^2}{(s+t)^2 s} J(s) + \frac{(2t+s)s^2m^2}{(s+t)^2 t} J(t) + \frac{stm^2}{2(s+t)^2}(1-2\frac{m^2(s+t)}{st})K(s,t) \\
& + \frac{2(2s^2-st+2t^2)m^2}{st} + \frac{(s+t)}{6} \Big] \\
& A(g+,g+,g+,g-;q)_m \\
= \;& -2\frac{K_{13}^{\wedge 2} p_2^+ p_4^+}{K_{43}^{\wedge} K_{32}^{\vee} K_{21}^{\vee} K_{14}^{\wedge}} \Big[-\frac{(2t+s)tm^2}{(s+t)s}(1-\frac{4m^2}{s})I(s) - \frac{(2s+t)sm^2}{(s+t)t}(1-\frac{4m^2}{t})I(t) \\
& + \frac{2(2s+t)t^2m^2}{(s+t)^2 s} J(s) + \frac{2(2t+s)s^2m^2}{(s+t)^2 t} J(t) + \frac{stm^2}{(s+t)^2}(1-2\frac{m^2(s+t)}{st})K(s,t) \\
& + \frac{4(2s^2-st+2t^2)m^2}{st} + \frac{(s+t)}{3} \Big]
\end{aligned}
\tag{6–12}
$$

In contrast to the massless case, the external leg factors are included in the results below for the helicity conserving amplitudes, since we can perform wave function renormalization now.

$$
\begin{aligned}
& A(g+,g+,g-,g-;s)_m \\
= \;& \frac{-2K_{12}^{\wedge 4} p_3^+ p_4^+}{K_{43}^{\wedge} K_{32}^{\wedge} K_{21}^{\wedge} K_{14}^{\wedge} p_1^+ p_2^+} \Big[(\frac{m^2}{2s} - \frac{2m^2}{3t} - \frac{2m^4}{st} + \frac{4m^4}{3t^2} + \frac{1}{12})I(t) + \frac{m^4}{s^2}K(s,t) \\
& - \frac{2m^2}{s} + \frac{4m^2}{3t} + \frac{1}{18} - \frac{1}{6}\log \delta e^{\gamma} m^2 - \frac{1}{3} \Big] - \frac{1}{6}\times + \frac{1}{3} \\
& A(g+,g+,g-,g-;q)_m \\
= \;& -2\frac{-2K_{12}^{\wedge 4} p_3^+ p_4^+}{K_{43}^{\wedge} K_{32}^{\wedge} K_{21}^{\wedge} K_{14}^{\wedge} p_1^+ p_2^+} \Big[(\frac{m^2}{s} + \frac{2m^2}{3t} - \frac{4m^4}{st} + \frac{8m^4}{3t^2} - \frac{1}{3})I(t) + (-\frac{m^2}{s} + \frac{2m^4}{s^2})K(s,t) \\
& - \frac{4m^2}{s} + \frac{8m^2}{3t} + \frac{19}{9} + \frac{2}{3}\log \delta e^{\gamma} m^2 - \frac{2}{3} \Big] + \frac{2}{3}\times - \frac{4}{3}
\end{aligned}
\tag{6–13}
$$

$$
\begin{aligned}
&A(g+,g-,g+,g-;s)_m = \frac{-2K_{13}^{\wedge 4}p_2^+p_4^+}{K_{43}^{\wedge}K_{32}^{\wedge}K_{21}^{\wedge}K_{14}^{\wedge}p_1^+p_3^+} \\
&\Big[(-\frac{tm^2(17st+s^2+4t^2)}{6(s+t)^3s}+\frac{2tm^4(2t+5s)}{3(s+t)^2s^2}+\frac{t(5st-2s^2+t^2)}{12(s+t)^3})I(s) \\
&+(-\frac{sm^2(17st+t^2+4s^2)}{6(s+t)^3t}+\frac{2sm^4(5t+2s)}{3(s+t)^2t^2}+\frac{s(5st-2t^2+s^2)}{12(s+t)^3})I(t) \\
&+(\frac{2stm^2}{(s+t)^3}-\frac{s^2t^2}{(s+t)^4})(J(s)+J(t))+(-\frac{2stm^2}{(s+t)^3}+\frac{m^4}{(s+t)^2}+\frac{s^2t^2}{2(s+t)^4})K(s,t) \\
&+\frac{2m^2(2t^2+2s^2+3st)}{3(s+t)st}+\frac{s^2+t^2+11st}{18(s+t)^2}-\frac{1}{6}\log\delta e^\gamma m^2-\frac{1}{3}\Big]-\frac{1}{6}\times+\frac{1}{3} \\
&A(g+,g-,g+,g-;q)_m = -2\frac{-2K_{13}^{\wedge 4}p_2^+p_4^+}{K_{43}^{\wedge}K_{32}^{\wedge}K_{21}^{\wedge}K_{14}^{\wedge}p_1^+p_3^+} \\
&\Big[(\frac{tm^2(5s^2+2t^2-5st)}{3(s+t)^3s}+\frac{4tm^4(2t+5s)}{3(s+t)^2s^2}-\frac{t(5s^2+2t^2+st)}{6(s+t)^3})I(s) \\
&+(\frac{tm^2(5t^2+2s^2-5st)}{3(s+t)^3t}+\frac{4sm^4(5t+2s)}{3(s+t)^2t^2}-\frac{s(5t^2+2s^2+st)}{6(s+t)^3})I(t) \\
&+(\frac{4stm^2}{(s+t)^3}+\frac{st(s^2+t^2)}{(s+t)^4})(J(s)+J(t))+(\frac{m^2(s-t)^2}{(s+t)^3}+\frac{2m^4}{(s+t)^2}-\frac{st(s^2+t^2)}{2(s+t)^4})K(s,t) \\
&+\frac{4m^2(2t^2+2s^2+3st)}{3(s+t)st}+\frac{19s^2+19t^2+47st}{9(s+t)^2}+\frac{2}{3}\log\delta e^\gamma m^2-\frac{2}{3}\Big]+\frac{2}{3}\times-\frac{4}{3} \qquad (6\text{–}14)
\end{aligned}
$$

The last numerical factors $-1/3$ and $-2/3$ inside each square bracket is due to the amputation of external legs: $[\lim_{p^2\to 0}\Pi(p^2)/p^2]^{1/2}$.

6.5 Photon Photon Scattering

The amplitude of photon-photon scattering can be obtained from the above results fairly easily, all we need to do is to replace $g^4\mathrm{Tr}[t^at^bt^ct^d]$ with e^4 and sum all the crossings. The reader might think that we should also remove the triangle diagrams from the amplitudes since these diagrams involve tri-gluon vertices which are absent in an abelian gauge theory. But, these diagrams will automatically cancel each other when we sum over all crossings. This cancellation goes by the name of $U(1)$ decoupling. The amplitudes are listed in the appendix.

When we sum over all the crossings, the counter term that is proportional to the four point vertex will vanish, while the pure number 2/3 will become 2, which has to

be subtracted to restore gauge covariance. We obtain the following photon scattering amplitude:

$$
\begin{aligned}
A(+,+,+,+) &= \frac{ie^4}{4\pi^2}\frac{4K^{\wedge}_{43}K^{\wedge}_{32}K^{\wedge}_{21}K^{\wedge}_{14}}{p_1^+p_2^+p_3^+p_4^+st}\left[2-\frac{4m^4}{st}K(s,t)-\frac{4m^4}{su}K(s,u)-\frac{4m^4}{tu}K(t,u)\right]\\
A(+,+,+,-) &= \frac{ie^4}{4\pi^2}\frac{stK^{\wedge 2}_{13}p_2^+p_4^+}{2uK^{\wedge}_{43}K^{\vee}_{32}K^{\vee}_{21}K^{\wedge}_{14}}\left\{2+\left[\frac{4m^2}{s}+\frac{4m^2}{t}+\frac{4m^2}{u}\right][J(s)+J(t)+J(u)]\right.\\
&\left.+\left[-\frac{2m^2}{u}-\frac{4m^4}{st}\right]K(s,t)+\left[-\frac{2m^2}{t}-\frac{4m^4}{su}\right]K(s,u)+\left[-\frac{2m^2}{s}-\frac{4m^4}{tu}\right]K(t,u)\right\}\\
A(+,+,-,-) &= \frac{ie^4}{4\pi^2}\frac{-tK^{\wedge 4}_{12}p_3^+p_4^+}{sK^{\wedge}_{43}K^{\wedge}_{32}K^{\wedge}_{21}K^{\wedge}_{14}p_1^+p_2^+}\\
&\left\{\left[\frac{8m^2}{s}+\frac{4m^2}{t}-\frac{2t}{s}-1\right]I(t)+\left[\frac{8m^2}{s}+\frac{4m^2}{u}-\frac{2u}{s}-1\right]I(u)\right.\\
&+\left[\frac{8m^2}{s}-\frac{4t^2+4st+2s^2}{s^2}\right]\left[J(t)+J(u)\right]+\left[\frac{2m^2}{t}-\frac{4m^4}{st}\right]K(s,t)+\left[\frac{2m^2}{u}-\frac{4m^4}{su}\right]K(s,u)\\
&\left.+\left[\frac{2(4t^2+4st+s^2)m^2}{stu}-\frac{4m^4}{tu}+\frac{2t^2+2st+s^2}{s^2}\right]K(t,u)-2\right\}\\
A(+,-,+,-) &= \frac{ie^4}{4\pi^2}\frac{-stK^{\wedge 4}_{13}p_2^+p_4^+}{u^2K^{\wedge}_{43}K^{\wedge}_{32}K^{\wedge}_{21}K^{\wedge}_{14}p_1^+p_3^+}\\
&\left\{\left[\frac{8m^2}{u}+\frac{4m^2}{t}-\frac{2t}{u}-1\right]I(t)+\left[\frac{8m^2}{u}+\frac{4m^2}{s}-\frac{2s}{u}-1\right]I(s)\right.\\
&+\left[\frac{8m^2}{u}-\frac{4t^2+4ut+2u^2}{u^2}\right]\left[J(t)+J(s)\right]+\left[\frac{2m^2}{t}-\frac{4m^4}{ut}\right]K(u,t)+\left[\frac{2m^2}{s}-\frac{4m^4}{su}\right]K(s,u)\\
&\left.+\left[\frac{2(4t^2+4ut+u^2)m^2}{stu}-\frac{4m^4}{ts}+\frac{2t^2+2ut+u^2}{u^2}\right]K(t,s)-2\right\} \qquad (6\text{–}15)
\end{aligned}
$$

The spinor structure above has been set up to be uni-modular and invariant under crossings of two legs. The results here agree with [27] and [31]. Note that in the first term of Eq.(127.18) of [31], the authors seemed to have left out terms of $-4/s+2/t$ and $-4/s+2/u$ in the coefficient of $B(t)$ and $B(u)$ (their B function is effectively our I function) respectively, as Eq.(127.18) will not lead to Eq.(127.20) without those two terms.

CHAPTER 7
CONCLUSIONS AND FUTURE WORK

7.1 Conclusion

To conclude, I have studied the renormalization of gauge theory on the light cone world sheet. In order to do so, I computed all the four point amplitudes in gauge theory. The box reduction technique was developed to extract the artificial divergences and IR divergences. The artificial divergences are the rational functions containing $1/q^+$ poles, they come from the light cone gauge propagators and were shown to cancel in a gauge invariant quantity. The IR divergences, regulated by setting q^+ away from zero, were combined with the Bremsstrahlung contributions to give a Lorentz covariant scattering cross section. The calculation of Bremsstrahlung contributions was also done in the light cone fashion to facilitate the comparison with the virtual processes. A mismatch in the rational parts of the amplitudes were prevalent, the restoration of gauge covariance was only partially addressed. Finally, the scattering of gluon by gluon with general massive matter was computed for completeness, and the light by light scattering amplitudes were obtained along the way.

Next I give some discussion on some unresolved issues and an outlook for the future work.

7.2 Restoring Gauge Covariance in the Light Cone

In [13, 14, 15], we insisted on only allowing counters terms that are polynomials in the target space. Thus, when we saw that there was a hanging four-point vertex in an amplitude, we could not put in a four point vertex as a counter term, but instead we modified the self-energy by a term const$\times p^2$ to adjust the strength of the exchange diagrams. But this scheme does not restore the gauge covariance for all the amplitudes.

Here I suggest a new system of putting in counter terms. Diagrams such as $\Pi(g^+, g^+)$ enter the amplitudes as 'double quartic' graphs, similarly $\Gamma(g+, g-, g^+)$ enters as 'quartic swordfish' diagrams, both of which are treated as 1PIR graphs in the canonical light cone formalism.

Treating them as 1PIR graphs forbids us to adjust their strength, for they usually contribute a multiple of four point vertices, which is not a polynomial in the momenta.

In Chapter 4, I compared $\Pi(g+,g-;s)$ with $\Pi(g^+,g^+;s)$ and $\Pi(g+,g-;q)$ with $\Pi(g^+,g^+;q)$. Here I give the result again:

$$\begin{aligned}
\Pi(g+,g-;s) &= p^2\left[\frac{5}{18}-\frac{1}{6}\log p^2\delta e^\gamma\right]\\
\Pi(g^+,g^+;s) &= p^{+2}\left[\frac{4}{9}-\frac{1}{6}\log p^2\delta e^\gamma\right]\\
\Pi(g+,g-;q) &= p^2\left[\frac{26}{9}-\frac{4}{3}\log p^2\delta e^\gamma\right]\\
\Pi(g^+,g^+;q) &= p^{+2}\left[\frac{20}{9}-\frac{4}{3}\log p^2\delta e^\gamma\right]
\end{aligned}$$

The non-rational parts of the self-energy contributions are the same regardless of the index on $\Pi^{\mu\nu}$. We have also reason to believe that, when there is no infrared divergence, the rational part should also match due to Lorentz covariance. More specifically, vacuum polarization should be of the form $\Pi^{\mu\nu}=\left(g^{\mu\nu}p^2-p^\mu p^\nu\right)\Pi(p^2)$. This tells us that

$$\begin{aligned}
\Pi(g+,g-) &= \epsilon_\wedge\cdot\epsilon_\vee p^2\Pi(p^2)=-p^2\Pi(p^2)\\
\Pi(g+,g^+) &= 0\\
\Pi(g^+,g^+) &= -p^{+2}\Pi(p^2)
\end{aligned}$$

Hence, apart from the factor of p^2 and p^{+2}, $\Pi(g+,g-)$ should be equal to $\Pi(g^+,g^+)$. Therefore, we have to invoke counter terms to force this equality. I chose to associate to each $\Pi(g^+,g^+;s)$ a term $-1/6$, and to $\Pi(g^+,g^+;q)$ a term $2/3$, I cannot quite find what is the correct value for $\Pi(g^+,g^+;g)$ because of the infrared divergence. So I simply defined it to be $-1/3$, chosen such that these counter terms vanish with $\mathcal{N}=4$ SYM field content. These counter terms are going to affect the four point vertex that is derived from the exchange diagrams.

The gluon vertex correction diagram has a similar problem:

$$
\begin{aligned}
\Gamma(g+,g-,g+;s) &= \frac{-2p_3^+}{p_1^+p_2^+}K_{2,1}^{\wedge}\left[\frac{1}{6}\log p_o^2\delta e^{\gamma}-\frac{1}{9}\right]\\
\Gamma(g+,g-,g^+;s) &= -(p_1^+-p_2^+)\left[\frac{1}{6}\log p_o^2\delta e^{\gamma}-\frac{5}{18}\right]\\
\Gamma(g+,g-,g+;q) &= \frac{-2p_3^+}{p_1^+p_2^+}K_{2,1}^{\wedge}\left[\frac{4}{3}\log p_o^2\delta e^{\gamma}-\frac{32}{9}\right]\\
\Gamma(g+,g-,g^+;q) &= -(p_1^+-p_2^+)\left[\frac{4}{3}\log p_o^2\delta e^{\gamma}-\frac{26}{9}\right]
\end{aligned}
$$

The logarithmic piece matches, so I will associate to $\Gamma(g,g,g;s)$ a term $-1/6$, to $\Gamma(g,g,g;q)$ a term $2/3$ and to $\Gamma(g,g,g;g)$ a term $-1/3$ to enforce the total agreement between $\Gamma(g+,g-,g+)$ and $\Gamma(g+,g-,g^+)$. Again, the number for $\Gamma(g,g,g;g)$ is hand picked so that there is no need for counter terms in $\mathcal{N}=4$ SYM. These counter terms will affect the strength of the exchange vertex.

There are also mismatches between $\Gamma(s,s,g+)$ and $\Gamma(s,s,g^+)$, which we cannot easily determine due to the IR divergence, so we throw in two arbitrary numbers and adjust these two numbers to make all the amplitudes work. The numbers are determined to be $-1/2$ for $\Gamma(s,s,g+)$ and 0 for $\Gamma(s,s,g^+)$ and $\Gamma(q,q,g)$.

Note that all of the modifications above can be achieved by polynomials in the external momenta[1] . I shall report how this counter term system is working out. First, I list all amplitudes in Table.7-1, note that by s-pt I mean the 4 point vertex that is derived from the s-channel exchange diagram.

The effect of the old regularization scheme is listed in Table.7-2.

We see by comparing 7-1 and 7-2 that all the bosonic amplitudes are fixed as long as there is only one species of scalar, while fermionic amplitudes generally have problems.

The new scheme gives Table.7-3.

By comparing 7-1 and 7-3, all the mismatches are fixed. But of course, this scheme answers as many questions as it raises. The loose threads include how to determine the counter term

[1] the structure $\left(-2p_3^+/p_1^+p_2^+\right)K_{2,1}^{\wedge}$ doesn't look like a polynomial, but actually its p^+ dependence comes from the polarization vectors

for those diagrams that have IR divergences, and whether they vanish in $\mathcal{N}=4$ SYM and how to realize them on the light cone world sheet. Finally, I want to point out an interesting observation that whenever a genuine four point vertex (meaning not derived from an exchange diagram) exists, the amplitude will have a constant mismatch.

7.3 Triangle Anomaly

Although I have stuck to the adjoint representation, in which the cubic invariant d^{abc} is zero, it is still necessary to look at how anomaly calculation turn out in the light cone. The first

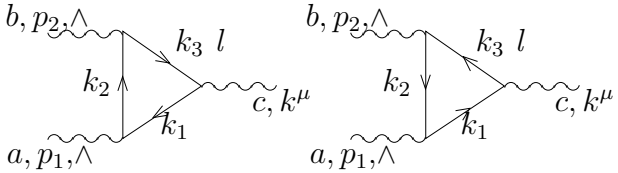

Figure 7-1. Triangle anomaly

diagram of Fig.7-1 is given by

$$\begin{aligned}
& -\mathrm{Tr}\left[it^b it^a it^c\right] \frac{\mathrm{Tr}\left[\epsilon_2\cdot\bar{\sigma}(q-k_2)\cdot\sigma\epsilon_2\cdot\bar{\sigma}(q-k_1)\cdot\sigma(k_3-k_1)\cdot\bar{\sigma}(q-k_3)\cdot\sigma\right]}{(-i)(q-k_2)^2(-i)(q-k_1)^2(-i)(q-k_3)^2} \\
= \; & i\mathrm{Tr}\left[t^b t^a t^c\right] \frac{2\langle\eta|(q-k_2)|k_1-k_2]\langle\eta|(q-k_1)(k_3-k_1)(q-k_3)|k_2-k_3]}{(-i)(q-k_2)^2(-i)(q-k_1)^2(-i)(q-k_3)^2} \\
= \; & -2\mathrm{Tr}\left[t^b t^a t^c\right] \langle\eta|(q-k_2)|k_1-k_2] \\
& \left\{\frac{\langle\eta|(q-k_3)|k_2-k_3]}{(-i)(q-k_2)^2(-i)(q-k_3)^2} - \frac{\langle\eta|(q-k_1)|k_2-k_3]}{(-i)(q-k_2)^2(-i)(q-k_1)^2}\right\}
\end{aligned} \tag{7–1}$$

After the usual steps of momentum integrals:

$$\begin{aligned}
& \int \frac{-idx_i}{16\pi^2}\Big\{ -\langle\eta|x_3(k_3-k_2)|k_1-k_2]\langle\eta|x_2k_{2\,\perp}+x_3k_{3\,\perp}|k_2-k_3] \\
& \qquad +\langle\eta|x_2(k_2-k_1)|k_2-k_3]\langle\eta|x_1k_{1\,\perp}+x_2k_{2\,\perp}|k_2-k_3]\Big\} \\
= \; & -\frac{i}{16\pi^2}\frac{2K_{12}^{\vee}}{3p_1^+p_2^+}\left(p_2^+(k_2+2k_3)^{\vee}+p_1^+(k_1+2k_2)^{\vee}\right)
\end{aligned} \tag{7–2}$$

The second diagram of Fig.7-1 is similar:

$$
\begin{aligned}
& -\mathrm{Tr}\left[it^b it^a it^c\right] \frac{\mathrm{Tr}\left[\epsilon_2\cdot\bar{\sigma}(k_3-q)\cdot\sigma(k_3-k_1)\cdot\bar{\sigma}(k_1-q)\cdot\sigma\epsilon_1\cdot\bar{\sigma}(k_2-q)\cdot\sigma\right]}{(-i)(q-k_2)^2(-i)(q-k_1)^2(-i)(q-k_3)^2} \\
= \;& i\mathrm{Tr}\left[t^b t^a t^c\right] \frac{2\langle\eta|(k_3-q)(k_3-k_1)(k_1-q)|k_1-k_2]\langle\eta|(k_2-q)|k_2-k_3]}{(-i)(q-k_2)^2(-i)(q-k_1)^2(-i)(q-k_3)^2} \\
= \;& -2\mathrm{Tr}\left[t^b t^a t^c\right] \langle\eta|(k_2-q)|k_2-k_3] \\
& \left\{\frac{\langle\eta|(k_1-q)|k_1-k_2]}{(-i)(q-k_2)^2(-i)(q-k_1)^2} - \frac{\langle\eta|(k_3-q)|k_1-k_2]}{(-i)(q-k_2)^2(-i)(q-k_3)^2}\right\}
\end{aligned}
\tag{7–3}
$$

After the momentum integral:

$$
\begin{aligned}
& \int \frac{-idx_i}{16\pi^2}\Big\{ -\langle\eta|x_1(k_1-k_2)|k_2-k_3]\langle\eta|x_1 k_{1\,\perp} + x_2 k_{2\,\perp}|k_1-k_2] \\
& \qquad\qquad +\langle\eta|x_2(k_2-k_3)|k_1-k_2]\langle\eta|x_2 k_{2\,\perp} + x_3 k_{3\,\perp}|k_2-k_3]\Big\} \\
= \;& -\frac{i}{16\pi^2}\frac{2K_{12}^\vee}{3p_1^+p_2^+}\left(p_1^+(k_2+2k_1)^\vee + p_2^+(k_3+2k_2)^\vee\right)
\end{aligned}
\tag{7–4}
$$

So the sum of these two diagrams gives

$$
\frac{i}{8\pi^2}\mathrm{Tr}\left[\{t^a,t^b\}t^c\right]\frac{2K_{12}^\vee}{p_1^+p_2^+}\left(p_1^+(k_2+k_1)^\vee + p_2^+(k_3+k_2)^\vee\right) \tag{7–5}
$$

The right handed fermion gives the same contribution as above (the Feynman diagram itself gives a negative sign relative to the left handed contribution, while the trace factor gives a second negative sign). But if we put t^c to be 1 and study the axial $U(1)$ current (commonly known as the abelian anomaly), the divergence of this current will be twice the above result. Or we can keep the theory chiral, and look at the divergence of the chiral current (know as the non-abelian anomaly) only. Note that the difference between these two cases is of order A^3, which will not show up here.

$*F\wedge F$ is of the form $K_{12}^\vee K_{12}^\vee/(p_1^+p_2^+)$ and 0 if the two gluons have different helicity. So some subtractions have to be made for Eq.7–5 to be of the correct form (again, due to the regulator we used, Eq.7–5 depends on each dual momenta). I haven't shown the calculation for the case when the two gluons having different helicity, the result is non-zero, so it has to be subtracted by counter terms too. Here, we see that the counter terms associated to three-point

function are populating fast, there may or may not be an economical choice of counter term(s) that will take care of all these problems.

7.4 Two-Loop and n-Point Amplitudes

The commonly adopted method for calculating one loop n-point amplitude is to use (generalized) unitarity [25, 26] to calculate box-coefficients, and to use recursion relations to recycle old results. And the results can be checked partially by looking at its collinear limit soft limit and multi-particle factorization properties.

We have basically calculated the four particle amplitude in the light cone gauge by brute force, should there be a need to obtain amplitudes with more legs or even higher loop amplitudes, to way to proceed is certainly not brute force.

Let us focus on the $\mathcal{N} = 4$ SYM theory as a first step. We know that in this theory, all integrands can be reduced to scalar boxes. This is very useful if we are using dimension regulation since the IR (or collinear) divergences are regulated. But we'd like to stick to our IR regulator, so scalar boxes have to go through some more subtractions to become infrared safe. I don't know yet how is this going to tell on the procedure of computing box coefficients.

The IR divergence is local in the sense that it is present whenever there is a four-point MHV subtree in the loop diagram, so the one loop IR structure we found in Chapter 5 will persist into a higher point amplitude. This feature perhaps can help us to define an IR safe part in an amplitude and 'bootstrap' it to a larger amplitudes.

Table 7-1. List of mismatches in all the amplitudes

Amplitude	s-exch	t-exch	s-pt	t-pt	const
$A(g+,g+,g-,g-;s)$	0	0	-	-1/6	1/2
$A(g+,g+,g-,g-;q)$	0	0	-	2/3	-2
$A(g+,g+,g-,g-;g)$	0	0	-	-1/3	1
$A(g+,g-,g+,g-;s)$	0	0	-1/6	-1/6	0
$A(g+,g-,g+,g-;q)$	0	0	2/3	2/3	0
$A(g+,g-,g+,g-;g)$	0	0	-1/3	-1/3	0
$A(s,s,g+,g-)$	0	0	-1/2	-	1/2
$A(g+,s,g-,s)$	0	0	-	-	2
$A(s,s,s,s)$	0	0	-1/2	-1/2	0
$A(q-,q-,\bar{q}-,\bar{q}-)$	-	0	-	-1/3	0
$A(q-,\bar{q}-,q-,\bar{q}-)$	0	0	-1/3	-1/3	0
$A(s,s,q-,\bar{q}-)$	0	-	-2/3	-	0
$A(g+,g-,q-,\bar{q}-)$	-1/3	0	-1/3	0	0
$A(g+,g-,q+,\bar{q}+)$	-1/3	0	-1/3	0	0
$A(g+,q-,g-,\bar{q}-)$	0	0	-	0	0

Table 7-2. List of the effect of the old counter terms schemes

Amplitude	s-exch	t-exch	s-pt	t-pt	const
$A(g+,g+,g-,g-;s)$	-1/6	-1/6	-	0	0
$A(g+,g+,g-,g-;q)$	2/3	2/3	-	0	0
$A(g+,g+,g-,g-;g)$	-1/3	-1/3	-	0	0
$A(g+,g-,g+,g-;s)$	-1/6	-1/6	0	0	0
$A(g+,g-,g+,g-;q)$	2/3	2/3	0	0	0
$A(g+,g-,g+,g-;g)$	-1/3	-1/3	0	0	0
$A(s,s,g+,g-)$	-1/2	-1/2	0	-	0
$A(g+,s,g-,s)$	-1/2	-1/2	-	-	0
$A(s,s,s,s)$	-1/2	-1/2	0	0	0
$A(q-,q-,\bar{q}-,\bar{q}-)$	-	1/3	-	0	0
$A(q-,\bar{q}-,q-,\bar{q}-)$	1/3	1/3	0	0	0
$A(s,s,q-,\bar{q}-)$	1/6	-	0	-	0
$A(g+,g-,q-,\bar{q}-)$	1/3	0	0	0	0
$A(g+,g-,q+,\bar{q}+)$	1/3	0	0	0	0
$A(g+,q-,g-,\bar{q}-)$	0	0	-	0	0

Table 7-3. List of the effect of the new counter terms scheme

Amplitude	s-exch	t-exch	s-pt	t-pt	const
$A(g+,g+,g-,g-;s)$	-1/3	-1/3	-	-1/6	0
$A(g+,g+,g-,g-;q)$	4/3	4/3	-	2/3	0
$A(g+,g+,g-,g-;g)$	-2/3	-2/3	-	-1/3	0
$A(g+,g-,g+,g-;s)$	-1/3	-1/3	-1/6	-1/6	0
$A(g+,g-,g+,g-;q)$	4/3	4/3	2/3	2/3	0
$A(g+,g-,g+,g-;g)$	-2/3	-2/3	-1/3	-1/3	0
$A(s,s,g+,g-)$	-1	-1	-1/2	-	0
$A(g+,s,g-,s)$	-1	-1	-	-	0
$A(s,s,s,s)$	-1	-1	-1/2	-1/2	0
$A(q-,q-,\bar{q}-,\bar{q}-)$	-	0	-	1/3	0
$A(q-,\bar{q}-,q-,\bar{q}-)$	0	0	1/3	1/3	0
$A(s,s,q-,\bar{q}-)$	-1/2	-	1/6	-	0
$A(g+,g-,q-,\bar{q}-)$	1/3	0	1/3	0	0
$A(g+,g-,q+,\bar{q}+)$	1/3	0	1/3	0	0
$A(g+,q-,g-,\bar{q}-)$	0	0	-	0	0

APPENDIX A
SPINOR NOTATION IN THE LIGHT CONE

$$\gamma^\mu = \begin{vmatrix} 0 & \sigma^\mu \\ \bar{\sigma}^\mu & 0 \end{vmatrix} \quad \sigma^\mu := (\mathrm{I}, \vec{\sigma}) \quad \bar{\sigma}^\mu := (\mathrm{I}, -\vec{\sigma})$$
$$\epsilon_{ab} = \epsilon^{ab} = \epsilon^{\dot{a}\dot{b}} = \epsilon_{\dot{a}\dot{b}} = i\sigma_2$$
$$p_a = \epsilon_{ab} p^b \quad p^a = p_b \epsilon^{ba}$$
$$|p\,] := p_{\dot{a}} \quad |p\,\rangle := p^a \quad [p| := p^{\dot{a}} \quad \langle p| := p_a \tag{A–1}$$

So far the spinor notations are common to all, and in the last line of Eq.A–1, I have conformed to the 'hep-ph' notation: $|p\,]$ is assigned a lower index while $|p\,\rangle$ an upper index.

In light cone, unlike what we had in Section 2.1, the reference spinor is fixed to be

$$\eta^\alpha = \eta^{\dot{\alpha}} = \begin{vmatrix} 1 \\ 0 \end{vmatrix} \quad \eta_\alpha = \eta_{\dot{\alpha}} = \begin{vmatrix} 0 \\ -1 \end{vmatrix} \tag{A–2}$$

We can define the light cone version spinor as

$$p^\alpha = \begin{vmatrix} -\frac{p^\wedge}{p^+} \\ 1 \end{vmatrix} \quad p_{\dot{\alpha}} = \begin{vmatrix} 1 \\ \frac{p^\vee}{p^+} \end{vmatrix} \tag{A–3}$$

The spinors satisfy the Dirac equation if p is light like. Note that they don't have the correct normalization, namely $p \cdot \sigma^{\alpha\dot{\alpha}} \neq p^\alpha p^{\dot{\alpha}}$, but they have the merit that $p^\alpha = (-p)^\alpha$. The polarization vectors of gluon can be written as

$$\epsilon_{\wedge \dot{a}a} = \sqrt{2}\frac{|p\,]\langle \eta\,|}{\langle \eta\,|p\,\rangle} = -\sqrt{2}|p\,]\langle \eta\,|, \quad \epsilon_{\vee \dot{a}a} = \sqrt{2}\frac{|\eta\,]\langle p\,|}{[p\,|\eta\,]} = -\sqrt{2}|\eta\,]\langle p\,| \tag{A–4}$$
$$K^\wedge_{ij} = p_j^+ p_i^+ \langle p_j\,|p_i\,\rangle, \quad K^\vee_{ij} = p_i^+ p_j^+ [p_i\,|p_j\,]$$
$$[\,\eta\,|\,p_i\,|\,p_j\,\rangle = \langle\, p_j\,|\,p_i\,|\,\eta\,] = \frac{\sqrt{2}}{p_j^+} K^\wedge_{ji}, \ \langle\,\eta\,|\,p_i\,|\,p_j\,] = [\,p_j\,|\,p_i\,|\,\eta\,\rangle = \frac{\sqrt{2}}{p_j^+} K^\vee_{ji} \tag{A–5}$$

The K_{ij}'s satisfy

$$
\begin{aligned}
\sum_j K^\mu_{ij} &= 0 \\
p_i^+ K^\mu_{jk} + p_k^+ K^\mu_{ij} + p_j^+ K^\mu_{ki} &= 0 \\
K^\wedge_{li} K^\wedge_{jk} + K^\wedge_{lk} K^\wedge_{ij} + K^\wedge_{lj} K^\wedge_{ki} &= 0 \\
\sum_j \frac{K^\wedge_{ij} K^\vee_{jk}}{p_j^+} &= p_i^+ p_k^+ \sum_j \frac{p_j^2}{2p_j^+}
\end{aligned}
\tag{A–6}
$$

The third line of Eq.A–6 is called the Schouten identity: $[ij][kl] + [jk][il] + [ki][jl] = 0$.

In the current case we are dealing with, i, j run from 1 to 4, but only two of the six K_{ij}'s are independent, say K_{43} and K_{32}. And any product of K_{ij}'s with total helicity 4 can be reduced to either $(K^\wedge_{43})^4$ or $(K^\wedge_{43})^3 K^\wedge_{32}$. Product of helicity 2 can be reduced to $(K^\wedge_{43})^2$ and $K^\wedge_{43} K^\wedge_{32}$. Product of helicity 0 can be reduced to 1 and $K^\wedge_{32} K^\vee_{43}$. The reduction is in general a formidable task for human, but quite a piece of cake for computers, as all our calculations are done with computers.

APPENDIX B
FEYNMAN RULES

We remind the reader that $g+(-)$ corresponds to a $\wedge\,(\vee)$ on the gluon line, $q(\bar{q})$ corresponds to an incoming (outgoing) fermion line, $q+(-)$ corresponds to right(left) handedness, s corresponds to a scalar.

The fermion gluon vertex Fig.B-1 is given by

$$\begin{aligned} V(q-,\bar{q}-,g+) &= -2ig(t^a)_{bc}\frac{p_2^+}{q^+p_1^+}K^{\wedge}_{p_1,q}, \quad V(q+,\bar{q}+,g+) = -2ig(t^a)_{bc}\frac{1}{q^+}K^{\wedge}_{p_2,q} \\ V(q-,\bar{q}-,g-) &= -2ig(t^a)_{bc}\frac{1}{q^+}K^{\vee}_{p_2,q}, \quad V(q+,\bar{q}+,g-) = -2ig(t^a)_{bc}\frac{p_2^+}{q^+p_1^+}K^{\vee}_{p_1,q} \end{aligned} \tag{B–1}$$

The gluon scalar vertex Fig.B-2 is given by

$$V\left(g+(-)\right) = -2ig(t^a)_{bc}\frac{1}{p_b^+ + p_c^+}K^{\wedge(\vee)}_{p_c,p_b} \tag{B–2}$$

Here we have used real scalar fields and hence it transforms in a real representation.

The gluon fermion 4 point vertex Fig.B-3 is given by

$$\begin{aligned} V(q-,\bar{q}-,g+,g-) &= -2ig^2(t^d)_{ce}(t^a)_{eb}\frac{p_2^+}{p_1^+ + p_4^+} + 2g^2 f^{dae}(t^e)_{cb}\frac{(p_3^+ - p_4^+)p_2^+}{(p_3^+ + p_4^+)^2} \\ V(q+,\bar{q}+,g+,g-) &= 2g^2 f^{dae}(t^e)_{cb}\frac{(p_3^+ - p_4^+)p_2^+}{(p_3^+ + p_4^+)^2} \\ V(q-,\bar{q}-,g-,g+) &= 2g^2 f^{dae}(t^e)_{cb}\frac{(p_3^+ - p_4^+)p_2^+}{(p_3^+ + p_4^+)^2} \\ V(q+,\bar{q}+,g-,g+) &= -2ig^2(t^d)_{ce}(t^a)_{eb}\frac{p_2^+}{p_1^+ + p_4^+} + 2g^2 f^{dae}(t^e)_{cb}\frac{(p_3^+ - p_4^+)p_2^+}{(p_3^+ + p_4^+)^2} \end{aligned} \tag{B–3}$$

The gluon scalar four point vertex Fig.B-4 is given by

$$\begin{aligned} & V(g+,g-,s,s) = V(g-,g+,s,s) \\ = \;& -ig^2\left[(t^a)_{ce}(t^b)_{ed} + (t^b)_{ce}(t^a)_{ed}\right] + g^2 f^{abe}(t^e)_{cd}\frac{(p_3^+ - p_4^+)(p_2^+ - p_1^+)}{(p_1^+ + p_2^+)^2} \\ & V(g+,g+,s,s) = V(g-,g-,s,s) = 0 \end{aligned} \tag{B–4}$$

For tri-gluon vertex Fig.4-3

$$V(g,g,g) = -gf^{abc}[\epsilon_1^* \cdot \epsilon_2^*(p_1-p_2)\cdot\epsilon_3^* + \epsilon_2^* \cdot \epsilon_3^*(p_2-p_3)\cdot\epsilon_1^* + \epsilon_3^* \cdot \epsilon_1^*(p_3-p_1)\cdot\epsilon_2^*]$$

Setting $\mu,\nu = \wedge$, $\rho = \vee$, the above becomes

$$\begin{aligned} V(g+,g+,g-) &= gf^{abc}[(p_2-p_3)^+\frac{p_1^\wedge}{p_1^+} - (p_2-p_3)^\wedge + (p_3-p_1)^+\frac{p_2^\wedge}{p_2^+} - (p_3-p_1)^\wedge] \\ &= 2gf^{abc}\frac{(p_1+p_2)^+}{p_1^+p_2^+}K_{21}^\wedge \end{aligned} \tag{B–5}$$

The gluon four point vertex receives contribution from two sources: the left diagram in Fig.B-6 is simply the covariant four point vertex:

$$V_1 = ig^2\left\{f^{abe}f^{ecd}[g^{\mu\sigma}g^{\nu\rho} - g^{\mu\rho}g^{\nu\sigma}] + f^{dae}f^{ebc}[g^{\mu\nu}g^{\rho\sigma} - g^{\mu\rho}g^{\nu\sigma}] + f^{cae}f^{ebd}[g^{\mu\nu}g^{\rho\sigma} - g^{\mu\sigma}g^{\nu\rho}]\right\} \tag{B–6}$$

The second is obtained by shrinking a propagator.

$$\begin{aligned} V_2 &= g^2f^{dae}f^{ebc}[\epsilon_1^*\cdot\epsilon_4^*(p_4-p_1)_\alpha]\frac{ig^{\alpha+}g^{\beta+}(p_1+p_4)^2}{(p_1^+ + p_4^+)^2(p_1+p_4)^2}[\epsilon_2^*\cdot\epsilon_3^*(p_2-p_3)_\beta] \\ &= ig^2f^{dae}f^{ebc}\frac{(\epsilon_1^*\cdot\epsilon_4^*)(\epsilon_2^*\cdot\epsilon_3^*)(p_4-p_1)^+(p_2-p_3)^+}{(p_1^+ + p_4^+)^2} \end{aligned}$$

There are two cases in which the gluon four point vertex is nonzero:

$$\begin{aligned} V(g+,g+,g-,g-) &= 2ig^2\left[-f^{dae}f^{ebc}\frac{p_1^+p_3^+ + p_2^+p_4^+}{(p_1^+ + p_4^+)(p_2^+ + p_3^+)} + f^{ace}f^{ebd}\frac{p_3^+p_2^+ + p_1^+p_4^+}{(p_1^+ + p_3^+)(p_2^+ + p_4^+)}\right] \\ V(g+,g-,g+,g-) &= 2ig^2\left[f^{abe}f^{ecd}\frac{p_2^+p_3^+ + p_1^+p_4^+}{(p_1^+ + p_2^+)(p_3^+ + p_4^+)} + f^{dae}f^{ebc}\frac{p_1^+p_2^+ + p_3^+p_4^+}{(p_1^+ + p_4^+)(p_2^+ + p_3^+)}\right] \end{aligned} \tag{B–7}$$

When using these vertices, we need to watch the indices of structure constants closely: not all terms are going to make contributions to $\mathrm{Tr}[t^at^bt^ct^d]$.

The fermion four point vertex comes from contracting a pair of three point vertices connected by a gluon propagator. It is given by (for configuration of Fig.B-7)

$$V(q,q,\bar{q},\bar{q}) = -4ig^2(t^e)_{da}(t^e)_{cb}\frac{p_3^+p_4^+}{(p_1^+-p_4^+)^2} \tag{B–8}$$

with the obvious restriction that fermion line 1 and 4 having the same handedness while 2 and 3 having the same handedness.

The scalar four point vertex Fig.B-8 comes from contracting a pair of three point vertices connected by a gluon propagator. It is given by

$$V(s,s,s,s) = -ig^2(t^e)_{ab}(t^e)_{cd}\frac{(p_3^+-p_4^+)(p_1^+-p_2^+)}{(p_1^+ + p_2^+)^2} \tag{B–9}$$

The scalar fermion four point vertex Fig.B-9 also comes from contracting a gluon propagator:

$$V(s,s,\bar{q},q) = -ig^2(t^e)_{ab}(t^e)_{cd}\frac{2p_3^+(p_2^+-p_1^+)}{(p_1^+ + p_2^+)^2} \tag{B–10}$$

with the restriction that the fermion lines having the same handedness.

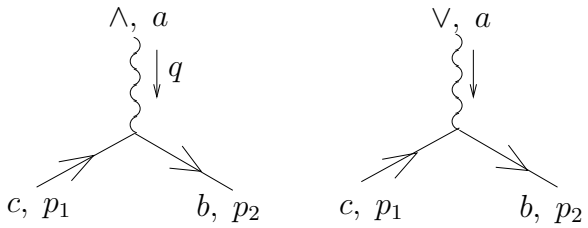

Figure B-1. Gluon-fermion-fermion 3 point vertex

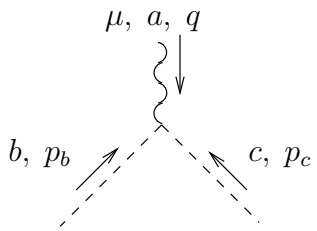

Figure B-2. Gluon-scalar-scalar 3 point vertex

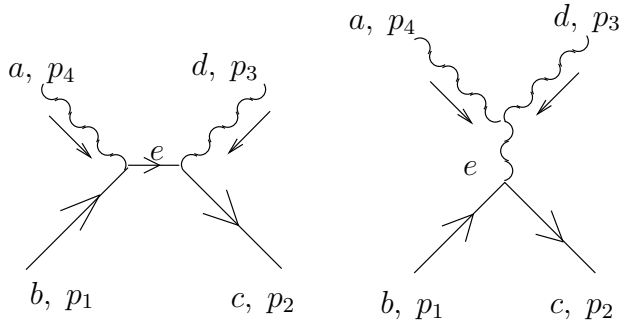

Figure B-3. Two diagrams contribute to the fermion-gluon 4 point vertex. Note these are not exchange diagrams but rather four point vertices gotten through cancelling a $1/p^2$ factor in a fermion propagator or a gluon propagator, see Eq.2–25

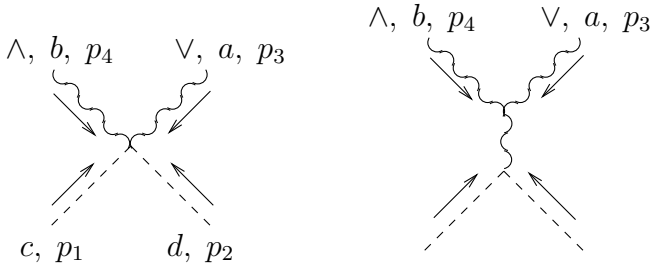

Figure B-4. Scalar-gluon 4 point vertex. Again, the second diagram is not an exchange diagram but rather a four point vertex obtained through shrinking a gluon propagator

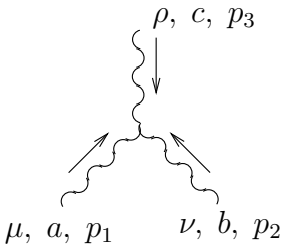

Figure B-5. Tri-gluon vertex

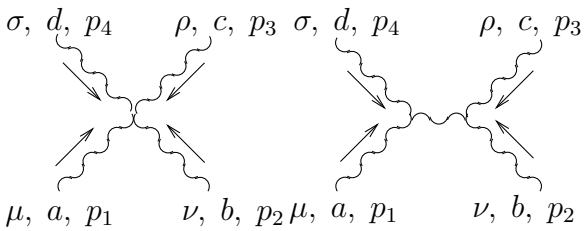

Figure B-6. Gluon 4 point vertex

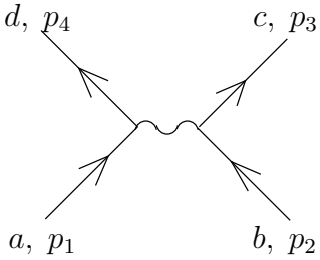

Figure B-7. Fermion 4 point vertex

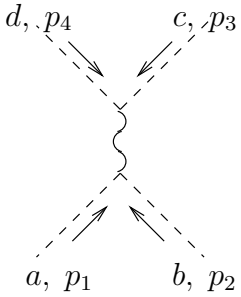

Figure B-8. Scalar 4 point vertex

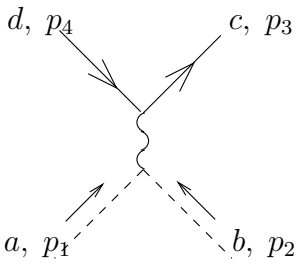

Figure B-9. Scalar Fermion 4 point vertex

REFERENCES

[1] G. 't Hooft, *Nucl. Phys.* **B72** (1974) 461. J. M.

[2] Maldacena, Adv. Theor. Math. Phys. **2**, 231 (1998).

[3] S.S. Gubser, I.R. Klebanov and A.M. Polyakov, Phys. Lett. **B428** (1998) 105,[arxive:hep-th/9802109]

[4] E. Witten, , Adv. Theor. Math. Phys.**2**: 253, 1998, [arxive:hep-th/9805028]

[5] J. Maldacena, Phys. Rev. Lett. **80**, 4859 (1998), [arXive:hep-th/9803002]

[6] K. Bardakci and C. B. Thorn, Nucl. Phys. **B626**, 287 (2002).

[7] C.B. Thorn, Nucl.Phys.**B637**:272-292 (2002).
Erratum-ibid.**B648**:457,2003. [arXive:hep-th/0203167]
S. Gudmundsson, C.B. Thorn, T.A. Tran, Nucl.Phys.**B649**:3-38 (2003).
[arXive:hep-th/0209102]

[8] C.B. Thorn Nucl.Phys.**B699**:427-452 (2004).[arXive:hep-th/0405018]

[9] S. Gudmundsson, C.B. Thorn, Phys.Rev.D**66**:076001 (2002). [arXive:hep-th/0203232]

[10] Z.Xu, D.H.Zhang and L.Chang, Nucl. Phys. **B291**:392 (1987)

[11] L. Dixon, Calculating Scattering Amplitudes Efficiently [arXive:hep-ph/9601359]

[12] G. Chalmers and W. Siegel Phys.Rev.D**63**:125027,2001[arXive:hep-th/0101025]
G. Chalmers and W. Siegel Phys.Rev.D**59**:045013,1999. [arXive:hep-ph/9801220]
G. Chalmers and W. Siegel Phys.Rev.D**59**:045012,1999[arXive:hep-ph/9708251]

[13] D. Chakrabarti, J. Qiu and C. B. Thorn, Phys. Rev. D**72**, 065022 (2005)
[arXiv:hep-th/0507280].

[14] D. Chakrabarti, J. Qiu and C. B. Thorn, Phys. Rev. D**74**, 045018 (2006)
[arXiv:hep-th/0602026].

[15] J. Qiu, Phys. Rev. D**74**, 085022(2006) [arXiv:hep-th/0607097].

[16] T.D. Lee and M. Nauenberg, Phys. Rev. **133**, B1549 (1964).

[17] M.T. Grisaru and H.N.Pendleton, Nucl. Phys. **B124** (1977) 81-92

[18] G. Passarino and M. Veltman, Nucl. Phys. **B160**:151 (1979)
D.B. Melrose, Nuovo Cimento **40A**:181(1965)
W.van. Neerven and J.A.M. Vermaseren, Phys.Lett. **137**B:241(1984)
G.J.van Oldenborgh and J.A.M. Vermaseren, Z.Phys. **C46**:425(1990)

[19] S. Mandelstam, Nuclear Physics **B213**, 149 (1983). G. Leibbrandt, Physical Review D**29**, 1699 (1984). D.M.Capper, J.J.Dulwich and M.J.Litvak, Nuclear Physics **B241** (1984) 463-476

[20] S. J. Parke and T. R. Taylor, Phys. Rev. Lett. **56** (1986) 2459.

[21] M. Mangano, S, Parke and Z. Xu, Nucl.Phys **B298** (1988) 653-672

[22] F. Berends and W. Giele, Nucl.Phys **B294** (1987) 700-732

[23] Z. Kunszt, A. Signer and T. Trocsanyi Nucl.Phys **B411** (1994) 397 [arXiv:hep-ph/9305239].

[24] Z. Kunszt and D. Soper, Phys. Rev. D**46**:192 (1992).

[25] R. Britto, F. Cachazo and B. Feng, Nucl.Phys. **B725** (2005) 275-305 [arXiv:hep-th/0412103].
R. Britto, F. Cachazo and B. Feng, Nucl.Phys. **B715** (2005) 499-522 [arXiv:hep-th/0412308].

[26] Z. Bern, L. Dixon, D.C. Dunbar, D.A. Kosower, Nucl.Phys. **B425** (1994) 217-260[arXiv:hep-ph/9403226]
C.F. Berger, Z. Bern, L. Dixon, D. Forde, D.A. Kosower, Phys Rev D**74**, 036009 (2006)

[27] R. Karplus and M. Neuman Phys.Rev. 83, 776 (1951)[arXive:hep-ph/0604195]

[28] S. Gudmundsson, C. B. Thorn, and T. A. Tran, Nucl. Phys. **B649** (2002) 3, [arXiv:hep-th/0209102]

[29] N. I. Ussyukina, A. I. Davydychev, Phys. Lett. B **298**, 363 (1993)

[30] Andrei I. Davydychev [arXiv:hep-ph/9307323]

[31] V.B.Berestetskii, E.M.Lifshitz and L.P.Pitaevskii Quantum Electrodynamics Landau and Lifshitz Course of Theorectical Phyiscs, Vol.4 page 570

BIOGRAPHICAL SKETCH

Jian Qiu was born in 11.2.1979 in Shanghai, China. He was raised up in a small town Le-Ping in the Jiang-Xi province, where he finished the first two years of elementary school. He moved back to Shanghai in 1988 and went to elementary school, middle school and high school there. From the sixth to the twelfth grade, he also took part in competitions in remote controlled race car.

After graduating from Shi-Er high school in 1998, he was admitted to Fudan University to study physics. He was first interested in Nuclear physics, then slowly shifted his interest to theoretical physics and mathematics. He then graduated from Fudan University in 7.2002 with the bachelor's degree.

In the same month, he left China and came to the University of Florida to pursue his graduate study in physics. And he has been in the Physics Department ever since.